Predictive Modeling of Organic Pollutant Leaching and Transport Behavior at the Lysimeter and Field Scales.

Dissertation

zur Erlangung des akademischen Grades Doctor rerum naturalium

vorgelegt der Fakultät Forst-, Geo- und Hydrowissenschaften
der Technischen Universität Dresden

von Edward Akwasi Amankwah MSc.

Gutachter:

Prof. Dr. Rudolf Liedl, TU Dresden
Prof. Dr. Peter Grathwohl, Eberhard-Karls-Universität Tübingen
Prof. Dr.-Ing. Peter-Wolfgang Gräber, TU Dresden.

Dresden, Mai 2007

Abstract

Soil and groundwater pollution has become a global issue since the advent of industrialization and mechanized agriculture. Some contaminants such as PAHs may persist in the subsurface for decades and centuries. In a bid to address these issues, protection of groundwater must be based on the quantification of potential threats to pollution at the subsurface which is often inaccessible. Risk assessment of groundwater pollution may however be strongly supported by applying process-based simulation models, which turn out to be particularly helpful with regard to long-term predictions, which cannot be undertaken by experiments. Such reliable predictions, however, can only be achieved if the used modeling tool is known to be applicable.

The aim of this work was threefold. First, a source strength function was developed to describe the leaching behavior of point source organic contaminants and thereby acting as a time-dependent upper boundary condition for transport models. For general application of these functions dimensionless numbers known as Damköhler numbers were used to characterize the reaction of the pollutants with the solid matrix. Two functions were derived and have been incorporated into an Excel worksheet to act as a practical aid in the quantification of leaching behavior of organic contaminant in seepage water prognoses. Second, the process based model tool SMART, which is well validated for laboratory scale data, was applied to lysimeter scale data from two research centres, FZJ (Jülich) and GSF (München) for long term predictions. Results from pure forward model runs show a fairly good correlation with the measured data. Finally, the derived source term functions in combination with the SMART model were used to assess groundwater vulnerability beneath a typical landfill at Kwabenya in Ghana. The predicted breakthrough time after leaking from the landfill was more than 200 years considering the operational time of the facility (30 years). Considering contaminant degradation, the landfill would therefore not cause groundwater pollution under the simulated scenarios and the SMART model can be used to establish waste acceptance criteria for organic contaminants in the landfill at Kwabenya.

Zusammenfassung

Seit dem Beginn der Industrialisierung und der mechanisierten Landwirtschaft wurde die Boden- und Grundwasserverschmutzung zu einem weltweiten Problem. Einige Schadstoffe wie z. B. PAK können für Jahrzehnte oder Jahrhunderte im Untergrund bestehen. Um diese Probleme behandeln zu können, muss der Schutz des Grundwassers basierend auf der Quantifizierung potentieller Gefährdungen des zumeist unzugänglichen Untergrundes erfolgen. Risikoabschätzungen von Grundwasserverschmutzungen können jedoch durch die Anwendung prozess-basierter Simulationsmodelle erheblich unterstützt werden, die sich besonders im Hinblick auf Langzeitvorhersagen als hilfreich erweisen und nicht experimentell ermittelbar sind. Derart zuverlässige Vorhersagen können jedoch nur erhalten werden, wenn das verwendete Modellierwerkzeug als anwendbar bekannt ist.

Das Ziel dieser Arbeit bestand aus drei Teilen. Erstens wurde eine Quellstärke-funktion entwickelt, die das Ausbreitungsverhalten organischer Schadstoffe aus einer Punktquelle beschreibt und dadurch als zeitabhängige obere Randbedingung bei Transportmodellen dienen kann. Im Hinblick auf die allgemeine Anwendbarkeit dieser Funktion werden als Damköhler-Zahlen bekannte, dimensionslose Zahlen verwendet, um die Reaktion von Schadstoffen mit Feststoffen zu charakterisieren. Zwei Funktionen wurden abgeleitet und in ein Excel-Arbeitsblatt eingefügt, das ein praktisches Hilfsmittel bei der Quantifizierung des Freisetzungsverhaltens organischer Schadstoffe im Rahmen der Sickerwasserprognose darstellt. Der zweite Teil dieser Arbeit beinhaltet die Anwendung des prozessbasierten und mittels Laborexperimenten validierten Modellwerkzeugs SMART für Langzeitprognosen auf der Lysimeterskala anhand von Daten zweier Forschungszentren, FZJ (Jülich) und GSF (München). Ergebnisse reiner Vorwärtsmodellierungsläufe zeigten gute Übereinstimmungen mit den gemessenen Daten. Im dritten Teil wurden die erhaltenen Quellstärkefunktionen in Kombination mit dem SMART-Modell eingesetzt, um das Grundwassergefährdungspotential unter einer typischen Deponie in Kwabenya, Ghana, einzuschätzen. Die vorhergesagten Durchbruchszeiten nach einer Leckage in der Deponie betragen über 200 Jahre bei einer Betriebszeit von 30 Jahren. Unter Berücksichtigung des Schadstoffabbaus verursacht die Deponie somit keine Grundwasserverunreinigung im Rahmen der simulierten Szenarien und das SMART-Modell kann verwendet werden, um Schadstoffgrenzwerte für organische Schadstoffe in der Deponie in Kwabenya festzulegen.

Acknowledgements

Work for this study has been partly financed by the Bundesministerium für Bildung und Forschung (BMBF, grant 02WP0198 and IPS04/4P2) and published with the support of the Institute for Groundwater Management, Technische Universität Dresden.

I will like to express my profound gratitude to Professor Rudolf Liedl, my supervisor who has supported this study since the beginning of the journey and has demonstrated this by his constructive discussions. Many thanks to Professor Peter Grathwohl and Professor Peter-Wolfgang Gräber for their co-supervisory and review roles in the research work. Working under my Professors' supervision has brought my knowledge of Groundwater Management to levels of understanding far beyond my expectations. The remarkable leadership of my supervisors has inculcated in me a sense of professionalism, discipline in team work and friendship.

I am also grateful to the special assistance given to me by Professor Eberle in co-ordinating and providing data for the "Sickerwasserprognose" project. Special thank to all other Professors and Friends whom I have worked with in the Institute and who in various ways have contributed to my evolution as a professional. They contributed by providing a congenial atmosphere which made this scientific work much interesting than I anticipated.

Furthermore I am grateful to Mr. Dietze, Mr. De Aguinaga and Mr. Hope for their assistance in formatting and reading through this manuscript. Finally I am indebted to all my family members and all well wishers whose timely words of encouragement have always been a footstool.

Contents

SYMBOLS AND ABBREVIATIONS

Symbols

$1/n_{Fr}$	Freundlich exponent [-]
A	grain size [L]
A	cross-sectional area [L^2]
B(C)	degradation kinetics [$ML^{-3}T^{-1}$]
c	dissolved solute concentration in intraparticle pores...[ML^{-3}]
c_{max}	maximum dissolved solute concentration in intraparticle pores [ML^{-3}]
C	total mobile solute concentration [ML^{-3}]
C_0	initial solute concentration [ML^{-3}]
C_C	mobil particle concentration [ML^{-3}]
$C_{C,\,o}$	particle input concentration [ML^{-3}]
C_D	dissolved solute concentration [ML^{-3}]
C_D	dissolved solute input concentration [ML^{-3}]
C_{INP}	tracer in flow concentration [ML^{-3}]
C_I	observed tracer concentration [ML^{-3}]
C_{eqm}	equilibrium solute concentration [ML^{-3}]
C_{sat}	saturated vapour phase concentration [ML^{-3}]
C_∞	total mobile long-term concentration [ML^{-3}]
D	dispersion coefficient [L^2T^{-1}]
D_p	coefficient of molecular diffusion [L^2T^{-1}]
D*	hydrodynamic dispersion coefficient [L^2T^{-1}]
D_{mec}	coefficient of molecular diffusion [L^2T^{-1}]
D_a	Damköhler number [-]
$D_{a,bio}$	Damköhler number for biodegradation [-]
D_{a1}	the ratio of mass transfer rate to advection [-]
D_{a2}	the ratio of biodegradation rate to advection [-]
D_{a3}	the ratio of biodegradation to mass transfer rate [-]
$D_{a,des}$	Damköhler number for desorption [-]
D_e	effective diffusion coefficient [L^2T^{-1}]
D_{app}	apparent diffusion coefficient [L^2T^{-1}]
D_{eff}	effective diffusion coefficient [L^2T^{-1}]

F	mass flux into soil grain $[ML^{-2}T^{-1}]$
F_{max}	maximum mass flux into soil grain $[ML^{-2}T^{-1}]$
f_{oc}	fraction of organic carbon [-]
$g(\tau)$	PDF of travel times $[T^{-1}]$
$g_{matrix}(\tau)$	PDF of travel times in matrix region $[T^{-1}]$
$g_{pref}(\tau)$	PDF of travel times in preferential flow region $[T^{-1}]$
j	diffusive flux $[ML^{2}T^{-1}]$
k_j	particle j deposition rate coefficient $[T^{-1}]$
k_{LH}	Langmuir-Hinshelwood parameter [-]
K_f	unsaturated hydraulic conductivity $[LT^{-1}]$
K	maximum substrates concentration $[T^{-1}]$
Ks	half saturation constant $[ML^{-3}]$
K_o	kinetic reaction rates $[T^{-1}]$
k_{oc}	distribution coefficent standardised on the content of organic carbon $[L^{3}M^{-1}]$
K_d	partitioning coefficient between contaminant and soil matrix $[L^{3}M^{-1}]$
$K_{d,c}$	partitioning coefficient between contaminant and particles $[L^{3}M^{-1}]$
K_{Fr}	Freundlich coefficient $[(MM^{-1})(ML^{-3})^{-1/nFr}]$
K_L	Langmuir sorption coefficient $[L^{3}M^{-1}]$
K_T	affinity parameter [-]
l	diffusion length [L]
M_{diff}	contaminant mass within soil grain [M]
M_p	mass of particle [M]
M_s	solid mass [M]
n	degradation order [-]
n_e	effective porosity [-]
n_{ip}	intraparticle porosity [-]
p	number of particles [-]
P_c	particle dry solid density [-]
PV	pore volume [-]
r	radial coordinate [L]
R	retardation factor [-]
RT	residence time [T]
S_{matrix}	ratio of sorbed solute mass per unit mass of soil matrix [-]

S_{cm} ratio of sorbed solute mass per unit mass of mobile particle [-]

S_{cim} ratio of sorbed solute mass per unit mass of immobile particle [-]

s substrate concentration [ML^{-3}]

S_w degree of saturation [-]

t time [T]

t_l observed tracer travel time [T]

$T_{1/2}$ half life [T]

v pore water velocity [LT^{-1}]

Q Darcy flow [L^3T^{-1}]

q specific flux [LT^{-1}]

q_s solid phase concentration [ML^{-3}]

M/A solid mass per unit cross sectional area [ML^2]

W/F water – solid ratio [L^3M^{-1}]

v_{matrix} flow velocity in matrix region [LT^{-1}]

v_{pref} flow velocity in preferential flow region [LT^{-1}]

x vertical coordinate [L]

X_b biomass concentration [ML^{-3}]

Greek symbols

α volume fraction of preferential flow [-]

α* characteristic mixing length [-]

β contaminant mass ratio not subject to particle-facilitated transport [-]

β_T heterogeneity parameter [-]

ε porosity [-]

θ water content [-]

λ degradation rate [T^{-1}]

λ’ modified degradation rate [T^{-1}]

ρ solid density of soil matrix grain [ML^{-3}]

ρ_b bulk density of soil matrix [ML^{-3}]

ρ_c solid density of particle [ML^{-3}]

ψ matrix potential [L]

τ travel time of a conservative tracer [T]

τ_a travel time of a conservative tracer in homogeneous soils [T]

$\bar{\tau}$	mean travel time of a conservative tracer [T]
ζ	tortuosity factor [-]
σ_c	volume of the immobile particle per unit volume [-]
Γ(τ,t)	reaction function [-]

Abbreviations

AMA	Accra Metropolitan Authority
2,4-D	2,4-Dichlorphenoxyacetic
BBA	Richtlinie fur die Priifung von Nagetierbekampfungsmitteln gegen Wanderratten
BBodSchV	Bundes-Bodenschutz- und Altlastenverordnung
BESSY	Batch Experiment Simulation System
BMBF	Bundesministerium für Bildung und Forschung
BMU	Federal Ministry for Environment, Nature Conservation and Nuclear Safety
BTC	Breakthrough Curve
DCE	Dichlorethylene
CDE	Convection-Dispersion Equation
CDE	Convection-Dispersion Equation
CLT	Convective Lognormal Transfer function model
DDT	Dichloro-Diphenyl-Trichloroethane
NAPL	Non Aqueous Phase Liquid
DNAPL	Dense Non Aqueous Phase Liquid
DND	Damköhler number distribution
ETFM	Extended Transfer Function Model
FAO	Food and Agricultural Organization
FD	Finite Difference
GRACOS	Groundwater Risk Assessment at Contaminated Sites
GLEAMS	Groundwater Loading Effects of Agricultural Management System
GTFM	Generalised Transfer Function Model
GWN	Groundwater flow rates
IPD	Intraparticle diffusion
LEA	Local Equilibrium Assumption

MOC	Method of Characteristics
PAH	Polycyclic Aromatic Hydrocarbons
PCE	Perchloroethylene
PDF	Probability Density Function
PERMO	Pesticide Leaching Model
PFM	Piston Flow Model
PRZM	Pesticide Root Zone Model
P4	Point of Compliance
PV	Pore Volume
RIZA	Rijksinstituut voor Integraal Zoetwaterbeheer en Afvalwaterbehandeling (Institute for Inland Water Management and Waste Water Treatment)
RTD	resident time distribution
SMART	Streamtube Model for Advective and Reactive Transport
SOM	Soil organic matter
TCE	Trichloroethylene
TDR	Time Domain Reflectometry
TOC	Total Organic Carbon
TVD	Total Variation Diminishing
VARLEACH	Variable Leaching
VOC	Volatile Organic Compounds
SVOC	Semi Volatile Organic Compounds

LIST OF FIGURES

LIST OF TABLES

Chapter 1

1 INTRODUCTION

1.1 Motivation

The quests for human survival and quality of life have led to enormous anthropogenic activities on the environment. Many soils and groundwater have therefore been adversely affected due to the proliferation of chemical industries and mechanised and fertilised agriculture. These environmental concerns could become a menace to posterity if left unchecked. Most of these contaminants diffuse through the soil, vadose zone and eventually into the aquifers. The contaminants are numerous and their sources of contamination are many. Common chemicals such as trichloroethylene, 1,1,1-trichloroethane, tetrachloroethane, benzene and carbon tetrachloride used in industries as solvents have been found in many multiple sources. (Fusillo, Hochreiter, and Lord 1985). The use of fertilisers and septic tanks discharges have resulted in high levels of nitrate concentration in groundwaters (Flipse et al. 1984). Mechanised agriculture areas have further compounded the problem of groundwater contamination (Pionke and Urban 1985). Moreover the use of specialised synthetic organic chemicals have also increased contamination. (Rothschild et al.,1982). Engineered landfills in rural and urban areas have also been well reported of causing contamination (Noss and Johnson 1984; McLeod 1984). Many leakages have also occurred in Petroleum underground storage tanks (Krammer 1982, Oliver and Saitar 1985). The extent of contamination depends on the nature of the contaminant and hydrogeology of the area. Most of the contaminants occur in nature as either point sources or distributed sources. Examples of point source contamination are municipal waste sites (landfill), industrial discharges, leaks and spills, leaks from underground storage tanks containing solvents, brines, gasoline and heating fuels, snow dumps, spillages during road and rail transport of chemicals and stockpiles of raw materials and industrial waste. Distributed sources occur as a result of effluent from latrines and cesspits, leaking sewers and septic tanks, oil and chemical pipelines, lawn, garden and parkland fertilisers and pesticides, road de-icing chemicals, oil and grease from motorised

vehicles, wet and dry deposition from smoke stacks and fill material containing construction waste.

In a bid to address these concerns, the problem of groundwater contamination must be addressed holistically. The United Nations in its report for sustainable development pointed out the accelerated degradation of groundwater systems through pollution of aquifers, the economic implications of not balancing groundwater demand and supply management and the lack of public awareness about the importance of groundwater resource management (International Water and Sanitation Center, 2003). The European community fifth framework program, Energy, Environment and Sustainable development called for guidelines for groundwater risk assessment at contaminated sites (GRACOS research project). The European Landfill Directive (Council Directive 1999/31EC, 1999) also called for the provision and protection of the environment, soil and groundwater from the adverse effects of toxic pollutants. In Germany about 74 % of the source of drinking water is from groundwater (Federal Ministry for Environment, Nature conservation and Nuclear safety (BMU) report, January 2006), hence the sustainable use and protection of groundwater is crucial. The German BMBF issued a research initiative ”Sickerwasserprognose” which involved an extensive research work. The main objective of this research activity is to propose a method that can reliably predict the concentration and mass of pollutants at the point of compliance, i.e. at the groundwater table, in accordance with the German Soil Protection Act (BBodSchV, 1998). One major item of “Sickerwasserprognose” is the model-based prediction of groundwater pollution. Corresponding tools have to account for all relevant processes, which are responsible for a decrease (sorption, biodegradation) or an increase of groundwater pollution risk (particle-facilitated transport, preferential flow). For organic contaminants, recent studies on these processes and process interactions have been done, e.g., by (Rahman 2002), (Cata 2003), (Schmidt 2003), (Bold 2004), (Cai 2004), (Christ 2004), (Henzler 2004), (Madlener 2004), and (Susset 2004). Most of these authors used the modeling software SMART (Streamtube Model for Advective and Reactive Transport). So far, all SMART applications were limited to laboratory scale problems, i.e. relying on data which have been obtained under fully controlled conditions. In this thesis quantification and predictions at the lysimeter scale are studied for conservative and reactive transport under unsaturated conditions.

1.2 Objective and justification of the thesis

Among the persistent contaminants in the environment are organic pollutants such as polycyclic hydrocarbon compounds. Quantifying and predicting contamination at the groundwater table is therefore necessary to assess the potential threats to pollution. The objectives of the thesis are:

(1) to determine a source strength function for the quantification of the possible temporally variable discharge behaviour of organic pollutants from point sources of pollutant,

(2) to quantity the discharge behaviour for proper control and management of polluted sites, and its associated effects on underground waters,

(3) to simulate the ageing of the source by time dependent modelling which would eventually aid in developing remediation strategies for the control of the pollutants,

(4) to determine the temporal change of the pollutant concentration in the seepage water at the transition from the pollutant source to the transport zone,

(5) to simulate transport and reactive processes by using the source strength function as a time-dependent upper boundary condition for pollutants migrating to the ground-water level (point of the compliance),

(6) to quantify the fate of organic pollutants such as Polycyclic Aromatic Hydrocarbons (PAHs) at the lysimeter scale,

(7) to demonstrate the predictive capabilities of the reactive transport model, SMART at the lysimeter and field scales,

(8) to predict the longterm contaminant breakthroughs at the outlet (an index of groundwater table) of lysimeter data from Jülich and GSF-München research centers,

(9) to predict the fate of PAHs at a field scale landfill at Kwabenya in Ghana.

1.3 Structure of the thesis

The primary topic of this thesis is long term process based modelling of organic non-volatile compounds at the lysimeter scale and the scenario based modelling of the Kwabenya landfill in Ghana. Chapter 1 gives the problem statement, aims and justification of the thesis. In chapter 2 the general overview of non-volatile organic compounds, especially PAHs, is discussed. The application of lysimeters in the environment and solute transport are also reviewed. Chapter 3 presents the methodology, description of the important processes triggering the migration of contaminants in the vadose zone. Some of the existing analytical and numerical methods are given. Moreover, Damköhler numbers, which are used to quantify the relative importance of the major source and transport processes, are also discussed. In addition, the main model SMART, which was used throughout this work is discussed in detail. Chapters 4 deals with the derivation and identification of source term functions to describe the leaching behaviour of organic pollutants. Again Chapter 4 discusses how the contaminant is modelled at the source zone, the use of regression analysis for the derivation of a source term function which could be used as a time-dependent upper boundary condition for ensuing pollutants migrating to the transport zone. Rosen's analytical solutions which show the proximity of the numerical solutions are also introduced. Chapter 5 is dedicated to the longterm modelling of lysimeter data. Chapter 5 also discussed the preparation and analysis of the input data needed for the transport modelling of the Jülich and München lysimeters. Uncalibrated forward model results are compared with the observed lysimeter data in the short term. Based on the relevant processes in the transport zone, the long term fate of the contaminants at the lysimeter outlets (a representation of the point of compliance between the saturated and unsaturated zone) is predicted. Chapter 6 presents the application of the derived source term functions and SMART to a proposed field scale landfill at Kwabenya, a sub urban town in Ghana. Again Damkökler numbers are exploited to elucidate the major driven processes. Summary and conclusions of this thesis are given in Chapter 7.

Chapter 2

2 CONTAMINANTS IN THE ENVIRONMENT

2.1 Types of contaminants in the environment

Different types of contaminants occur in groundwater depending on the type of site and the site activities. The following groups of contaminants may be identified:

1. Halogenated and non halogenated VOCs: They are hydrocarbon compounds that evaporate readily at room temperature and are usually found at locations including burn pits, chemical manufacturing plants and disposal areas such as marine sediments, disposal wells and leach fields, landfills and burial pits, leaking storage tanks, dry cleaning shops, pesticide and herbicide mixing areas, solvent degreasing areas, surface impoundments, and vehicle maintenance areas. Halogenated VOCs have a halogen (fluorine, chlorine, bromide, iodine) attached to it while non halogenated VOCs are without a halogen. Examples of such compounds include 1-Chloro-2-propene Carbon tetrachloride, Hexachlorobutadiene, 1,1-Dichloroethane, Vinyl chloride, Chloroform, ethanol and vinyl acetate.

2. Halogenated and non halogenated SVOCs: They are semi volatile organic compound that have boiling points above 200 ^{o}C. They are usually found in sites such as wood preservation sites in addition to the sites stated above. Examples of these compounds are Benzedrine, benzoic acid, isoprophorone, anthracene, naphthalene, pyrene and phenanthrene. Pesticides such as andrin, chlordane, Malathion and DDT form a subgroup of halogenated SVOCs.

3. Fuels: They are a group of chemicals produced by refining and manufacturing of petroleum or natural gas to generate heat and energy in combustion processes. Sites where fuel contamination may be found include aircraft, storage and service areas, and solvent degreasing areas and in addition to those locations mentioned above. Most of the non halogenated VOCs and / or SVOCs are also fuels. Typical fuel contaminants encountered at many sites

include creosol, phenol, toluene, fluorine, fluoranthene, naphthalene, propane and benzene.

4. Metals and metalloids: Metals are usually hard, with high melting point and electrical conductivity. They heat well while metalloids are usually semi conductors whose properties are between metals and non metals. They are usually found at electroplating and metal finishing shops, landfills and burial pits, paint striping and sand blasting areas. Metals and metalloids contaminants include mercury, lead, chromium, cadmium, nickel, zinc and arsenic.

5. Explosives: They are usually chemicals produced as explosive and repellents. They are usually located in contaminant sites such as marine sediments, disposal wells, leach fields, landfills and burial pits. Examples are nitroaromatics, trinitrobenzenes, picrates, nitrocellulose TNT and 2, 4-DNT (2, 4-Dinitrotoluene) Nitroglycerine (EPA Roadmap, 2005).

2.2 The behavior of polycyclic aromatic hydrocarbons in the environment

PAHs in the environment are a large group of compounds with a similar structure comprising two or more benzene or other aromatic hydrocarbon rings with carbon and hydrogen atoms only. They are formed through incomplete combustion of carbon compounds. The unmeticulious use of petroleum and charcoal products leads to the input of aromatic hydrocarbons into the environment. PAHs vary with respect to sources, chemical and physical characteristics and are predominantly found in particulate phase under ambient conditions (UBA, 1998). Concern over PAH emissions relates to their health effects. With a view to the amount and the size of the contaminated sites the largest potential risk for groundwater contamination emerges from coking plants and gas industry. PAH containing tar oils can be DNAPL which can sink to the bottom of the aquifer. Laboratory experiments have shown that the desorption of PAH from soils occurs very slowly. At times the adsorption of PAH on coal particles is very strong. They can form a long term contamination source with contaminations which could persist for centuries.

Aromatic hydrocarbons belong to the most important ground water contaminants with very slow degradation tendencies leading to the formation of long contaminant plumes and pollutant transport over long distances. Such processes endanger the drinking water supply in many areas. Diffuse emissions through combustion of coal or gasoline cause a widespread pollution of air and soil, especially close to main traffic roads, and massive punctual contaminations due to spills during transport and at sites of storage and refinement of petroleum and coal products. When large amounts of aromatic hydrocarbons enter environments with limited oxygen supply such as aquifers. This slows down the degradation of aromatic compounds so that long pollutant plumes are transported in aquifers endangering drinking water supply in many areas. Other natural sources also exist in the environment. Anaerobic bacteria produce benzene and toluene during fermentation of aromatic aminoacids (Jüttner and Henatsch, 1986; Jüttner, 1988; Fischer-Romero et al., 1996). Certain termite species use naphthalene to fumigate their nests (Chen et al., 1998). Moreover incomplete combustion of organic materials also produces polynuclear aromatic hydrocarbons, for instance when forest fires occur (Hirner et al., 2000). However, it has also been shown that degradation of petroleum products in the subsurface can lead to alteration of oils which may have ecologic implications (Aitken et al., 2004).
Modelling PAHs could therefore help in formulating risk assessment principles which can lead to management practices that would ensure the safety of drinking water.

2.3 Lysimeters

Lysimeters are field devices containing a soil column and vegetation, used for measuring actual evapotranspiration. (Fetter, 2005). They may also be defined as containers with a given soil volume and depth. They are either filled undisturbed or disturbed, installed plane to the surface and are used to collect seepage water (drainage/leachate) which is gained by means of different methods at the lysimeter bottom (Lanthaler, 2004). Depending on functions and characteristics such as the soil size and fractions, weighability, the soil filling techniques and the vegetation cover, lysimeters may be grouped according to the following types: weighable and non weighable lysimeters, monolithic lysimeters, groundwater lysimeters and large lysimeters. According to (Muller, 1996) the term lysimeter originated from the Greek words “lusis” meaning solution and “metron” meaning measure. Originally it was designed to measure soil leaching (Kutilek and Neilsen, 1994) but due to the

increase of pollution and groundwater contamination (BAL, 1993) in the last decades, it has been applied in the field of research studies such as soil hydrology, hydrogeology, water economy, agriculture and forest economies, ecology and environmental protection. The FAO applied it to study crop water balance and evapotranspiration (FAO, 1982). In many European currents lysimeters have been used for registration of plant protection products and research purposes (Hance and Führ, 1992). For instance the German pesticide testing guidelines (BBA, 1990) were established for the registration and regulation of lysimeters in Germany. This has provided many local authorities and decision makers with a tool for the idenfication of vulnerable areas where specific monitoring actions and preventive measures for the protection of water could be studied. Though an ideal lysimeter may not exist (Seeger et al. in Böhm et al. 2002), lysimeter contribution to the risk assessment of groundwater is enormous. The concentration measured at the bottom of lysimeters, filled with one or more soils representative of the local territorial could be used as an index of risk for groundwater even though contaminant transport may vary between the field and the lysimeters (Bergström and Jarvis, 1994). Moreover they enable a close mass balance of contaminants in soils.

2.4 Modelling at the lysimeter scale

Modelling has become an integral part of water management and research in the field of water science and agric economy. Many models have been developed for different purposes and scales. In this section the application of models to contaminant leaching is discussed. Tracer investigation and numerical modelling in lysimeters on the movement of water and solids from the surface of the soil through the un-saturated and saturated zones of an aquifer enable to quantitatively predict the impact of different measures on to the whole subsurface system. Many single component and multicomponent analytical and numerical models have been developed to simulate and predict water and leaching behaviour of solutes in the unsaturated zone and the water table through lysimeters.

The following models though not used in this work are discussed briefly due to their comparative usage to the model SMART 2200 (Finkel, 1999) that was used: GLEAMS (Leonard et al., 1987 and Rekolainen et al., 2000b), PELMO 2.02 (Klein et

al., 2000), PRZM-2 (Trevisan et al., 2000), VARLEACH (Trevisan et al., 2000), SIMULAT 2.3 (Aden and Diekkrüger, 2000), MACRO 3.1 and 4.0 (Jarvies et al., 2000), WAVE (Vanclooster et al., 2000a) and LEACHP (Dust et al., 2000). Details of the models may be seen in the attached references. All the models were applied as 1-D flow with no horizontal components to lysimeter data sets. They are deterministic and process based and have the potential to predict without calibration. The main medium by which contaminants flow is by waterflow hence a proper description is necessary. Two main approaches were identified. In the first four models, a simple capacity approach was used in which drainage only occurs above a user specified soil water content without considering hydraulic gradients. This makes those models weak to circumvent upward fluxes and groundwater tables. In the last four models (SIMULAT, MACRO, WAVE and LEACHP), water flow is described by the Richards equation in which hydraulic gradients and hydraulic conductivity function describe the water flow. Contaminant transport is evaluated by convection, i.e. taking the product of the soil water flux and chemical concentrations for the first four models. The rest which are more physically based, involve the hydrodynamic dispersion and molecular diffusion coefficients and solve the convection-dispersion equation (CDE). Such description usually encounters numerical dispersion due to the choice of correct combination of layer thickness (spatial discretization) and time steps. All the models considered reversible and equilibrium sorption processes. The models GLEAMS, PRZM2, VARLEACH, MACRO and WAVE considered linear sorption which requires a combination of fraction of organic content (foc) and distribution coefficient between organic matter or organic carbon and soil matrix (Koc) or linear distribution coefficient (Kd), while the models PELMO, SIMULAT and LEACHP took into account non linear Freundlich sorption which requires an extra parameter, the Freundlich exponent, n, to describe the nonlinearity of the isotherm. All the models took into account first order degradation. Parameters such as degradation rate or degradation half life to depends on depth of soil profile, soil water content and temperature were described. With the exception of the model SIMULAT, all the models considered contaminant (in this case pesticides) passive uptake by plants which calls for the inclusion of a concentration stream factor to cater for selective uptake. Only the LEACHP model considered gas phase and surface volatilization based on Henry's law. The model HYDRUS-1D 3.0 (Simunek et al., 2005) has recently also been used by Concalves et al. (2006) to analyse water flow and multicomponent solute transport in three soil

lysimeters irrigated with different water quality to evaluate salinization and alkalinity risk. The model solves the Richards equation by taking into account variably saturated water flow and different forms of the convection-dispersion equation that takes into account solutes, carbon dioxide and heat transport. Additionally the flow equation includes a sink term that deals with water uptake by plant roots. Models such as HYDRUS-2D, 3D (Sansoulet, 2006) and SiWaPro-1D, 2D (Kemmesies, 1999) perform similar functions of flow and transport as described above.

SMART is the Streamtube Model for Advective and Reactive Transport that takes into account most of the major processes that lead to the contamination or leaching of solutes from the soil to the groundwater table. Processes considered in SMART are advection, sorption/desorption (equilibrium and kinetic), biodegradation, particle facilitated transport and preferential flow. Details of model conceptualization and numerical implementation are given in section three.

2.5 Conceptual Scheme: separated and integrated approaches

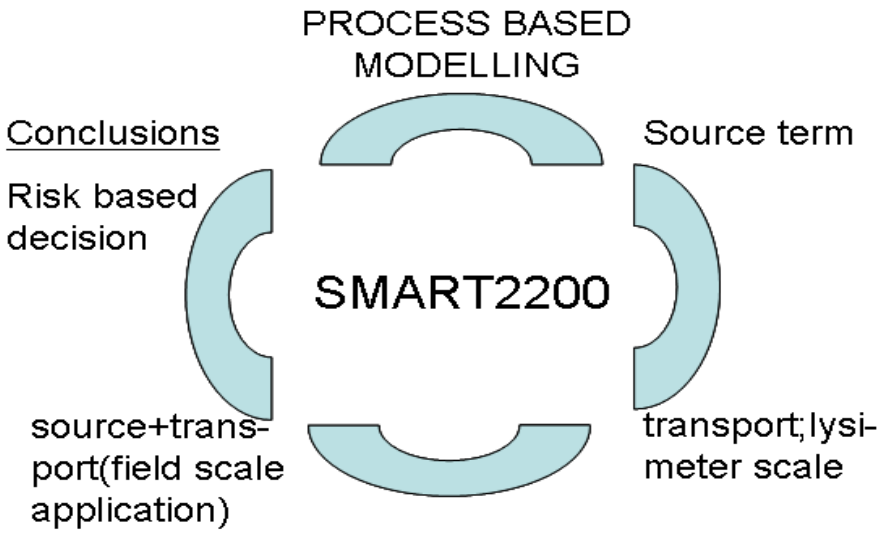

Fig. 2.1: Scheme of work

The figure 2.1 above puts the process based modelling of this study in three perspectives.

1. The development of a source strength function which could predict the behaviour of non volatile organic pollutant leaching at the basement of a source zone.
2. The quantification and prediction of contaminants at the outlet of a lysimeter over a long period. The outlet of the lysimeters could serve as good index of risk for groundwater providing the local authorities and the decision makers with a tool for the identification of the areas at risk of pollution, where specific monitoring actions and prevention measures for the protection of waters can be studied (Francaveglia et al., 2000).
3. A scenario based modelling of a typical landfill in Ghana which extends the model tool SMART into field scale applications.

After applying SMART through this cycle, the model tool which has been tested and validated at the laboratory scale (Bold, 2004) would have been employed as well up to the field scale, the ultimate aim of groundwater risk assessment.

The source strength function was achieved through scenario based modelling considering major processes such as advection, desorption kinetics and biodegradation and the use of Damköhler numbers to quantify the relative importance of each of the processes. Usually laboratory experiments are performed to quantify the contaminant release at the base of a source zone. For instance, Susset (2004) described the assessment of groundwater risk due to pollutant emission from contaminated soils through leaching column tests. But laboratory experiments may not last long enough to establish equilibrium between the solutes and the soil matrix. This may lead to lower concentration measurements. However the expected maximum concentration released could be achieved through longterm modelling. For this purpose the model assumes steady state release with no ageing of the pollutant source.

The second objective is achieved through transport modelling.
Figure 2.2 shows the procedure of groundwater risk assessment through the use of lysimeters. The lysimeter cross section shows a pile of contaminated material on top

of an undisturbed transport layer of porous medium with measuring instruments such as tensiometers, temperature sensors and TDR probes. The plot on the right of figure 2.2 depicts the increase of contaminant concentration in seepage water at maximum mass flux, F_{max} (non equilibrium) until a maximum concentration C_{max} is reached. Maximum concentration is established when equilibrium occurs during desorption and dissolution from residual phase. A decrease in concentration in the seepage water further down the transport distance occurs due to biodegradation. Mean contaminant concentrations rather than total compositions of the contaminants are quantified at the base of the lysimeter through forward modelling involving all the relevant processes. Not only is the inaccessibility of the point of compliance a problem but also the contaminant compositions are highly variable and depend on local conditions. Hence the uses of mean breakthrough concentrations give a better estimate than extreme values of concentration (Grathwohl and Susset, 2001).

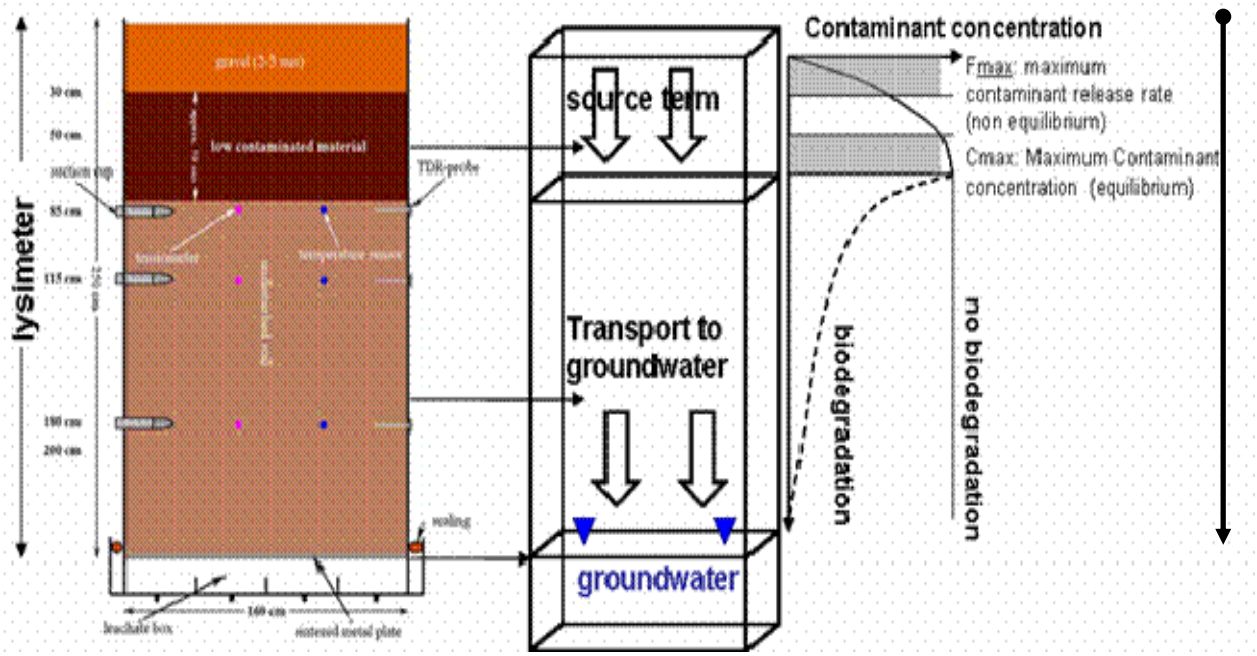

Fig. 2.2: Left, a cross section of a test lysimeter. The figure in the middle shows contaminant quantification procedure of the lysimeter which is separated into source term and transport term material and measurements. The diagram shows maximum concentration build up during desorption and a decrease in the seepage water after a long transport distance due to biodegradation.

Figure 2.3 below shows a typical concentration profile of a scenario based modellling of a typical landfill in which the source zone contamination is depleting into the unsaturated transport zone. In the integral approach, the source zone and the transport zone are modelled together as a single unit. In the separated approach, the concentration at the bottom of the source zone is taken as the upper boundary condition of the transport zone. The concentration profile in Fig. 2.3 shows the extent of kinetic interactions within the system but not due to dispersion. For this thesis the integral approach was not used but rather the application of the source strength function as upper boundary condition for solute spreading in the transport zone modelled with SMART.

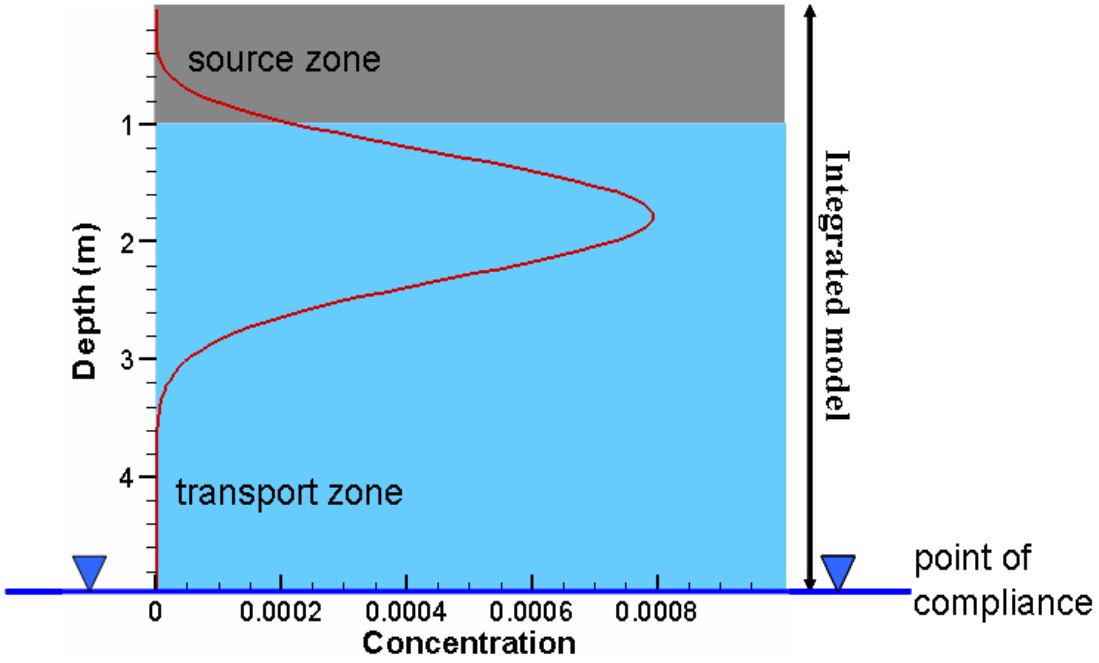

Fig. 2.3: A concentration profile showing the source and transport zones of a landfill.

Chapter 3

3 METHODOLOGY : PROCESS BASED MODELLING

A model may be defined as a selected simplified version of a real system, which approximately simulates the latter's excitation-response relations that are of interest. A system includes the domain and phenomena that take place within the domain (Bear, 2001). In modeling the reality is simplified but not reproduced. In recent times models are increasingly applied in water management and research to predict the responses of systems.

3.1 Modelling approaches

Model approaches differ depending on the nature of problem being addressed, data needs and other complexities involve. According to (Addiscott and Wagenet, 1985) models may be classified as deterministic or stochastic, mechanistic or functional, and numerical or analytical. Also other approaches could be based on spatial scale (pore scale or global scale), temporal scale considerations (instantaneous or decades), level of complexity (scientific or decision making) and level of integrity (holistic or reductionistic)

Indeed the scope of modelling could be very wide. According to Figure 3.1 below, which was adopted from the STOWA/RIZA (1999) report, the approaches could be seen from two extremes with different degrees of combinations in between. Firstly, models can be fully data oriented (based on measurements from the field). An example is the Archydro data model by Maidment (2003) which provides a standardized framework for storing information. And secondly, fully process oriented models follow a deterministic approach based on physical processes. Here the physical processes are assumed to be known and stored in the model in a form of equations. The ensuing parameters in the equations are supplied in the form of time series. For instance, the SMART (Finkel, 1999) model used in this thesis contains routines to simulate hydrologic solute transport processes. Usually many models consist of a combination of these two extremes.

Neural networks approaches establish an empirical relationship between cause and effects. A correlation is therefore derived between the input and output data sets through the process of calibration so any needed future output could be predicted for new available input data sets. In soft hybrid model approaches, physical processes such as conservation of equations are included in the modelling in addition to the input-output data based calibration. Numerical models with data assimilation rather focus on physical process knowledge and integrate the data about the physical processes in such a way that both the data and process description are accounted for explicitly.

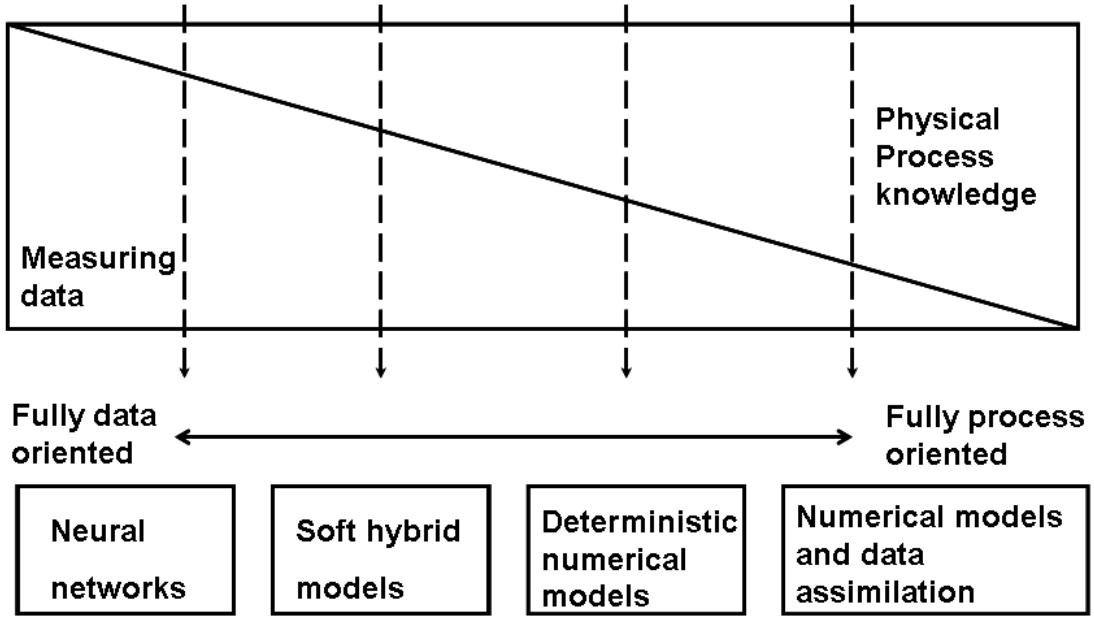

Fig. 3.1: Modelling approaches (adopted from STOWA/RIZA Good Modelling Practise report, 1999)

3.2 Modelling of Solute Transport in Porous Media

Figure 3.1 above shows clearly the extent of modelling approaches applied in water and solute transport through porous media. Most of the models differ in the underlying model concept and partial differential equations describing the system. Flow and solute transport in the vadose zone have been simulated with models such as FEFLOW (Diersch, 2002), HYDRUS (Simunek et al., 1998) and MACRO (Jarvis et al., 2000). Water flow in the vadose zone is usually described by the Richards equation (Richards, 1931). Neglecting the flow of air for simplification purposes the Richards equation is given in 1-D form as:

$$\frac{\partial \theta}{\partial t} = \frac{\partial}{\partial x}\left[K_f(\psi)\left(\frac{\partial \phi}{\partial x}\right)\right] \qquad 3.1$$

where θ is the water content [-], t is the time [T], ψ is the matrix potential [L], $K_f(\psi)$ is the unsaturated hydraulic conductivity [LT^{-1}] at given ψ, ϕ is the total soil-moisture potential [L] and x [L] is the spatial coordinate corresponding to the vertical direction and oriented positively downward. The unsaturated hydraulic conductivity $K_f(\psi)$ could be estimated by Van Genuchten (1980) parameters based on the soil properties.

Depending on the assumption of solute movement, many approaches exist as mentioned in section 2.4. Four of such solute transport approaches are further briefly described.

1. The conversion dispersion equation (CDE) (van Genuchten and Wierenga, 1976) : Solute transport in 1-D steady flow field may be described by

$$\frac{\partial C_D}{\partial t} = D\frac{\partial^2 C_D}{\partial x^2} - vC_D \qquad 3.2$$

where C_D is the dissolved solute flux concentration [ML^{-3}], v is the flow velocity [LT^{-1}] and D is the hydrodynamic dispersion coefficient [L^2T^{-1}]. The CDE assumes perfect mixing of solute in the lateral direction. The solute movement is driven by pore water velocity variations. Various representation of the velocity variations in the 1-D CDE

have been developed by Parker and van Genuchten (1984) and Bresler and Dagan, (1981).

2. Convective Lognormal Transfer function model (CLT) : Solute transport is represented by the use of transfer functions in which system output flux are described as a function of the input function. Using the idea of probability density functions to describe the distribution of transport times from the inlet to the outlet and the concept of stochastic convection transport, transfer functions are generated to characterise the solute transport processes (Jury, 1982; White et al., 1986; Jury and Scotter 1994). CLT assumes that the travel time of solute molecules is a linear function of transport distance without lateral mixing. This assumption may however be insufficient in complex soil settings to describe the movement to solute through the porous media. The CLT which is based on stochastic convective transport has been shown by field experiments to predict solute transport well at the first 3 m of the top soil. The predictions were however poor at deeper depth where layering occurred (Butters et al. 1989; Roth et al. 1991). Nonetheless Zhang (1995) and Jacques et al. (1998) compared solute transport results of CLT and CDE using column data and field experiments respectively and came to a conclusion that the CLT gives better predictions than CDE.

3. Extended Transfer Function Model (ETFM) (Lui and Dane, 1996): The model described the concept of partial mixing with a changeable constant which represents the level of horizontal mixing and an extension of the transfer function models. Its range of applicability is between the CDE and CLT as described in points 1 and 2. The model is however restricted to characterizing solute transport described by either a quadratic or linear increase in the solute travel time in a steady state flow field with depth.

4. Generalised Transfer Function Model (GTFM) (Zhang, 2000): In heterogeneous media, effective transport parameters such as dispersive coefficient, D, and average linear water velocity, v, can be applied to the macroscopic mean transport equations to describe the solute movement (Gelhar and Axness, 1983). The CDE in this case assumes a Fickian mixing (high degree) within flow paths. The PDF of travel time by an impulse input follows the so called Fickian PDF (Jury and Roth, 1990). The GTFM

describes solute transport processes in heterogeneous media similar to the CLT but with two additional parameters which characterise the depth dependency of the mean and standard deviation of the logarithmic travel time. The GTFM can describe or predict not only the models described in points 1, 2 and 3 above but can also characterise solute transport in heterogeneous media in which changes in the soil moisture content and pore water velocity causes the mean travel time to increase with depth non-linearly. Moreover it is applicable to heterogeneous systems in which the scale dependency of the dispersivity to the travel distance results in a power law (Zhang et al., 2000).

3.3 Eulerian and Lagrangian numerical solutions

Many solutions have been developed to solve solute transport equations such as 3.2. Several analytical solutions exist that can solve the equations with different level of simplified boundary conditions. For instance (Ogata and Banks, 1961; Ogata, 1964; Thomann and Mueller,1987; O'Loughlin and Bowmer, 1975; Rose, 1977; Runkel, 1996) solve the CDE equation under steady state and spatially constant model parameters with simplified boundary conditions. The transport equation could therefore be solved numerically when other arbitrary boundary and transient conditions with distributed model parameters are considered. Solution methods normally employed in solving the CDE are Finite Difference (FD), Finite Element (FE), Total Variation Diminishing (TVD), Random Walk (RW) and Method of Characteristics (MOC). Two of such numerical model approaches are discussed.

1. Eulerian Approach: This approach considers changes in fluid properties or the rate of change of the fluid motion such as the orientation of non spherical distribution at a fixed point in the fluid mesh. The mesh therefore presents a fixed reference frame. It is therefore applied when fixed sampling or predictions are made in space and time. The set of concentration distributions can be described by the Fokker-Planck ordinary differential equation which reduces to the convective diffusion equation under conditions of dilute suspensions (Adamczyk et al., 1983; Jia and Williams, 1990; Peters and Ying, 1991). Examples of application are flow and diffusion equations.

The Eulerian approach is more responsive to analytical approximations and numerical solutions than the Lagrangian approach. The FD, FE and TVD solution

techniques are all based on the Eulerian approach. The model tool MT3D (Zheng 1990; Zheng and Wang, 1999) includes Eulerian approaches to predict concentration of conservative solutes at any time in space. Its FD scheme is efficient, convenient and produces good mass balances but may lead to either over prediction in source concentration or prediction of negative concentrations in contaminant flow processes in which advection dominates. It also has the disadvantage of introducing computational errors in algorithms which leads to numerical dispersion that cannot be separated from physical dispersion. Results from the FD approach can be improved by using smaller time steps and grid size. However the required computational effort may restrict the fine discretization.

2. Lagrangian Approaches: They describe the trajectories of single particles encroaching a collector surface. This approach considers changes in the fluid properties as the fluid moves along a trajectory. The mesh is therefore deformed or moves with the fluid in a fixed grid. It is mostly applied when the evolvement of a solute in space is predicted. It is governed by the Newton's second law and leads to the Langevin-type equation when combined with Brownian motion (thermal random force), the solution of which produces stochastic trajectories (Gupta and Peters, 1985; Russel et al., 1989; Ramaro et al., 1991). An example is the pure advection (without dispersion) equation. The model tool SMART (Finkel et al., 1999; Finkel, 1999) uses the Lagrangian approach to track the trajectory motion of conservative parcels of solute in an Eulerian steady state flow field. The heterogeneous model domain was discretised along flow paths by the travel time of the conservative solute. It is perfectly applied in pure advective processes but becomes complex when other processes such as dispersion, sources are involved in a heterogeneous medium.
In order to reduce numerical problems, overshooting and/or undershooting of source concentrations, a mixture of the Eulerian and Lagrangians approaches may be used. Examples of such solution options are Method of Characteristics, Modified Method of Characteristics and Hybrid Method of Characteristics (Zheng 1990; Zheng, 1996).

3.4 SMART

The numerical code SMART (Streamtube Model for Advective and Reactive Transport) was developed by Finkel (1999) a the Centre for Applied Geosciences, Universität Tübingen. It is based on the Lagrangian approach of describing flow paths by the use of probability density functions (PDF) of travel time of inert tracers (Dagan and Cvetkovic, 1996). The PDF is used as an input for the reactive transport modelling. This allows the decoupling of conservative transport from physicochemical processes. The approach ensures a good mass balance, is almost free from numerical dispersion and consumes less time during numerical computations (Thiele et al., 1995a, b; Batycky et al., 1996). It is designed for use as a pure forward model involving input parameters which can be derived from independent laboratory or field scale experiments. Solute transport through heterogeneous media is represented by an ensemble of 1-D streamtubes with infinitesimal cross-sectional area and time dependent concentrations.

3.4.1 SMART: Assumptions and heterogeneity implementation

The SMART model assumes:

(1) The flow field is at steady state.

(2) The variability of the velocity field completely describes the hydraulic heterogeneities within the porous medium. The travel time approach does not allow heterogeneity of the hydrogeochemical parameters.

(3) Dispersion of solute plumes is solely attributed to macroscopic hydraulic heterogeneities, i.e pore scale dispersion and molecular diffusion is neglected.

The third assumption which neglects diffusion is unrealistic in general but is a reasonably valid approximation in application scenarios where advection becomes dominant (Finkel et al., 1999). In this approach solute in the form of parcels moves and spreads out in the streamtube from an injection plane (i.e. source zone of the lysimeter) to a control plane (outlet of the lysimeter) normal to the mean flow direction (Fig 3.2). The parcel flow shows how non-uniformity in the hydraulic properties causes the spatial spreading of the fluid parcels along the streamtubes. The spreading is similar to macro scale solute dispersion.

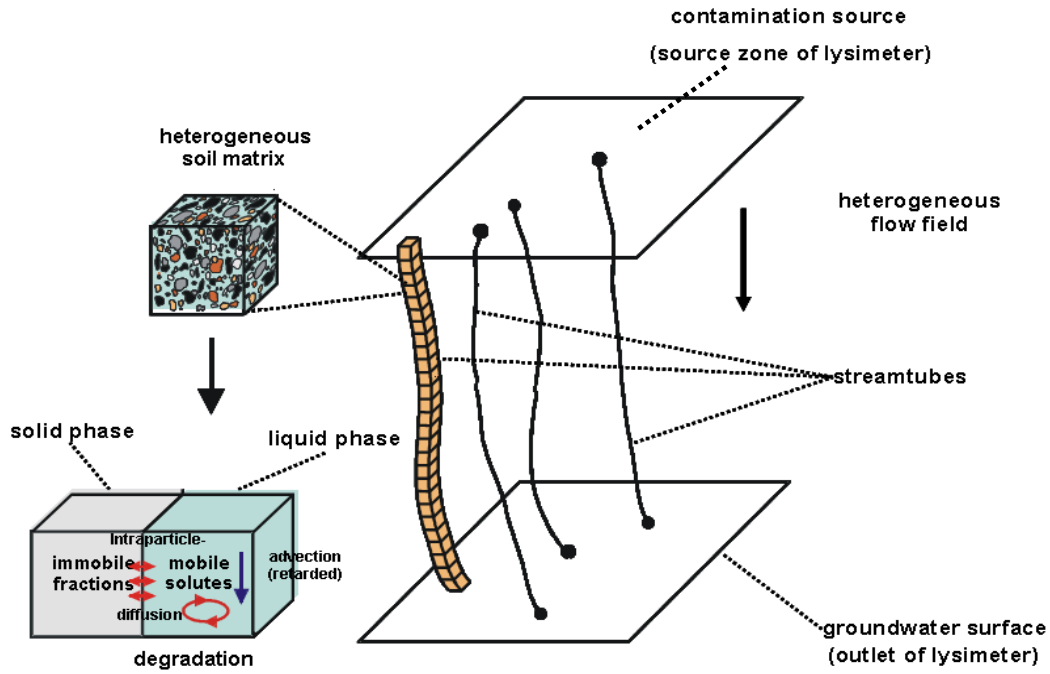

Fig. 3.2: Conceptual illustration of the streamtube model SMART (adopted and modified from Finkel et al., 1998b)

The time independent solute concentration at the control plane (base of lysimeter) is given by

$$C_r(t) = \int_0^\infty g(\tau)\Gamma(\tau,t)d\tau \qquad 3.3$$

where *t* is time [T] and τ represents the travel time of a conservative tracer through the lysimeter [T]. The function $\Gamma(\tau, t)$, is the reaction function which represents the reactive processes for a continuous injection with unit input concentration. It simulates the concentration profiles for each time step. The variations in the arrival times (hydraulic heterogeneities) are accounted for by the PDF $g(\tau)$. Depending on the processes of consideration, different expressions of $g(\tau)$ are given in the sections ahead. According to Peter (2002) evaluation of equation 3.3 is tantamount to simulating reactive transport along a single streamtube when the physico-chemical parameters are spatially constant. The PDF of travel times for conservative transport in an ensemble of streamtubes accounts for the distribution of travel times which represents the hydraulic heterogeneities. Soil and lithological heterogeneities are

accounted for by a matrix of mass fractions of different lithological units and grain size classes which must be the same in every model cell. This ensures a smooth transfer of relevant parameters measured in the laboratory to the lysimeter or field scales with respect to the lithological fractions and grain size distribution.

3.4.2 Numerical implementation of conservative transport in SMART

The integral solute contaminant equation 3.3 is discretised to a finite equation

$$C(t) = \sum_{l=1}^{n} g(\tau_l)\Gamma(\tau_l, t)\Delta\tau \qquad 3.4$$

where l is the time step index and $\Delta\tau$ is the cell discretization by travel time of the 1-D streamtube model. The cell length corresponding to the travel distance of particles is given by

$$\Delta x_{cell} = v_x * \Delta\tau \qquad 3.5$$

where v_x is the average flow velocity. The breakthrough curve C (t) is evaluated after the generation of the PDF and calculation of the reaction functions. The conservative transport is evaluated independently from the reactive process and can be described by the PDF of travel time for conservative transport between the two control planes. This approach has the advantage of using measured data from a conservative tracer test for deriving the PDF. Uncertainties with respect to conservative transport are thus greatly reduced. The conservative tracer breakthrough can therefore be evaluated as follows :

1. Generation of PDFs based an tracer test data

1a. From a tracer experiment with Dirac input (instantaneous injection), the PDF is generated from the measured concentrations by the equation

$$g(\tau_l) = \frac{C_l}{\sum_{l=1}^{n}\left[C_{l+1}\left(t_{l+1} - t_l\right)\right]} \qquad 3.6$$

1b. From a tracer experiment for a constant tracer injection, the PDF is generated from the measured concentrations by the equation

$$g(\tau_l) = \frac{\frac{C_{l+1} - C_l}{t_{l+1} - t_l}}{C_{INP}} \qquad 3.7$$

Where C_l [ML^{-3}] and t_l are the observed tracer concentration and travel time respectively, C_{INP} [ML^{-3}] is the constant tracer inflow concentration. It must be noted that equations 3.6 and 3.7 are only valid when the tracer recovery is 100%. The normalised output signal $C(\tau_l)/ C_{INP} = h(\tau_l)$ can be obtained by the integration of $g(\tau_l)$.

2…….Generation of PDFs using analytical models:

2a. Convection-dispersion equation (CDE) with pulse input in a homogeneous soil (Jury and Roth 1990). The PDF (Fickian PDF) of the travel time is given by the equation

$$g(\tau) = \frac{x}{2\sqrt{\pi D \tau^3}} \exp\left(-\frac{(x - v\tau)^2}{4D\tau}\right) \qquad 3.8$$

where v [$L\ T^{-1}$] is the linear velocity, x is the distance between injection and control planes [L], and D is the dispersion coefficient [$L^2\ T^{-1}$]. The same Fickian PDF but with modified mean and standard deviation of the natural logarithm of the travel times is applied by Zhang (2000) in the GTF model to account for heterogeneous systems in which the scale dependency of the dispersivity to the travel distance results in a power law.

A conversion of equation 3.8 to a discrete set of PDF values, as given by equations 3.6 and 3.7 is possible through

$$\frac{C}{C_{INP}} = \frac{1}{2}\left[erfc\left(\frac{x-v^*t_{i+1}}{2^*\sqrt{D^*t_{i+1}}}\right)+\exp\left\{\frac{v^*x}{D}\right\}^*erfc\left(\frac{x+v^*t_{i+1}}{2^*\sqrt{D^*t_{i+1}}}\right)\right]-\frac{1}{2}\left[erfc\left(\frac{x-v^*t_i}{2^*\sqrt{D^*t_i}}\right)+\exp\left\{\frac{v^*x}{D}\right\}^*erfc\left(\frac{x+v^*t_i}{2^*\sqrt{D^*t_i}}\right)\right] \qquad 3.9$$

2b. Piston flow model (PFM) in a homogeneous soil with uniform mean flow. It is given by the equation

$$g(\tau) = \delta(\tau - \tau_a) \qquad 3.10$$

where τ_a [T] is the travel time of a conservative tracer. Equation (3.8) reduces to equation 3.10 when dispersion is neglected.

2c. Bimodal PDF (Utermann et al., 1990). This takes into account both matrix and preferential flow. The equation is given by

$$g(\tau) = \alpha g_{pref}(\tau) + (1-\alpha) g_{matrix}(\tau) \qquad 3.11$$

where α is the volume fraction occupied by the preferential flow, g_{pref} is the PDF of the preferential flow zone and g_{matrix} is the PDF of the matrix zone.

3. Generation of PDF using numerical models

An inert tracer breakthrough curve can be simulated and evaluated numerically at the control plane (base of lysimeter) by an application model such at HYDRUS (Simunek, 1998) and WAVE (Vanclooster et al., 2000a). In application to SMART, the numerical breakthrough curves are transformed into PDFs in similar manner to PDFs generated from measured concentrations (equations 3.6 and 3.7).

3.4.3 Numerical implementation of reactive transport in SMART

The reaction function $\Gamma(\tau,t)$ in equation 3.3 is evaluated by performing simulations of one-dimensional advective–reactive transport. A series of concentration profiles are numerically approximated along the travel distance with respect to τ at distinct times t_z (z=1,2,3,…n). The discretization of the travel time and the corresponding PDF should always be equivalent to each other. Finkel (1999) employed a technique

which is capable of circumventing numerical dispersion problems inherited in many finite different and finite element models. In this technique the model grid is defined based on the travel time discretization $\Delta\tau$. Solute concentrations are represented in the form of a continuous series of large parcels (i.e. each parcel represents a given mass of the solute). Each parcel is advected to a new location on the cell grid for every time step with the retarded flow velocity. Average concentrations of each solute parcel are calculated on each grid cell. The concentration can be calculated as

$$C(\tau) = \frac{p^* m_p}{v_z} \qquad 3.12$$

where p is the number of parcels [-], m_p [M] is the mass of parcels and v_z [L^3] is the volume of cell. The solute concentrations are then redistributed from the cells to the parcels for the corresponding simulation of the next time step.

3.5 Modelling process

The ability to model a process depends on how well the process is understood. An initial level of understanding stimulates the development of a conceptual model while a higher level of understanding leads to the formulation of mathematical models and eventually results in a quantitative model which is capable of predicting natural systems and environments which have been adversely affected. Attempts to improve process based modelling understanding has ameliorated tremendously the description and modelling of flow and transport processes in the subsurface (Anderson, 1984). The following subsections discuss the relevant processes and transport mechanisms in nature and many contaminated sites and, where appropriate, their application and implementation in SMART.

3.5.1 Advection

Advection is the process of transport of pollutants at the same speed as the average linear transport velocity of groundwater or the movement of pollutants through a geologic formation in response to a pressure gradient. During solute spreading, sharp concentrations fronts of solutes maintain their shapes. It is usually referred to as convection when the transport is in response to temperature induced density

gradients (Anderson, 1984). Advection does not take into account microscopic processes but follows the bulk Darcian flow vectors. Moreover it is also described as the transport along pathlines. Pure advective transport can be evaluated from the results of the flow model with path line models (e.g. particle tracking and Method of Characteristics). Known specific fluxes within cells can be used to calculate advective fluxes.

$$q = \frac{Q}{A} \qquad 3.13$$

where Q [L^3 T^{-1}] is the discharge of flow, q [L T^{-1}] is specific flux or Darcy velocity, and A [L^2] is cross-sectional area for water flux. The pore velocity which determines the advective flux is given by

$$u = \frac{q}{n_e} \qquad 3.14$$

where u [L T^{-1}] is pore velocity and n_e [-] is the effective porosity.
In pure advection transport problems the Lagrangian approach is employed to eliminate numerical dispersion. In the SMART code pure advection is represented as a flug-flow or piston-flow model (equation 3.10).

3.5.2 Diffusion and dispersion

Diffusion is the spreading of compounds through the effects of random molecular motion. The compounds passively move and transfer mass from an area of higher concentration to area of lower concentration causing mixing in the direction of their concentration gradient. It primarily starts from movement of molecules and results in variation of concentrations. Solute emanating from a point source by diffusion in the absence of hindrance or advection to movement will lead to a Gaussian distribution of the concentration, with the width of the plume growing with the square root of time. The higher molecular activity in gases causes spreading due to diffusion about 100 times faster than in the liquid phase (Selker et al., 1999). Diffusion rate changes with the square root of temperature (measured in Kelvin) and since temperatures vary

little in typical groundwater, variation of diffusion tends to be very low in groundwaters (Selker et al., 1999). The diffusive mass flux is determined through the concentration gradient and the effective coefficient of diffusion of the porous media. The diffusive flux is described by Fick's first law

$$J_i = -D_i \frac{\partial c}{\partial x} \qquad 3.15$$

where J_i [M L^{-2} T^{-1}] is the diffusive flux of chemical i. D_i [L^2 T^{-1}] is the coefficient of molecular diffusion and $\frac{\partial c_i}{\partial x}$ [M L^{-3} L^{-1}] is the concentration gradient. The molecular diffusion coefficient depends on solvent temperature, solvent viscosity, molecular size and shape. According to (Neretnieks, 2002), the magnitude of diffusive distance can be approximated by the equation

$$l = 2.2\sqrt{D_i * t} \qquad 3.16$$

where l [L] is the distance of diffusive transport for which the mean concentration equals 50% of the maximum concentration and t [T] is typical time. The effective molecular diffusion coefficient D_e [L^2 T^{-1}] is given by the relation

$$D_e = \zeta * D_i \qquad 3.17$$

where ζ [-] is the tortuosity factor.

Dispersion is the mixing that occurs as a result of differences in velocities of neighbouring parcels of fluid at different scales. At pore scale dispersion leads to the separation of intergranular particles and mixing of solutes (Selker et al., 1999). Natural sediments are heterogeneous and lead to a non uniform velocity distribution which causes the smearing of fronts above the pore scale. This additional mixing process is termed macro-dispersion. The presence of macro dispersion has been confirmed by field studies (Skibitzkie and Robinson, 1963; Anderson, 1979). Groundwater moves at rates that are both greater than and less than the average linear velocity. This is due to hydrodynamic dispersion, a phenomenon caused by

mechanical dispersion and molecular diffusion. Mechanical dispersion is basically caused by three phenomena:

1) As fluid moves through the pores, it will move faster in the center of the pores than along the edges. This causes an accelerated arrival of contaminant at a point of discharge.
2) Some of the particles will travel along longer flow paths in porous media than other particles to go the same linear distance. This caused the smearing of concentration fronts.
3) And some pores are larger than others, which allow the fluid flowing through these pores to move faster (Fetter, 1993). Dispersion is a mechanism of dilution which causes mixing with unpolluted groundwater and the spread of contaminants into greater volumes in aquifers than normal groundwater velocity vectors would predict. It is more important in predicting transport away from point sources than diffused sources. Slichter (1905) predicted an s-shape breakthrough curve owing to dispersion from his laboratory experiment of flow through porous media.

Along the direction of flow the velocity variations within and between pores as well as the variation in the flow path length causes the dispersive effect know as longitudinal dispersion. Similar dispersive effects which are mainly due to the splitting of flow paths but normal to the mean flow path is know as transverse dispersion. The longitudinal dispersion is usually greater than the transverse dispersion. The combined effect of these two mechanisms is known as mechanical dispersion. Studies have found the mechanisms to be scale dependent (Anderson, 1984 , Gelhar et al., 1992).

Usually the process of molecular diffusion cannot be separated from mechanical dispersion in flowing groundwater. The two are therefore combined to define a new parameter called the hydrodynamic dispersion coefficient, D^* (Fetter, 1993)

$$D^* = D_{mec} + D_p \qquad 3.18$$

where D_p [L^2T^{-1}] is the pore diffusion coefficient and D_{mec} [L^2T^{-1}] is the coefficient of mechanical dispersion. The coefficient of mechanical dispersion is given by the relation

$$D_{mec} = \alpha^* v \qquad 3.19$$

where α [L] is the characteristic mixing length usually known as dispersivity and v is the average linear pore velocity [LT^{-1}].

Most field studies and flow and transport modelling are conducted at the macroscopic level. This may be due to measurement problems (Fried, 1975) and the use of the fundamental macroscopic Darcy (the use of unresolved velocity distribution and single average values in a representative elementary volume) equation in models. Taylor (1921, 1953) therefore suggested that dispersion could be represented by Fick's 1st law of diffusion. The mass flux due to dispersion is given by

$$J = -D^* \frac{\partial c}{\partial x} \qquad 3.20$$

where D^* is the hydrodynamic dispersion coefficient as given in equation 3.18.

Further studies from many researchers have found out that the Fickian representation of dispersion is only valid after some distance and certain length of time have elapsed in porous media and in rivers (Fisher, 1973; Matheron and DeMarsily, 1980; Gelhar and Axness, 1981; Dagan, 1982; Beltaos and Day, 1978). Only for long times or travel distances under special geologic conditions can the Fickian process accurately represent dispersion. Moreover other studies show that dispersion is non Fickian near the source of a contamination (Molinari et al., 1977; Lee et al., 1980; Pickens and Grisak, 1981b). Other approaches which are not discussed in detail in this thesis (Schwartz, 1977 and Smith and Schwartz, 1980, 1981a, 1981b) described dispersion by defining the hydraulic conductivities statistically. Dispersion close to a source therefore requires other terms of higher order. Therefore detailed characterisation of heterogeneities, hydraulic conductivity units, heads and gradient is needed for accurate prediction of contaminant transport (Anderson, 1984). In SMART, the Langrangian approach in which solutes moving along non interacting streamtubes are tracked do not account for dispersion. Hence

unsuitable in heterogeneous systems or geologic settings where dispersion is dominating the over all advective-dispersive transport process.

3.5.3 Preferential flow

The quests for management of land and chemical inputs on soil have increased recently as more and more chemicals and fertilizers are applied on land to ensure optimised crop yield. Unexpected chemicals have been found in drinking wells as well as ground waters Compounds which are highly degradable or highly sorbed have been found at higher concentrations and much more rapidly than would have been predicted in groundwaters. This would constitute a longterm hazard that posterity would have to deal with. This fast movement of solute endangers groundwater quality with an associated adverse effect on humans and aquatic systems. Recent studies have shown this phenomenon to be a process known as preferential flow which occurs in many natural geological and soil settings (Flury, 1996; Traub-Eberhard et al., 1995; Kladivko et al., 1991; Parlange et al., 1998). Again preferential flow has been observed in many laboratory and field studies (Pyrak et al., 1985; Abelin, 1986; Bourke, 1987; Haldeman et al., 1991). The process had actually been described earlier on by Lawes et al. (1882) who distinguished between preferential flow and matrix flow in field drain experiments. Preferential flow is the unequal and fast movement of water and solutes through porous media which is characterised by structural and textural inhomogeneous. Three mechanisms have been reported to be responsible for preferential flow processes: (i) macropore flow (bypass flow) is due to several soil forming factors such as soil fauna, tubes left from rotten roots, flow through non capillary cracks, subsurface erosion, aggregate, gabs and exclusion due to parts of pore area. High macropore routes form and persist in structured soils with flow fairly uniform near the upper horizons and becomes sparse as it drains down the unsaturated zone. (ii) Finger flow is due to the instability in wetting front which causes water to flow in channel or fingers. Fingers results from infiltration through dry sands, water flow from fine into coarse material (Akthar et al., 2003) and local variations in wetting characteristics of porous media. Hill and Parlange (1972) observed this mechanism in homogeneous media at low rate of infiltration. The higher the flow rate the higher the number of fingers formed and vice versa (Selker et al., 1996). This unstable wetting fronts results in preferred finger flow

paths which end up in fast transport to ground waters (Ritsema et al., 1998). (iii) Funnel flow is caused by the sloping geological layers which also cause water flow laterally or diagonally. Stones and lenses of different texture in sandy matrix result in preferred flow of the funnel nature. This diverging of flow due to layering or sloping (Welter et al., 2000) is important because monitoring wells emplaced to capture contaminants may miss entirely if the wells are located away from places where layering of the geological setting and funnelling are known to occur. Preferential flow is again known to affect other processes such as biodegradation and particle transport. Biodegradation rates were found to be initially less in macro pores than rates in matrix pores but later increased and exceeded matrix pore rates as a result of greater mass of substrate passing through and increase of microbial pollution with time in the macrospores (Pivetz and Steenhuis (1995), Pevetz et al., 1996; Utermann et al., 1990). Again Ryan and Elimelech (1996) demonstrated that particle transport is enhanced in macrospores due to their higher travel velocities.

Many analytical and numerical models have also been conducted to characterise preferential flow. (Van Dam et al., 1990; De Rooij, 1995) modelled flow and transport in water repellent soils with analytical approaches. Ritsema (2001) modelled 2-D flow and transport using finite element techniques described by Nieber (1996) and Ritsema et al. (1998) including preferential flow and hysteresis which affects water retention characteristics in repellent soils. He also used SWAP (Van Dam et al., 1997) in that same study which again incorporated preferential flow and hysteresis. Two-region stage models based on Coats and Smith (1964) in which chemical exchange is rate limited between soil matrix and preferential flow paths have been applied earlier. Multi layer models which encompass many flow paths have also been used (Ma et al., 1995; Jarvis et al., 1991a, b; Hutson and Wagenet, 1995; Steenhuis et al., 1990). Additionally (Skopp et al., 1981) considered a preferential flow model in which water is mobile in both matrix and macro pores while (Wallach et al., 1998) looked at other cases in which water in the matrix pores is considered stagnant (MIM models). The mobile-immobile (MIM) models (Skopp and Warrick, 1974; van Genuchten and Wierenga, 1976; van Genuchten and Dalton, 1986) are reported to provide good predictions for measured breakthrough curves since their concentrations are averaged and distributed uniformly across the lateral dimensions throughout the model domain.

In SMART, preferential flow is modelled as a conservative process by using the bimodal PDF approach after Utermann et al. (1990). Accounting for both matrix and preferential flow in porous media their formulation is given as

$$g(\tau) = \alpha\, g_{pref}(\tau) + (1-\alpha)\, g_{matrix}(\tau) \quad . \qquad 3.21$$

as shown in equation 3.11. Bold (2003) in his thesis demonstrated that the expected long term concentration at the control plane (outlet of lysimeter) taking into account sorption, biodegradation, particle-facilitated transport and preferential flow and assuming physico-chemical equilibrium between contaminants and particles is given by:

$$C_{\infty} = C_{INP}\left\{\alpha \exp\left[\frac{v_{pref}\,x}{2D_{pref}}\left(1-\sqrt{1+\frac{4\lambda' D_{pref}}{v_{pref}^{\,2}}}\right)\right]+(1-\alpha)\exp\left[\frac{v_{matrix}\,x}{2D_{matrix}}\left(1-\sqrt{1+\frac{4\lambda' D_{matrix}}{v_{matrix}^{\,2}}}\right)\right]\right\} \qquad 3.22$$

where C_{∞}[ML^{-3}] is total mobile long-term concentration, C_{INP}[ML^{-3}] is total mobile solute input concentration, α[-] is volume fraction of preferential flow, v_{pref} [LT^{-1}] and V_{matrix} [LT^{-1}] are flow velocities in preferential flow and matrix flow regions respectively, D_{pref} [L^2T^{-1}] and D_{matrix} [L^2T^{-1}] are the dispersion coefficients in preferential flow and matrix regions respectively, λ' [T^{-1}] is modified effective degradation rate accounting for all particles involved and x is the vertical coordinate. Bold (2003) successfully applied equation 3.21 to data from a lysimeter tracer (^2H) experiment conducted under steady state in an unsaturated medium by Seiler (2000). In this thesis preferential flow is not accounted for since the expected lysimeter breakthroughs to be modelled showed no signs of macropore flow·

3.5.4 Sorption/desorption

The rate at which solutes pass through the zone of aeration (vadose zone) and break through at the groundwater table partly depends on the interaction between the moving mass in the aqueous phase and the solid matrix in the immobile phase. Depending on the interfacial conditions, solute can either be sorbed into or desorbed from soil matrices. Two of such major fundamental phenomena that take place in soils and sediments are adsorption and absorption. Adsorption is the process in

which the solute accumulation is generally restricted to a surface or interface, for instance solid/liquid, solid/gas and liquid/gas. Absorption describes a process in which the solute penetrates the sorbent similar to solution in a solvent. Both processes may take place simultaneously due to the heterogeneous nature of soils and sediments. The term sorption is used to describe both absorptive and adsorptive processes. The solute in solution not yet sorbed is also referred to as sorptive (Grathwohl, 1997). In addition sorption processes also include chemisorption and ion exchange. Chemisorption occurs when the solute is incorporated on a sediment or soil surface by a chemical reaction (Fetter, 1991). Sorption is extremely important because of its ability to effectively affect the fate and impact of chemicals in the environment (Schwarzenbach et al., 1992).

3.5.4.1 Equilibrium sorption/desorption isotherms

Sorption isotherms relate the aqueous concentration to the sorbed concentration at a constant temperature. The aqueous concentration is assumed to be in equilibrium with the sorbed concentration if the sorptive uptake of the solvent by the sorbent is instantaneous or occurs in a time that can be neglected when compared to the advective time. The simplest case is when the concentration in the solid (q_s) is directly proportional to the corresponding equilibrium solute concentration (C_{eq}) in aqueous or vapour phase:

$$q_s = K_d C_{eq} \qquad 3.23$$

where K_d [L^3M] denotes distribution coefficient, which defines the ratio between the solute concentrations in aqueous and solids phases. q_s is frequently termed sorbate concentration but actually represents the ratio of sorbed mass to solid mass. K_d describes the partitioning and is equal to the slope of the sorption isotherm when sorption is linear. K_d becomes solute concentration dependent when sorption isotherms are nonlinear. Four models often used to describe nonlinear sorption isotherms in soils and sediments are described below.

(i) Freundlich model (Freundlich, 1909):

$$q_s = K_{Fr} C_{eq}^{1/n_{Fr}} \qquad 3.24$$

where K_{Fr} is the Freundlich sorption coefficient and $1/n_{Fr}$ is an empirical exponent. The relation becomes linear when $1/n_{Fr} = 1$. The value of K_{Fr} always depends on the units of q_s and C_{eq} respectively. Combining equations (3.23) and (3.24) yields the dependency of the distribution coefficient on the concentrations and is given by

$$K_d = K_{Fr} C_{eq}^{(1/n_{Fr})-1} \qquad 3.25$$

K_d becomes equal to K_{Fr} when $C_{eq} = 1$ for the selected concentration unit or $1/n_{Fr} = 1$.

(ii) Langmuir model. This model was originally developed to account for adsorption of gases on solids. It normally accounts for a maximum sorbate concentration, q_{smax}

$$q_s = \frac{K_L q_{smax} C_{eq}}{1 + K_L C_{eq}} \qquad 3.26$$

where K_L [L^3M^{-1}] is the Langmuir sorption coefficient, $q_s = q_{smax}$ if $K_L * C_{eq} >> 1$ and for very low concentrations, $q_s = K_L\, q_{smax}\, C_{eq}$.

(iii) BET model: This model was also meant for the adsorption of gases onto solid surfaces and accounts for capillary condensation of the solute in mesopores.

$$q_s = \frac{K q_{max} C_{eq}}{(C_{sat} - C_{eq})(1 + (K-1) C_{eq} / C_{sat})} \qquad 3.27$$

where C_{sat} is the saturation concentration in vapour. A linear relationship is obtained between aqueous and sorbed concentration if $C_{eq} << C_{sat}$. As C_{eq} approaches C_{sat}, q_s becomes infinitely large (capillary condensation of vapours, precipitation or clustering of solutes in aqueous solution) (Brunauer et al., 1938).

(iv) Toth isotherm: This isotherm is more flexible than Langmuir and BET isotherms in terms of description of environmental sorption data (Kinniburgh, 1986). It is given by

$$q_s = \frac{K_T q_{smax} C_{eq}}{(1+(K_T C_{eq})^{ß_T})^{1/ß_T}} \qquad 3.28$$

where K_T and $ß_T$ are affinity and heterogeneity parameters respectively. Fig. 3.3 below describes sorption isotherms.

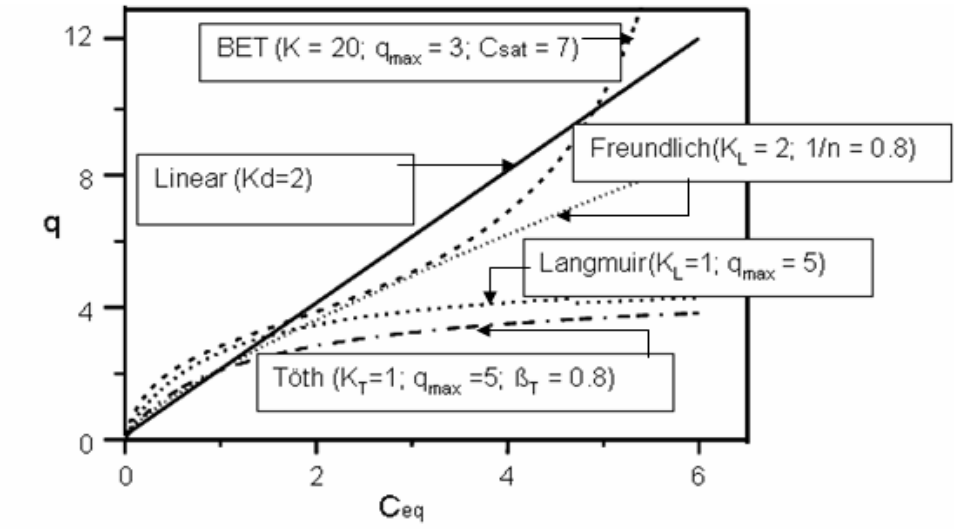

Fig. 3.3. Equilibrium sorption isotherms adopted from Grathwohl (1997).

3.5.4.2 Sorption / desorption Kinetics

Most organic substances spilled unto porous media have the tendency of interacting and reacting with the host matrix before leaching out. The sorption of the organic compounds in soils and sediments essentially takes place through the organic matter (SOM) contained in it (Karickhoff et al., 1979; Grathwohl, 1990; Kleineidam et al., 1999a). The sorption / desorption capacity depends on the natural SOM which develops differently in different heterogeneous compositions. Knowledge of the portion and the kind of SOM is therefore crucial for the estimation for the hydrophobic desorption of the organic pollutants. The SOM usually may be altered genetically or thermally. The sorption / desorption process may therefore be linear over a concentration range or independent of the concentration of the pollutant as described in section 3.5.4.1. The distribution coefficient can also be represented as

$$K_{\mathrm{d}} = K_{oc} f_{oc} \qquad 3.29$$

where f_{oc} [-] is the fraction of organic carbon and K_{oc} [L^3M^{-1}] is the distribution coefficient standardised on the content of the organic carbon. K_{oc} is usually empirically determined based on either the octanol water distribution (K_{OW}) coefficient or the solubility of the organic compound. In this study one of such linear regression equations for sorption studies published by Seth et al. (1999) and Allen-King et al. (2002) was used.

$$\log K_{oc} = -0.88 \log S + 0.07 \qquad 3.30$$

where S [Mol l^{-1}] is the aqueous solubility. This relation takes into account uncertainty limits in determining K_{oc} for hydrophobic organic compounds and also matches closely with other relations provided by (Xia and Ball, 1999). The saturated concentration (C_{max}) is observed in the source over a period of time depending on the level of contamination at equilibrium conditions. At non equilibrium or kinetic conditions, the effluent concentrations begin to decrease rapidly and usually show an extended period of tailing (Susset et al., 2004). The non equilibrium behaviour was clearly seen when desorption of the pollutants from porous soil matrix is limited by slow intraparticle diffusion. Susset found out that contaminant concentration in his column effluent initially decreases with the square root of time depicting that the most influential process in the intraparticle pore space is diffusion. This slow diffusion process within soil aggregates / particles and the organic matter have also been observed by many authors (Grathwohl, 1998; Kleineidam et al., 1999a; Rügner, 1997). Since the sorption / desorption equilibrium between the seepage water and solid matrix is normally not reached within the ensuing contact time, it makes sense to apply sorption / desorption kinetics especially when considering long term risk with strong sorbing organic pollutants. Figure 3.4 below shows the path and the diffusion processes of a contaminant sorbed in an intraparticle pore in the immobile phase as well as mobile phase in a water saturated media.

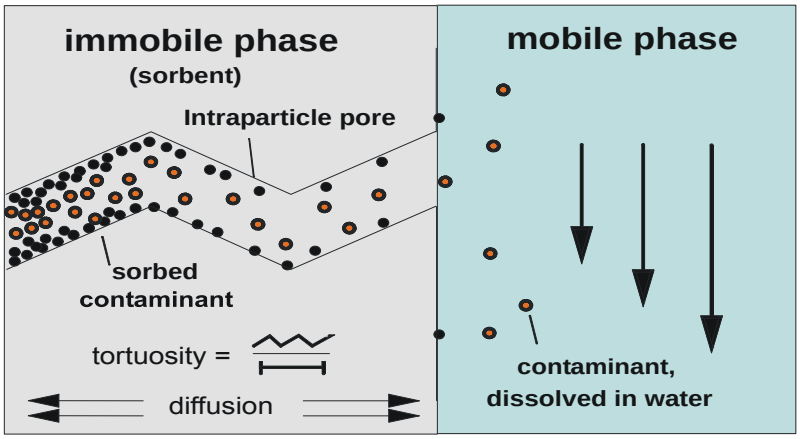

Fig. 3.4: Modelling of intraparticle diffusion (Grathwohl 1998)

The release rate depends on the pollutant properties such as diffusion coefficients, solubilities, mass and partitioning of the pollutant in the particles. Assuming a spherical nature of the particles, the sorption / desorption processes in water saturated media can be described by Fick`s second law in spherical coordinates given as:

$$\frac{\partial C}{\partial t} = D_{app}\left[\frac{\partial^2 C}{\partial r^2} + \frac{2\partial C}{r\partial r}\right] \qquad 3.31$$

where C [ML^{-3}] is the aqueous concentration, t [T] is time , r [L] is the radial distance from the centre of the spherical particle and D_{app} [L^2T^{-1}] is the apparent diffusion coefficient. According to equation 3.32 below the apparent diffusion coefficient assumes a linear isotherm between the sorbate and the aqueous concentrations and that the intraparticle tortuosity is inversely proportional to the intraparticle porosity. The apparent diffusion coefficient (D_{app}) takes into account the geometry of the pores and relates the aqueous diffusion coefficient (D_{aq}), intraparticle porosity (n_{ip}), the sorption / desorption distribution coefficient (K_d), and the material density of the particle (ρ) as

$$D_{app} = \frac{D_{aq} \cdot n_{ip}^2}{n_{ip} + (1 - n_{ip}) \cdot \rho \cdot K_d} \qquad 3.32$$

Using the local equilibrium assumption (LEA) in the interparticle pore space, the solute uptake or release can be described by the Fickian second law with a retardation factor

$$R = 1 + \frac{(1-n)\rho * \partial q_s}{n_e * \partial C_{aq}} \qquad 3.33$$

where ρ [ML-^{3}] is the particle density, n is total porosity and n_e [-] is the effective porosity. The derivative $\partial q_s / \partial C_{aq}$ represents the distribution coefficients in any of the equations (3.23 – 3.28) depending on which isotherm i.e. linear or non-linear isotherm is considered. The retardation factor [-] is accordingly modified to the form

$$R = 1 + \frac{1 - n_{ip}}{n_{ip} \cdot S_w} \cdot \rho \cdot \frac{\partial q_s}{\partial C_{aq}} \qquad 3.34$$

when the intraparticle pore diffusion is included. S_w is degree of saturation.

In SMART sorptive and desorptive processes are modelled based on how fast or slow the process proceeds. The fast (equilibrium) processes are modelled by using the parcel tracking approach as described in section 3.4. The retardation factor is computed as the ratio of total contaminant mass and contaminant mass dissolved in the mobile aqueous phase. The sorbed mass is obtained by equilibrium sorption isotherms such as the linear and Freundlich. Details may be referenced from Finkel (1999), Hüttmann (2001) and Bold (2004). The desorption behaviour of organic constituents is also implemented in SMART by calculating a retardation factor based on the organic carbon distribution coefficient (k_{oc}) of each constituent and fractional organic carbon in the soil (f_{oc}).

The time dependent concentration gradient (kinetic sorption / desorption) is modelled in SMART in two ways:

(i) analytically by a process in which solutes diffuse into the intraparticle pore of spherical grains (Crank, 1975) with concentration steps as boundary conditions at the surface and a linear equilibrium sorption inside (Finkel et al., 1998a);

(ii) numerically by coupling SMART with a finite difference solver for intraparticle diffusion, BESSY (Batch Experiment Simulation System), (Jaeger and Liedl, 2000),

which has been applied in sorption and desorption models with extended boundary conditions (Amankwah, 2003) and also coupled to the MT3D (Zheng, 1990) code to model reactive processes (Liedl and Ptak, 2003, Peter, 2002, Bold, 2004). The concentration gradients are resolved by dividing the spherical grains in shells with non equidistant nodes at which the difference equations are solved. By subdividing the grains into fractions of grain sizes with different lithocomponents, heterogeneous porous matrixes are catered for in the model. The numerical approach has an additional advantage of dealing with non linear sorption isotherms.

Moreover under unsaturated conditions, an analytical solution derived by Rosen (1954) and Crittenden et al (1986) for soils with homogeneous flow and physico-chemical reactions without biodegradation can be adopted:

$$C_D(t) = \frac{C_0}{2}\, erfc\left[\frac{1+\dfrac{\theta}{\rho_b\left(K_d+\dfrac{n_{ip}}{(1-n_{ip})\rho}\right)}\left(1-\dfrac{t}{PV}\right)}{\sqrt{\dfrac{4R^2\theta}{15D_{app}\rho_b\left(K_d+\dfrac{n_{ip}}{(1-n_{ip})\rho}\right)PV}}}\right] \qquad 3.35$$

Sorption / desorption is close to equilibrium if $\dfrac{3D_{app}\rho_b\left(K_d+\dfrac{n_{ip}}{(1-n_{ip})\rho}\right)PV}{\theta R^2} \geq 40$

where θ [-] is water content, ρ_b [ML^{-3}] is bulk density and PV [T] is the pore volume (travel time of a conservative tracer in a homogeneous soil). By this formulation an appropriate discretization can also be determined for the numerical model of sorption and desorption reactions.

3.5.5 Biodegradation

Petroleum and charcoal products are used for a large range of chemical synthesis and fuel in the industry. Some of these chemicals are carcinogenic and can find their way into the environment through point and diffuse emissions. They persist due to their inert and hydrophobic nature endangering humans and the ecosystem. Biodegradation is the only natural attenuation mechanism that has the potential to destroy the contaminants in-situ with nontoxic inorganic end products even though adsorption may contribute to the reduction of concentrations to some extent (Peter, 2002). Depending on the type of organic contaminant, bioavailability of the compound (usually accessible in the aqueous phase), environmental conditions (e.g. pH, temperature, EC and nutrients) and properties of the microorganisms (Wiedemeier et al., 1999; Alexander, 1999; Salanitro et al., 1997), the pollution risk expected at the groundwater table could be greatly reduced. With the exception of some metabolites which would be toxic biodegradation therefore becomes a reaction sink by which solute concentrations are reduced (Seagren et al., 1993). Since human activities though managed continue to pose a threat to the environment, many laboratory and field studies (Luthy et al., 1994) have been conducted to improve the understanding of the degradation process and see how the process could be augmented and enhanced during remediation (Franck, 1963; Nakahara et al., 1977; Jüttner and Henatsch, 1986; Nielsen and Christensen, 1994; Fischer et al., 1996; Guha et al., 1999).

3.5.5.1 Microbial degradation processes

The biodegradation process may involve (i) the conversion of contaminants to mineralized end-products through biological mechanisms (e.g. CO_2, H_2O, and salts). (ii) the biological process in which the contaminant is biotransformed into end-products which are not minerals (e.g. dehalogenation of PCE to TCE, DCE) and (iii) the process of extracting energy from organic chemicals through oxidation of the organic chemicals. These biotic processes may take place under aerobic or anaerobic conditions. The degradation process is aerobic when oxygen becomes the terminal electron acceptor. Oxygen atoms are incorporated into the organic

contaminant resulting in products with hydroxyl groups (Gibson and Subramanian, 1984; Cerniglia, 1984, 1992). The degradation capacity of oxygen related degradation has been found to be low due to the low solubility of oxygen in water and the slow diffusion process of oxygen into plumes (Wiedemeier et al., 1999). Based on the studies of Coover and Sims (1987), Groenewegen and Stolp (1976), and Sims (1990), Howard et al. (1991) predicted that the half-lifes of PAHs in soils could vary between 1-2 orders of magnitude and estimated an average value of 570 days. Other effects such as cometabolism and inhibition have also been observed (Bouchez et al., 1995; Wackett and Ellis, 1999). The degradation process is anaerobic when all available oxygen is depleted. Many studies have substantiated the biodegradation of organic compounds in the absence of oxygen (Kuhn et al., 1985; Zeyer et al., 1986; Grbic-Galic and Vogel, 1987; Meckenstock, 1999; Wiedemeier et al., 1999). The degradation is found to proceed in the following order of electron acceptor processes: denitrification (Evans et al., 1991; Song et al., 1999), manganese reduction, iron reduction (Lovely and Lonergan, 1990), sulfate reduction (Rabus et al., 1993; Beller et al., 1996), and methanogenesis (Beller and Edwards, 2000, Lovley et al., 1994b). According to Wiedemeier et al. (1999) the degradation capacity of the combined anaerobic processes is 97 % as against 3 % of aerobic process. Some laboratory studies have shown the anaerobic biodegradation of PAHs (Zhang and Young, 1997; Galushko et al., 1999; Meckenstock et al., 2000; Rockne et al., 2000; Annweiler et al., 2000). However field scale biodegradation of PAHs is still debatable.

3.5.5.2 Microbial degradation kinetics

Degradation kinetics studies the rate at which microbial / enzyme reactions occur. This offers insight into biodegradation mechanics of biomass growth and substrate depletion. Many biodegradation studies focus on the rate of biodegradation or biotransformation of pollutants to predict the kinetics of microbial uptake and growth. In single pure cultures, growth linked processes are often described by Monod kinetics (Monod, 1940) whilst nongrowth (enzymes) linked biodegradation is described by Michaelis-Menten kinetics. In other studies mixtures of bacterial cultures and substrates have been studied to determine the interaction, inhibition parameters, and effects caused by the substituents of the mixture in such environment (Meyer et

al., 1984; Egli., 1995; Reardon et al., 2002). Figure 3.5 below shows the phase growth of microbes.

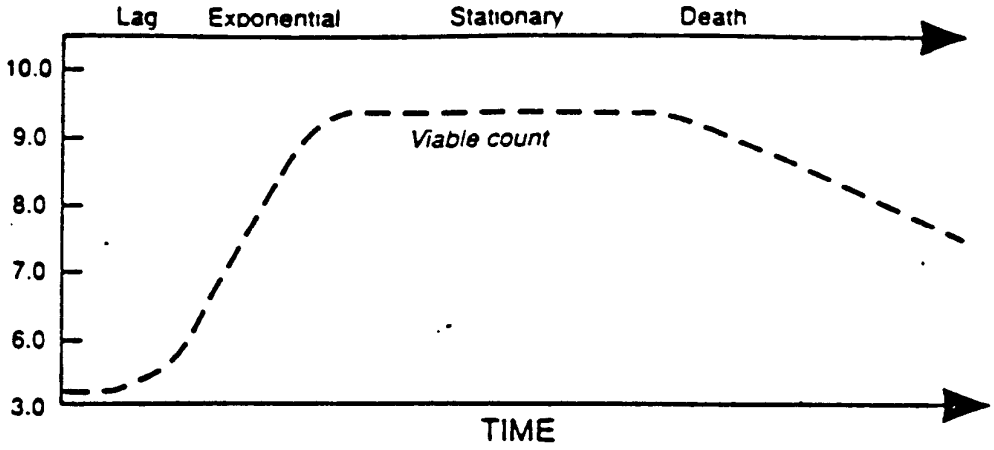

Fig. 3.5: Microbial growth phases adopted from Adriaens (2003)

The growth of microbes continues through a sequence of phases affected by time-dependent interactions between cell numbers and nutrient concentrations. During the lag phase, microbes adjust to the new substrate with no indication of increase of biomass or low initial cell counts. At the exponential growth phase, microbes are well adapted to the new substrate conditions and are characterized by a doubling of cell numbers until one or more of the nutrients become growth-limiting, and cell growth becomes flat (constant plateau). During the stationary phase there is no net growth of cells. This is due to the limiting substrate or electron acceptor and nutrients. The cell growth and death are therefore in a dynamic equilibrium. The death or decay phase results when the available substrate is depleted. The ensuing growth therefore becomes zero as the cell disintegrates and dies off.

3.5.5.3 Microbial degradation modelling

Biodegradation is usually accounted for by measuring the variables of substrate concentrations, microbe's population densities, and disappearance of organic molecules added to laboratory cultures or samples taken from the natural environments (Simkins et al., 1984, 1985). Different curves have been obtained and

modelled (Fig. 3.6). A summary of some of the models found in literature are described below.

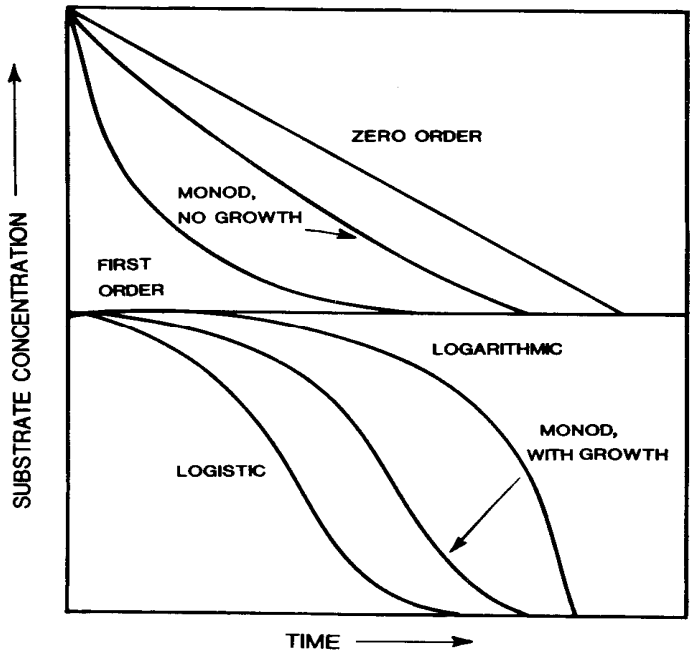

Fig. 3.6: Plots of microbial growth kinetics adopted from Meckenstock (2002)

The Monod substrate diffusion model is given by the equation

$$-\frac{dS}{dt} = \frac{kSX_b}{K_s + S} \qquad 3.36$$

where S [ML^{-3}] is the substrate concentration, X_b [ML^{-3}] is the biomass concentration, k [T^{-1}] is the maximum substrate utilization rate and K_S [ML^{-3}] is the half-saturation coefficient. If the organic compound is abundant, i.e. the substrate or major nutrients are not rate-limiting for growth ($S >> K_S$), equation 3.32 reduces to a zero order rate equation given by

$$-\frac{dS}{dt} = kX_b \qquad 3.37$$

The cell growth rate becomes equal to the maximum growth rate over the whole range of substrate concentration. If substrate concentrations are low in comparison to the affinity of the microorganism for a given substrate, i.e. the condition close to natural systems where the organic compound in the aqueous phase are accessible and hence suboptimal in terms of abundance ($S<<K_S$), equation 3.31 reduces to a first order equation given by

$$-\frac{dS}{dt} = \frac{kX_b}{K_s} S \qquad 3.38$$

The cell growth rate becomes first order in respect to substrate concentrations. In between the zero order and first order kinetic models, Monod kinetics with growth or Monod kinetics with no growth (Michaelis-Menten) models are used as shown in Figure 3.6. At higher values of substrate concentrations X_b, faster rates are predicted by Monod kinetics. Under conditions of low substrate and cell concentrations, the logistic kinetic model is used to describe the s-shape substrate diffusion curve. This type of growth kinetics is usually observed in ecology for growths which occurs as the substrate disappears (Slater, 1979; Simkins and Alexander, 1984). Logarithmic growth kinetics occurs under conditions when the initial substrate concentration is far greater than half saturation constant for growth and a low initial biomass concentration, such that cell doublings are not associated with significant mass loss. Multiple Monod kinetics formulations have been published by (Molz et al., 1986; Widdowson, 1991; Essaid and Bekins, 1997; Clemet et al., 1998). Biodegradation reactions have therefore been implemented in many solute transport codes. Codes such as Bioplume II (Rifai et al., 1988) and BIOID (Srinivasan and Mercer, 1988) model Monod type kinetics. Biochlor (Aziz et al., 1999) solves sequential reactions at different biodegradation zones. In addition RT3D (Clement, 1997) models biodegradation of oxidizable contaminants and SEAM3D (Waddill and Widdowson, 1998) solves purely kinetic biodegradation reactions. Moreover Bioscreen (Newell et al., 1996) and Bioplume III (Rifai et al., 1997) model biodegration of first order and instantaneous rate kinetics. The multicomponent transport code PHT3D, developed by (Prommer et al., 2001) is capable of modeling biodegradation of complex systems. Simpler multi-species models are simulated through a predefined reaction model.

3.5.5.4 Microbial degradation modeling in SMART

In SMART, two kinetic models are implemented, nth order kinetics as wells as Langmuir-Hinshelwood kinetics (Bold, 2003).

(i) The n^{th} order kinetics (similar to Alexander, 1999) can be described by the equation :

$$B(C) = \frac{\partial}{\partial t} C = -\lambda C^n \qquad 3.39$$

where B(C) is the degradation kinetics, C [ML^{-3}] is the concentration dissolved concentration at any time t [T], λ [T^{-1}] is the degradation rate of n^{th} order. The degradation rate therefore depends on the order of kinetics. By separating variables and solving for C, the concentration at any time t is given by

$$C(t) = C_0 e^{-\lambda t} \qquad 3.40$$

With a half life given by

$$T_{1/2} = \frac{\ln 2}{\lambda} \qquad 3.41$$

if n = 1, and

$$C(t) = C_0 \left[1 - (1-n)\lambda t\right]^{\frac{1}{1-n}} \qquad 3.42$$

with a half life given by

$$T_{1/2} = \frac{1 - 2^{n-1}}{(1-n)\lambda} \qquad 3.43$$

if $n \neq 1$.

C_0 [ML^{-3}] denotes the starting dissolved contaminant concentration at time t = 0 and $T_{1/2}$ [T] is the time at which the contaminant concentration reduces to half of the starting concentration.

(ii) The Langmuir-Hinshelwood kinetics is given by the equation:

$$B(C) = \frac{\partial}{\partial t} C = \frac{\lambda C}{1 + K_{LH} C} \qquad 3.44$$

where λ [T^{-1}] and K_{LH} [-] represent the two kinetic parameters. It is only valid for biodegradation scenarios in which the decay starts from a zero order kinetics and moves to a first order kinetics. An implicit solution to equation 3.39 is given by

$$\ln\frac{C}{C_o} + K_{LH}\frac{C}{C_o} = K_{LH} - \lambda t \qquad 3.45$$

With a half life of

$$T_{1/2} = \frac{K_{LH}/2 + \ln 2}{\lambda} \qquad 3.46$$

The parameter K_{LH} determines the order of the degradation kinetics. For K_{LH} = 0, the kinetics reduces to first order but tends to zero order as K_{LH} increases. Biodegradation is implemented in SMART by considering each model cell as independent batch system. Biodegradation with equilibrium sorption is coupled and solved iteratively while biodegradation with sorption kinetics is coupled with the integration of the intraparticle diffusion model BESSY with batch boundary conditions. The expected long term concentration with first order decay and reaction function that follows the CDE formulation is given by

$$C_\infty = C_o \exp\left[\frac{vx}{2D}\left(1 - \sqrt{1 + \frac{4\lambda D}{v^2}}\right)\right] \qquad 3.47$$

where C_o [ML^{-3}] is the input concentration and C_∞ [ML^{-3}] is the expected long term concentration at the point of compliance (Bold, 2003).

3.5.6 Particle-facilitated transport

3.5.6.1 Particle-facilitated transport in porous media

Particle facilitated or particle mediated transport, though not modeled in this thesis, is reviewed as part of the reactive code SMART. The terms particles and colloids are used interchangeably. Particles movement in porous media is well reported in literature (Avogadro et al., 1984; Marchy and Zachara., 1989; Moulin and Ouzounian, 1992; Ryan and Elimelech, 1995). Some of the particles or colloids though imperceptible can enhance the transport of solute which can endanger subsurface waters. According to (McCarthy et al., 2004) the impact of mobile colloid transport in terms of human risk from infiltrating pathogens and environmental and geological hazards from contaminant transport to groundwater can be significant. For instance colloid transport becomes increasingly important in high level nuclear waste repositories where the only form of transport is through fractures that may be developed in low permeability geological formations (Chryskopoulos and Abdel-Salam, 1995; Ryan and Elimelech, 1996). Also the effects of aqueous chemical conditions of colloid dispersion and permeability of geological settings have been carried out to improve the recovery of oil and gas (Khilar and Fogler, 1984; Cerda, 1987; Kia et al., 1987). Pathogens found in drinking wells are reported to have originated from sources such as sewage sludge, animal waste and septic fields and transported by microbial particles. Bacteria transport also has a dual role as a pathogen risk and a remedial option to degrade and or immobilize contaminants in groundwater (McCarthy and McKay, 2004). In several laboratory and field studies, particles have been found to enhance transport (McDowell-Boyer et al., 1986; Penrose et al., 1990) of contaminants such as radionuclides (Airey, 1986; Haldeman et al., 1991; McCarthy et al., 1998; Flurry et al., 2002), metals (McCarthy and Zachara, 1989; Grolimund et al., 1996; Karathanasis, 1999), organics (Vinten et al., 1983; Jonson-Logan et al., 1992), pesticides (de Jonge et al., 1998; Sprague et al., 2000; Williams et al., 2000), and inorganics in porous media (Gounaris et al., 1993). The enhancement has been attributed to the translocation of particle-reactive contaminant effects in soils (Steenhuis et al., 2005). PAH contaminants have also been reported sorbing to colloids thereby reducing their bioavailability (McCarthy and Jimenez, 1985) and consequently their uptake by microbes (Dohse and Lion, 1994).

However these PAHs could be partly available for microbes in the presence of some surfactants (Guha and Jaffe, 1996a, b; Guha et al., 1998). The particles may be in the form of clay minerals, oxides, carbonates, humic substances, microbial elucidates, bacteria, polystyrene microspheres and viruses (Higgo et al., 1993). They are mostly generated and become mobilized through processes such as chemical and physical perturbations (Lallay et al., 1987; Wood and Ehrlich, 1978; Gschwend and Reynolds, 1987), rapid infiltration of rainfall (Kaplan et al., 1993; Ryan et al., 1995), an increase in pH, decrease in ionic strength due to infiltration of dilute precipitation water (Frenkel, 1978; Abu-Sharar et al., 1987) and hydrodynamic detachment of their solutions (Abdel-Salam and Chrysikopoulos, 1995). Also increasing concentration of surfactants and dissolved organic matter and soil macropores can mobilize colloids or particles.

In groundwaters, the deposition of particles primarily controls the transport of colloids. Filtration theories are used to calculate and analyse the deposition rate in porous media. Details of the filtration theories based on the Langrangian and Eulerian approaches (section 3.3) applied to particles deposition may be referenced from (Adamczyk et al., 1983; Tien, 1989; Ryan and Elimelech, 1995).

In the unsaturated zone mechanisms such as advection and dispersion (Abdel-Salam and Chrysikopoulos, 1995; Lenhart and Saiers, 2002), preferential flow (Bourke, 1987; Steenhuis et al., 2001), diffusion (Yao et al., 1971; Schelde et al., 2002) sorption (Sposito, 1984; Toran and Palumbo, 1992; Schäfer at al., 1998a; Chu et al., 2001), film straining (Wan and Tokunaga, 1997), microbial contamination in aquifers (McCarthy and McKay, 2004) and other pore scale and air-water-solid interfaces (Lanhart and Saiers, 2002; Steenhuis et al., 2005) affect transport and distribution of particles.

3.5.6.2 Particle mediated transport modelling in SMART

In the subsurface several interactions between particles, contaminants and the host matrix can take place. According to Bold (2004) the significant interactions are between particle and matrix, contaminant and matrix, and contaminant and particle.

Biodegradation in the aqueous phase affects these interactions. In SMART the interaction process between particles and contaminant can be considered as (i) equilibrium (sorption rate of solute is significantly larger than its mass flow rate) (ii) kinetic (sorption rate of solute is comparable to its mass flow rate) and (iii) decoupled (no interaction). Assuming that immobilised particles have no effect on the effective porosity of the porous medium, the equation describing the transport of particles along a streamtube is given by

$$\frac{\partial}{\partial t}C_{c,j} + \frac{\partial}{\partial \tau}C_{c,j} = -K_j C_{c,j} \qquad 3.48$$

where $C_{c,j}$ [ML^{-3}] is the mobile particle concentration, j is an index characterising particle size and material [-] and K [T^{-1}] is the particle deposition rate coefficient. According to the right-hand side of equation (3.48) deposition is modelled by a first order rate law. If the interaction between particle and matrix can be described as an equilibrium process, then equation (3.48) is replaced by

$$\frac{\partial}{\partial t}\left(C_{c,j} + \frac{\rho_b s_{matrix}(C_{c,j})}{\theta} \right) + \frac{\partial}{\partial t}C_{c,j} = 0 \qquad 3.49$$

where ρ_b [ML^{-3}] is the bulk density of the porous medium, $s_{,matrix,}$ can be any type of equilibrium isotherm between particles and solid matrix, and θ [-] is the water content. Taking into account the sorption of contaminants by matrix, mobile and immobile particles and assuming a first order decay of the dissolved contaminants in the aqueous phase the contaminant transport for a single type of particle is described by the equation

$$\frac{\partial}{\partial t}\left[C_D + \frac{\rho_b S_{matrix}(C_D)}{n_e} + S_{cm}(C_D)C_c + \frac{S_{cim}(C_D)\rho_c \sigma_c}{n_e} \right] + \frac{\partial}{\partial \tau}\left[C_D + S_{cm}(C_D)C_c \right] = -\lambda C_D \qquad 3.50$$

where C_D [ML^{-3}] is the dissolved contaminant concentration, ρ_b [ML^{-3}] is the bulk density of the porous medium, ρ_c is the particle dry solid density, σ_c [-] is the volume of immobile particles per unit volume and λ [T^{-1}] is the first-order degradation rate constant. $S_{matrix}(C_D)$, $S_{cm}(C_D)$, $S_{cim}(C_D)$ are the ratios of sorbed solute mass per unit mass of solid matrix, mobile and immobile particles, respectively. The mechanisms

responsible for the contaminant and solid interactions determine the $S(C_D)$ relationships. If the reaction mechanism is fully decoupled i.e. the advective mass transfer is much faster than the solute mass transfer between mobile particles and the dissolved phase, the particle transport equation reduces to the equation

$$\frac{\partial}{\partial t}\left[C_D + \frac{\rho_b S_{matrix}(C_D)}{n_e}\right] + \frac{\partial C_D}{\partial \tau} = -\lambda C_D \qquad 3.51$$

The dissolved concentration C_D is calculated based on the known input parameters. Bold (2004) presented two solutions. (i) Given the total contaminant input concentration C_o entering the modelling domain, the dissolved contaminant concentrations in equations 3.50 and 3.51 can be calculated as

$$C_D = \beta C_o \qquad 3.52$$

where β [-] is the contaminant mass ratio not affected by particle mediated transport. (ii) Given that pre equilibration existed between contaminants and mobile particles entering the modelling domain and disregarding the volume of intra-particle pores of the particles, the dissolved contaminant concentration is given by the equations

$$C_D = C_o - S_{cm}(C_{D,o})C_{C,o} \qquad 3.53$$

where $C_{C,o}$ [ML^{-1}] is the concentration of mobile particles entering the model domain. The particle mediated transport is implemented in SMART by firstly modelling the particle-contaminant interactions as a retarded diffusion process. Secondly the calculated mobile and immobile particle concentrations are then applied to quantify the level of contaminant-particle interactions. The kinetic approach is applied by using the intraparticle diffusion model described in section 3.5.4.2 regarding each mobile and immobile particle in each cell equal to a lithocomponent in the integrated code BESSY. For the uncoupled transport, separate concentration calculations are made for contaminant in the dissolved phase and the sorbed phase on the particles. Assuming linear isotherms and physico-chemical equilibrium the expected long term equilibrium concentration C_∞ following the CDE formulation is given by the equation

$$C_\infty = C_o \exp\left[\frac{vx}{2D}\left(1 - \sqrt{1 + \frac{4\lambda' D}{v^2}}\right)\right] \qquad 3.54$$

where λ '[T^{-1}] is the modified biodegradation rate which is expressed by the equation

$$\lambda' = \frac{\lambda}{1 + \sum_j K_{d,c,j} C_{c,o,j}} \qquad 3.55$$

and $K_{d,c,j}$ [L^3M^{-1}] is the partitioning coefficient between contaminant and mobile particle *j*. Scenario calculations presented by Bold (2004) show an earlier breakthrough of contaminants when particle mediated transport is considered, illustrating the enhancement of contamination by particles in porous media. However the degree of enhancement somewhat depends on the bioavailability of the contaminants and the sorption between the particles and the contaminant. In addition to the numerous evidence of particle mediated transport cited in this section, de Jonge et al. (2004) in their review paper gave further evidence of colloids facilitating contaminant transport. DDT adsorbed unto suspended montmorillonite colloids was observed in a vertical transport of packed soil columns (Vinten et al., 1983) and in fractured clayey tills (Jorgensen and Frederecia, 1992). Atrazine transport in field lysimeters and soil columns have been found to occur with colloids and other contaminant complexes (Sprague et al., 2000; Seta and Karathanasis, 1999).

3.5.7 Damköhler numbers

In order to expand the scope and applicability of systems whilst still maintaining simplicity, dimensionless numbers are used to characterise the conditions and functions of solute transport in the environment. One kind of such numbers is Damköhler numbers which are used to describe the relative behaviour of reactive transport to flow mechanisms analogous to Peclet numbers which compare inertial forces to Brownian forces of fluids in motion (i.e. advective versus dispersive effects). Such numbers have the potential of reducing model parameters to the minimum.

Damköhler numbers (Da) are numbers used in chemical engineering and other disciplines to relate chemical reaction timescales to other phenomena occurring in a system. According to Fogler (1992) Da is defined as the ratio of the rate of consumption by reaction to rate of transport by advection. By combining residence

time distribution (RTD) and Damköhler distribution (DND), Carleton (2002) demonstrated the mechanistic nature of the removal process of a wetland under treatment. Seagren et al. (1993) used Damköhler numbers and NAPL dissolution rates derived from the one-dimensional advective-dispersion reaction equation which integrates first order interphase mass transfer relationship and first order biodegradation kinetics to detect whether equilibrium or non equilibrium exist and to investigate when flushing and biodegradation can efficaciously facilitate NAPL contamination dissolution in a saturated system.

For a general chemical reaction A → B of n-th order, the Damköhler number is defined as:

$$D_a = k_o C_o^{n-1} t \qquad 3.56$$

where k_o [L^3M^{-1}] is kinetic reaction rate constant, C_0 [ML^{-3}] is initial concentration, n [-] is reaction order and t [-] is time which represents a dimensionless reaction time, e.g. the dimensionless mean residence time.

Depending on the usage Damköhler numbers can also be described as Da_1: the ratio of mass transfer rate to advection rate, Da_2: the ratio of biodegradation rate to advection and Da_3: the ratio of biodegradation rate to mass transfer rate (Seagren et al., 1993).
In this thesis two Damköhler numbers were defined in the source term studies:
(i) Da_{des}, which describes the characteristic ratio of advection to desorption time scales and
(ii) Da_{bio}, which describes the characteristic ratio of advection to biodegradation time scales (Susset, 2004). In order to ensure the greatest possible range of application of the results, it was advantageous to set the characteristic time scales of the considered processes (advection, desorption, biodegradation) in relation to each other. In this way the material propagation behaviour did not depend on the absolute values of the three characteristic time scales, but on the relations of those time scales. Also the number of model parameters to be varied before the simulation runs were reduced. For general applications, bigger Damköhler numbers (*Da* >> 1) constitute faster reactions whilst smaller Damköhler numbers (*Da* << 1) constitute

slower reactions. Extreme cases, i.e. $Da \rightarrow +\infty$ und $Da = 0$, represent instantaneous reactions or no reaction processes respectively. With $Da = 1$, both the advective and reactive processes proceed at the same speed. According to Grathwohl (1997) and Bold et al. (2005) the Damköhler number for sorption / desorption taking into account pore scale geometries and grain sizes can be derived as

$$Da_{des} = \begin{cases} -\ln\left(1 - 6 \cdot \sqrt{\frac{D_{app} \cdot PV}{\pi \cdot a^2}} + 3 \cdot \frac{D_{app} \cdot PV}{\pi \cdot a^2}\right) & if \quad \frac{D_{app} \cdot PV}{a^2} < 0.1 \\ \pi^2 \cdot \frac{D_{app} \cdot PV}{a^2} - \ln\frac{6}{\pi^2} & if \quad \frac{D_{app} \cdot PV}{a^2} \geq 0.1 \end{cases} \qquad 3.57$$

where PV [T] is the pore volume, the characteristic time scale of advection, a [L] is grain radius, and D_{app} is the apparent diffusion coefficient which is quantified by equation 3.32 and applied in the kinetic sorption / desorption intraparticle diffusion model (see section 3.5.4.2). The characteristic time scale of microbial degradation can be quantified as the average life span

$$\bar{T} = \frac{\int_0^{+\infty} tC(t)\,dt}{\int_0^{+\infty} C(t)\,dt} \qquad 3.58$$

If the concentration-time relationship for first order microbial degradation described by equation 3.39 (see section 3.5.5.4) is used, then the resultant average life span is not identical with the radioactive half-life $T_{1/2}$, but rather the reciprocal value of the rate constant. Therefore the corresponding Damköhler number, Da_{Bio} (expresses the relative time scales of biodegradation to advection) for biodegradation is given by

$$Da_{bio} = \frac{PV}{\bar{T}} = \lambda \cdot PV = \ln 2 \cdot \frac{PV}{T_{1/2}} \qquad 3.59$$

The discharge behaviour of organic contaminants from a source of pollution can therefore be completely characterised on the basis of the equations (3.58) and (3.60) with the aid of the two Damköhler numbers Da_{des} and Da_{bio}.

The pore volume (PV) for a given source of contamination is given by the equation below:

$$PV = \frac{n \cdot S_w \cdot L}{Q} \qquad 3.60$$

where n [-] is porosity, S_w [-] is degree of water saturation, L [L] is the thickness of the source and Q [LT^{-1}] groundwater flux. In contaminant and seepage water ("Sickerwasserprognose") studies, breakthrough plots are sometimes expressed in units of concentrations versus water to solid mass ratios (W/F). W and F represent the time-independent volume of water passing through the source zone and the mass of solids in the source zone, respectively. A conversion between dimensionless time and water-solid mass ratio is given by the relations:

$$t' = \frac{M/A}{n_e \cdot L} \cdot W/F \qquad 3.61$$

where t' [-] is time normalised by pore volume, M/A [ML^2] is solid mass per unit cross-sectional area, and W/F [L^3M^{-1}] is the water-solid mass ratio. The normalised pore volume time is given by the equation:

$$t' = t/PV \qquad 3.62$$

This conversion assumes that groundwater flow is at steady state. The use of the normalised pore volume time t' offers a crucial advantage in the context of setting of tasks, because the retention time of the pollutant in the mobile phase is thereby included. This enters directly in the determination of the Damköhler numbers (Da_{des} and Da_{bio}) with which the relative contributions of desorption kinetics and the microbial degradation in the discharge behaviour are quantified.

Chapter 4

4 SOURCE TERM MODELLING

4.1 Introduction

One goal of this study was the development of a source term function for organic pollutants (in particular non volatile PAHs). This function was to quantify the time–dependent leaching behaviour of materials from sources of contaminants and serve as a practical tool in seepage water prognosis. The source term function included primarily measured variables (for example source term thickness, pollutant-solid distribution coefficients, seepage water flow rates and contents of typical pollutants).

4.2 Methodology

Initially, selections of realistic representative values and or ranges of values of measured variables for the leaching behaviour were made (thickness of source zone, pollutant solid interaction parameters such as foc, porosity and bulk density, flow rate, pollutant type etc.) to cover the relevant spectrum of leaching curves. Laboratory results (Henzler, 2004; Susset, 2004) mainly focusing on seepage water prognoses were also included. Series of linear forward simulations were run with the modelling tool SMART (Streamtube Model for Advective and Reactive Transport) for each combination of variables. Breakthrough curves of each simulated scenario were evaluated. Depending on the type and properties of the organic pollutant under consideration, different types of effluent leaching curves were obtained. Appropriate mathematical functions were then used to characterise these numerical curves. In general two groups of curves were obtained with coefficients which were obtained by fitting the analytical curves to the numerical curves while ensuring minimum discrepancies. The optimization of the curves and minimisation of the discrepancies were accomplished by the method of least squares. As a result of this step, the source strength function for the leaching behaviour of organic pollutants was obtained. This function does not only serve as seepage water management tool but also as a close-to-reality boundary condition for the transport modelling of organic contaminants in the subsurface.

4.3 Processes and modelling assumptions

In order to determine the source strength function, the major and relevant processes must be taken into consideration. Advection, desorption kinetics and microbial degradation were considered as relevant discharge processes. Advection accounted for the bulk movement of the fluid or liquid phase as polluted solutes deplete down to the transport zone. The depletion or release of the solutes from the solid grain matrix with time is accounted for by the desorption kinetics as described by the intraparticle diffusion model (section 3.5.4.2). Microbial degradation which accounts for the transformation of the solutes as they encounter microorganisms in the dissolved phased was modelled with a first order rate kinetics (see section 3.5.5). The following modelling assumptions were made:

- The flow in the unsaturated zone was at steady state with time invariant flow. This is acceptable for longterm investigations in which average concentrations are more representative rather than variations or extreme values.
- The model parameters that quantify the reactive processes such as desorption (n_{ip},ρ, K_d, D_{aq} und grain radius) and microbial degradation (λ and/or $T_{1/2}$) were spatially constant.
- The soil materials were homogeneous with respect to grain size and lithology.
- Desorption kinetics was simulated with the aid of the intraparticle diffusion model.
- Solute transport in the interparticle pores is purely advective i.e. there is no mass transfer between streamtubes (no dispersion).
- A concentration equilibrium existed between mobile and immobile phase at the beginning of simulation (t=0). This concentration equilibrium is determined by the distribution coefficient Kd.
- Microbial degradation is represented in the model by a first order rate law. Degradation occurred solely in the interparticle pore area.

4.4 Results and discussion

4.4.1 Input parameters and /or model parameter ranges

Table 4.1 below shows the results of the determination of appropriate ranges of the model parameters. Using Phenanthrene as model pollutant (representative of the PAH) and Ashes from burnt household waste (HMVA), which was made available from BAM in the context of the BMBF project "Sickerwasserprognose" as a reference material (Henzler, 2004) of the porous medium, the model parameters were varied.

Table 4.1: Selection of parameter ranges for the SMART process simulations with Phenanthrene as model pollutant and HMVA BAM as solid material.

Parameter	Range of values
Thickness of source (m)	0.5 – 1
Porosity (-)	0.24 – 0.33
Bulk density (kg/m³)	$2.57 \cdot 10^{3}$ – $2.73 \cdot 10^{3}$
Discharge (mm/a)	300 – 700
Aqueous diffusion coefficient (m²/s)	$6.5 \cdot 10^{-10}$ – $9.1 \cdot 10^{-10}$
Intraparticle porosity (-)	0.0001 – 0.015
Grain radius (m)	$1 \cdot 10^{-7}$ – $3 \cdot 10^{-7}$
Distribution coefficient (l/kg)	55.4
Initial pollutant mass per solid mass in the source (mg/kg)	0.8

4.4.2 Pollutants leaching simulations with SMART

The source strength function was derived from the results of many simulation runs with the model tool SMART when the parameters where varied. During the simulations the two Damköhler numbers, Da_{Des} and Da_{Abb} were varied in an interval of $0.001 \leq Da_{Des} \leq 1000$ and/or $0.001 \leq Da_{Bio} \leq 1000$ independently from each other by an order of magnitude. A small Damköhler number corresponds to a “slow desorption“ and / or a “slow biodegradation“. A big Damköhler number corresponds to a “fast desorption“ and / or a “fast biodegradation“.

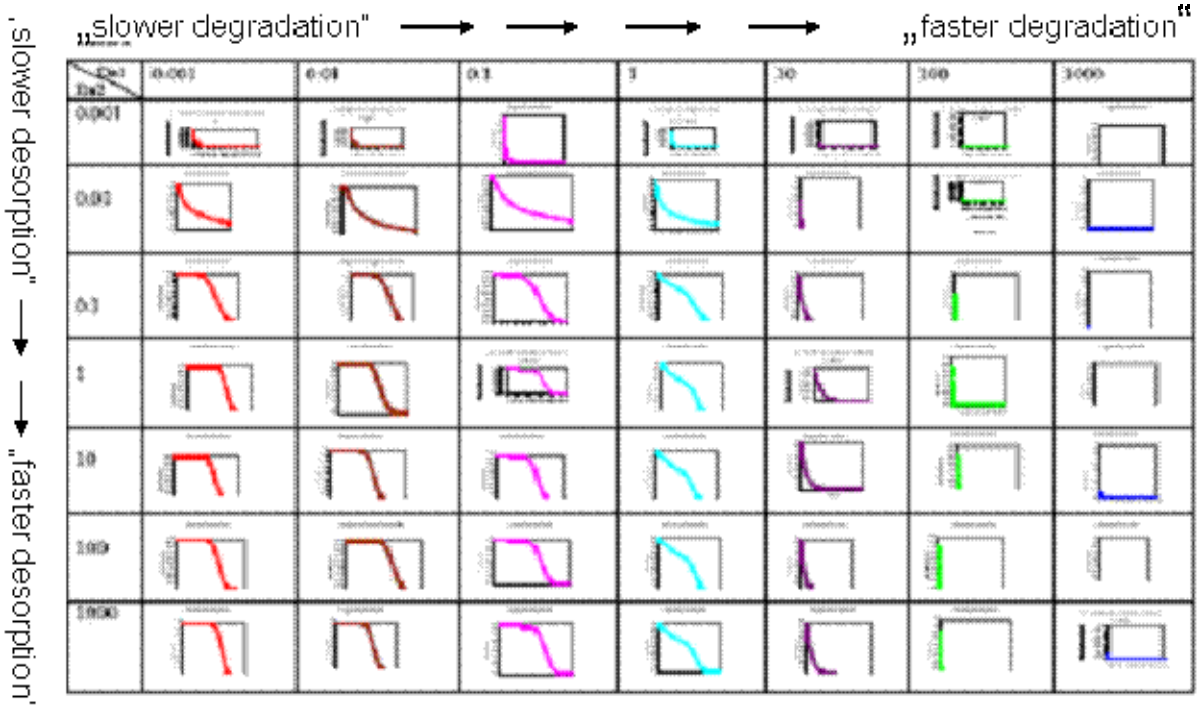

Fig. 4.1: Leaching behaviour of organic pollutants for Damköhler numbers from the intervals $0.001 \leq Da_{Des} \leq 1000$ and/or. $0.001 \leq Da_{Bio} \leq 1000$.

Figure 4.1 shows a general overview of the breakthroughs obtained from the SMART simulations. Two curve group types of concentration time curves could be derived qualitatively: (i) For the parameter interval $0.1 \leq Da_{Des} \leq 1000$, S-shaped curves (e.g. sigmoid) with points of inflexion were obtained and (ii) for the interval $0.001 \leq Da_{Des} \leq 0.1$ curves with positive curvature (“bent towards the left”) were found. The different shapes of the leaching behaviour depend on the time scale and the dominant process. There was a general sharp drop and little breakthrough concentrations in

regions where diffusion was very low. This may show the extent of the contact period between the solute pollutants and the surrounding matrix. Regions of faster desorption experienced long period of constant concentration in the effluent followed by a sharp drop. The higher rate of replenishment of the solutes from the immobile to mobile phase accounts for the long periods of constant relative concentration in the effluent. Again in regions where advection, desorption and degradation time scales were of equal importance, the leaching behaviour was a gradual process. Moreover regions of higher biodegradation time scales exhibited low effluent concentrations independent of the other processes. This may underscore the importance of biodegradation. Figures 4.2 and 4.3 below represent the two curve group types. The axes of coordinates in these illustrations represent the relative leaching concentration (ordinate axis) and the time (abscissa axis), normalised with the initial concentration C_o (t=0 at mobile – immobile phase equilibrium) and pore volume PV respectively. The normalised time t' [T] is given by equation (3.62).

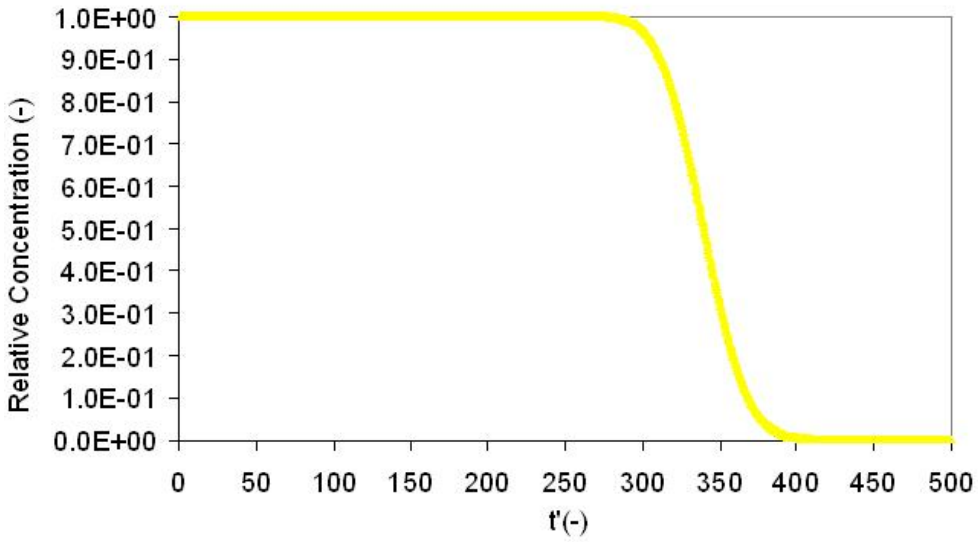

Fig. 4.2: S-shaped curve group type of the leaching behaviour for the case $0.1 \leq Da_{Des} \leq 1000$. The relative leaching concentration is represented as a function of dimensionless pore volume time t' after equation 3.63.

Figure 4.2 shows a constant value in the relative concentration for pore volume time from 0 to more than 300 and then decreases sharply up to 400 pore volumes. The curve then flattens to zero. As the desorption rate increases slowly the leaching in the

mobile phase remains at equilibrium until about 300 pore volumes when leaching proceeds sharply. Within 100 pore volumes the concentration drops to almost zero.

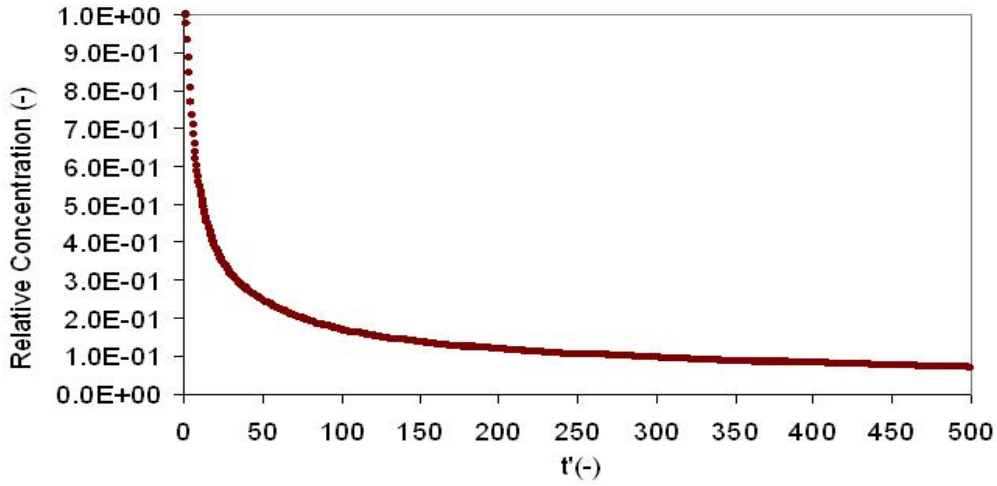

Fig. 4.3: Left bent curve group type of the leaching behaviour for the case $0.001 \leq Da_{Des} < 0.1$. The relative leaching concentration is represented as a function of dimensionless pore volume time t' after equation 3.63.

Figure 4.3 shows a sharp decrease in relative concentration for pore volume time ranging from 0 to 50 and then decreases steadily up to 470 pore volumes. The curve then flattens till the end of the simulation period. In this scenario the time scale of desorption is less than or equal to one-tenth of the time of advection. This relative sharp decrease in the relative concentration shows how fast the solute is leached out of the source zone. As more solute is released into the mobile phase, the rate of leaching becomes steady and then flattens until when the leaching drops close to zero. The scenarios are analogues to the long term tailing effects in tracer test experiments and pump and treat remediation technologies.

Both curve group types, behave similarly when $100 \leq Da_{Bio,}$ independent of the Damköhler number for desorption, Da_{Des}.

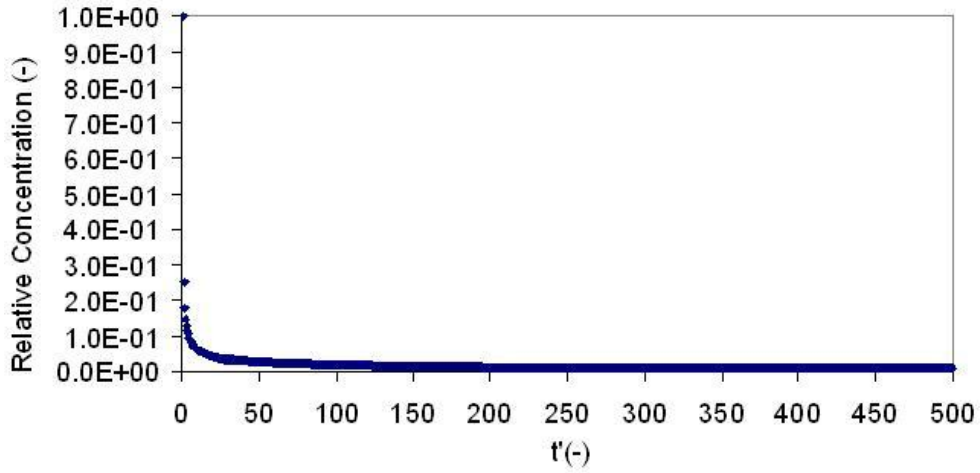

Fig. 4.4: Flattened curves of the leaching behaviour for cases $100 \leq Da_{Bio}$ and independent of the value of Da_{Des}. The relative leaching concentration is represented as a function of dimensionless pore volume time t' after equation 3.63.

Figure 4.4 shows almost a sudden drop in concentration to zero for all pore volume times. This scenario occurs when the microbial degradation rate is very fast such that almost all pollutants that get into the aqueous phase are degraded by the microbes leaving almost nothing to be observed as the outlet concentration.

4.5 Source term function

In order to characterise the leaching behaviour of the source pollution, a source term function was derived. Two general function types were basically identified, firstly those time dependent leaching behaviour for the cases $Da_{Des} > 0.1$ and secondly for $Da_{Des} < 0.1$. The function parameters for both relations were optimally adjusted to the series of SMART simulation runs conducted

4.5.1 Source term function for the parameter interval $0.1 \leq Da_{Des} \leq 1000$

In this section Damköhler numbers for desorption within the interval $0.1 \leq Da_{Des} \leq 1000$ were considered. The Damköhler number for degradation was varied for the entire parameter range under investigation, $0.001 \leq Da_{Bio} \leq 1000$. Using the appropriate SMART results from Figure 4.1 for Da_{Des} and Da_{Bio} the following source

strength function was determined for the ranges of values of the Damköhler numbers defined above:

$$\frac{c}{c_0} = \frac{\exp\left(-0.74 \cdot Da_{Bio} \cdot t'/R\right)}{1+\exp\left[3.45 \cdot \left(Da_{Des}\right)^{0.15} \cdot \left(t'-R\right)/R^{0.74}\right]} \qquad 4.1$$

Equation (4.1) shows the relative leaching concentration as function of the dimensionless time t'. In this equation the two Damköhler numbers, Da_{Des} and Da_{Bio} as well as the retardation factor R appear explicitly as function parameters. The constant values appearing as coefficients, powers and / or exponents were optimally determined by the adjustment of the source term function to the results of the SMART simulations by means of the method of the least squares (using Excel solver) up to two decimal places.

The following curves (Figures 4.5 – 4.8) resulted for the case of "very fast" desorption (Da_{Des} = 1000) when parameter values were adjusted for different values of the retardation factor R and the Damköhler number for degradation Da_{Bio} as shown in Table 4.2. The broken curves represent the source strength function in accordance with equation (4.1), and the coloured solid curves show the SMART results.

Table 4.2: Scenario parameters for very fast desorption leaching behaviour of Phenanthrene.

Parameters / Scenario	Retardation factor	Dades	Dabio
s1	10	1000	0, 0.01,1,10 and 1000
s2	32	1000	0, 0.01,1,10 and 1000
s3	105	1000	0, 0.01,1,10 and 1000
s4	340	1000	0, 0.01,1,10 and 1000

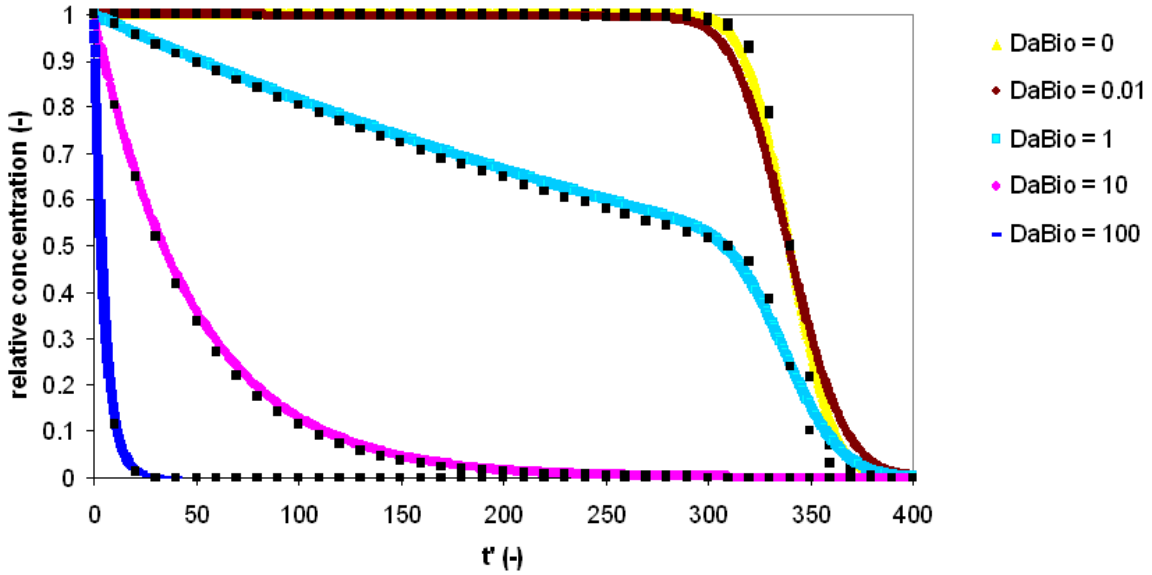

Fig. 4.5: Comparison of long term source strength functions of equation (4.1) (broken curves) with the SMART results (solid curves) for the case Da_{Des} = 1000 with a retardation factor of R = 340.

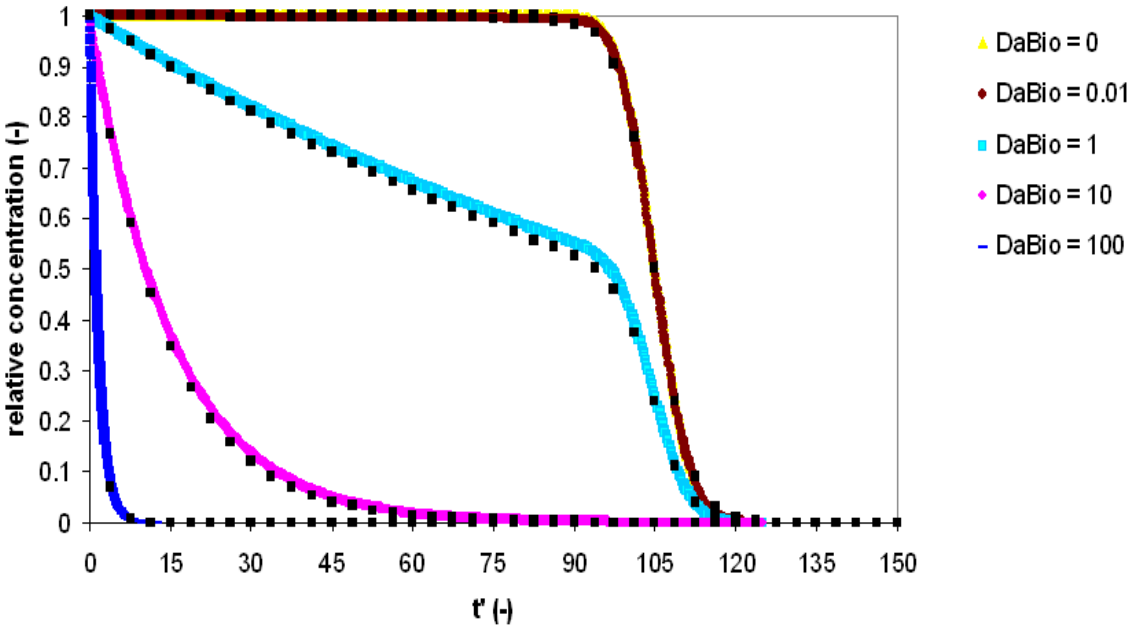

Fig. 4.6: Comparison of long term source strength functions of equation (4.1) (broken curves) with the SMART results (solid curves) for the case Da_{Des} = 1000 with a retardation factor of R = 105.

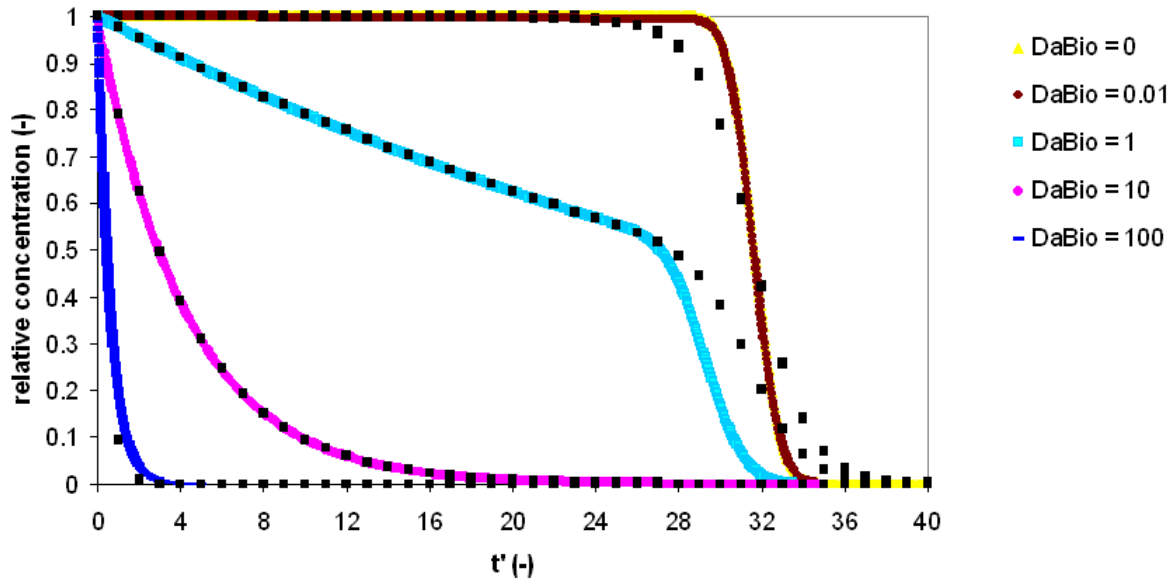

Fig. 4.7: Comparison of long term source strength functions of equation (4.1) (broken curves) with the SMART results (solid curves) for the case Da_{Des} = 1000 with a retardation factor of R = 32.

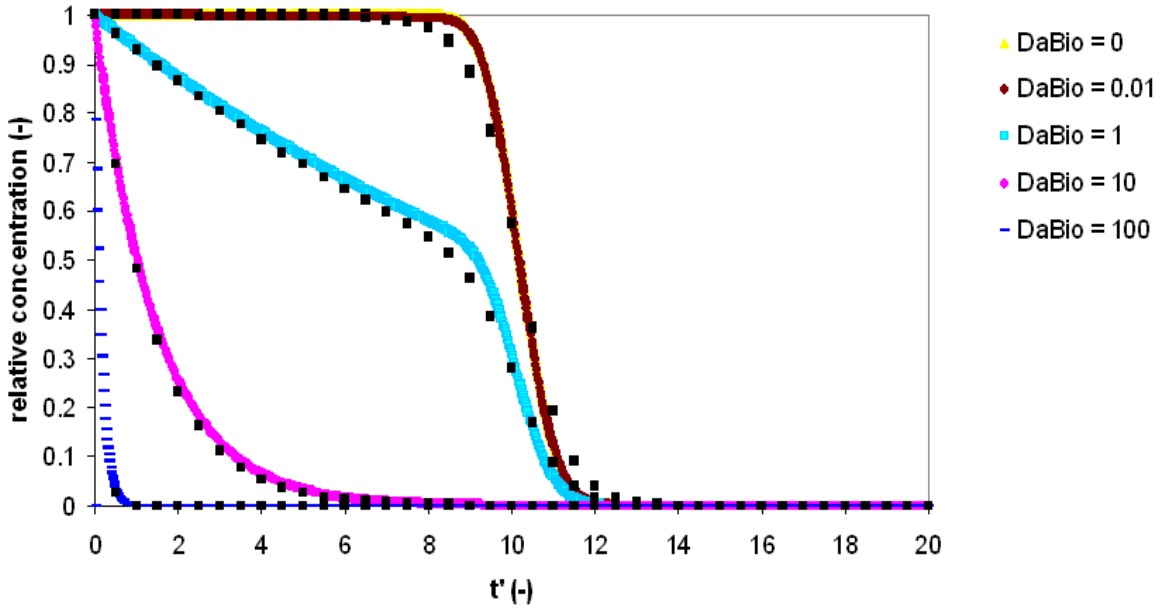

Fig. 4.8: Comparison of long term source strength functions of equation (4.1) (broken curves) with the SMART results (solid curves) for the case Da_{Des} = 1000 with a retardation factor of R = 10.

Figures 4.9 – 4.12 show a similar comparison as above, but the Damköhler number for desorption was set equal to 1, i.e. the characteristic time scale of the desorption was equal to the pore volume. The parameters R and Da_{Bio} were the same as in Table 4.2.

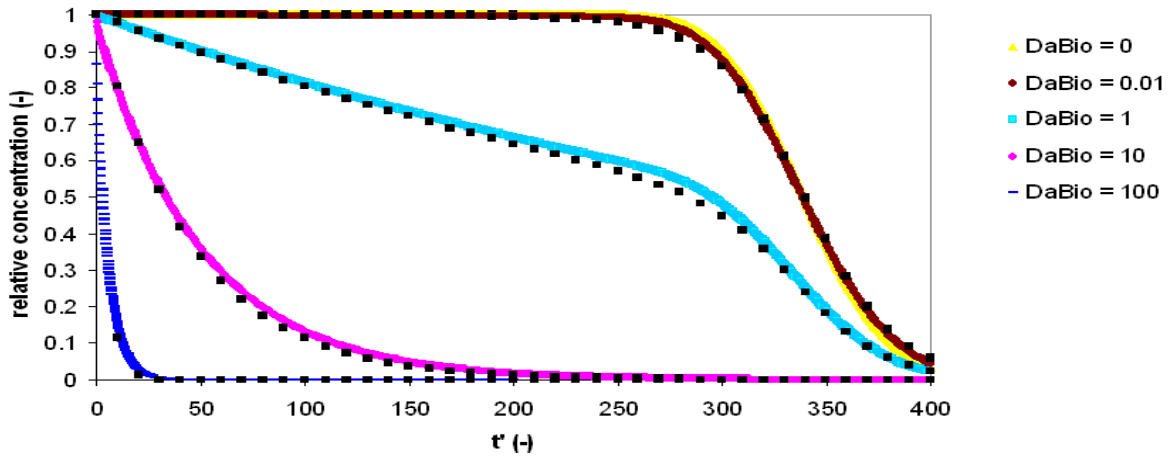

Fig. 4.9: Comparison of long term source strength functions of equation (4.1) (broken curves) with the SMART results (solid curves) for the case Da_{Des} = 1 with a retardation factor of R = 340.

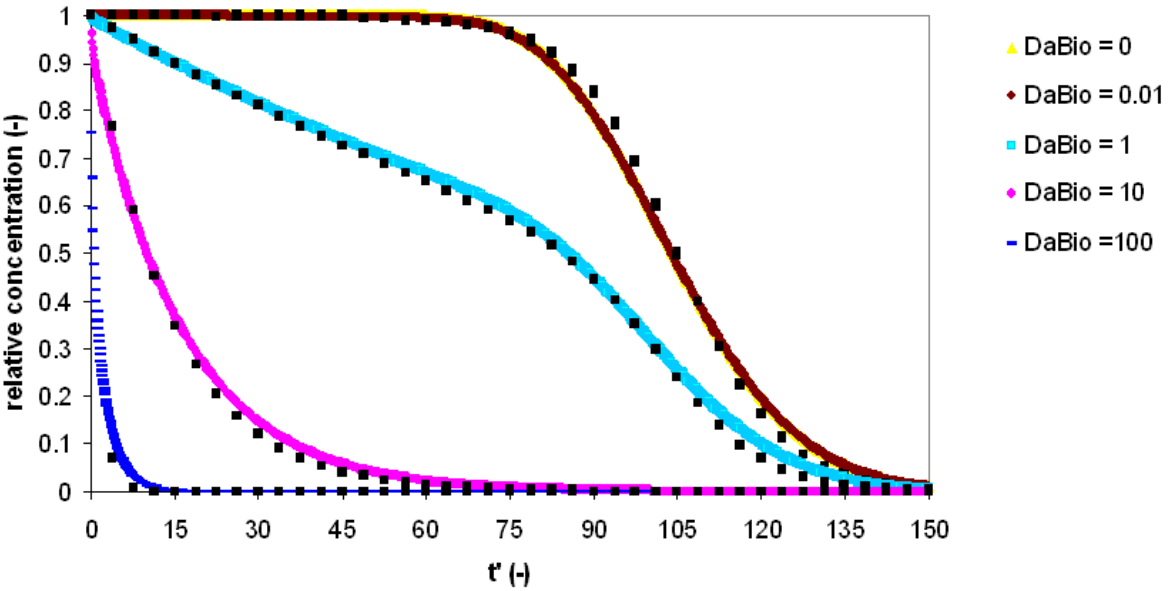

Fig. 4.10: Comparison of long term source strength functions of equation (4.1) (broken curves) with the SMART results (solid curves) for the case Da_{Des} = 1 with a retardation factor of R = 105.

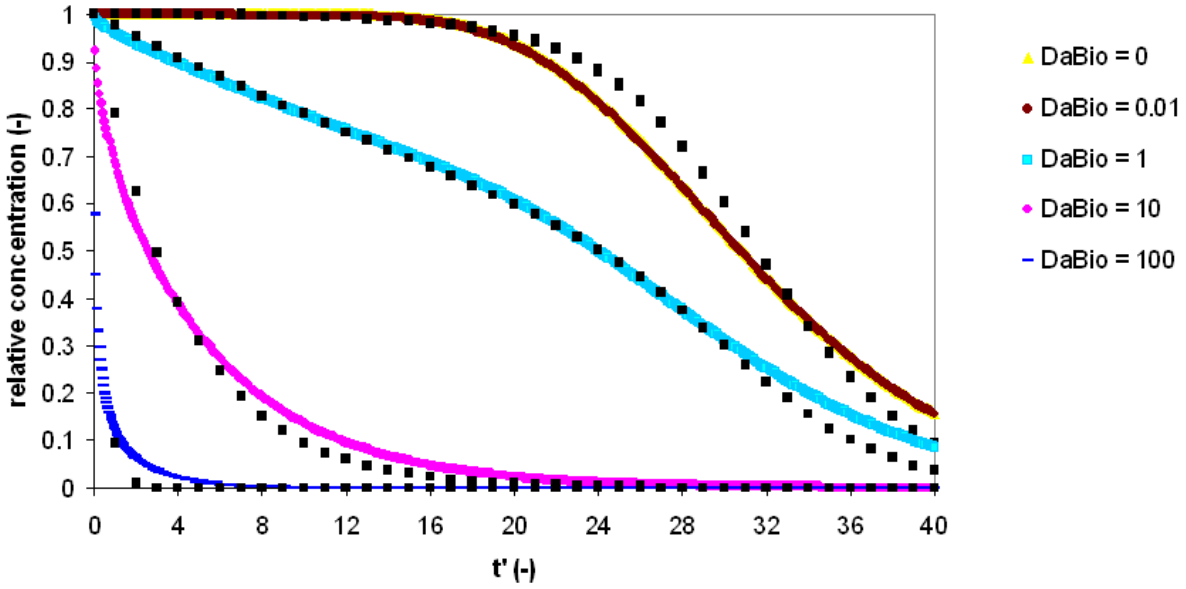

Fig. 4.11: Comparison of long term source strength functions of equation (4.1) (broken curves) with the SMART results (solid curves) for the case Da_{Des} = 1 with a retardation factor of R = 32.

.

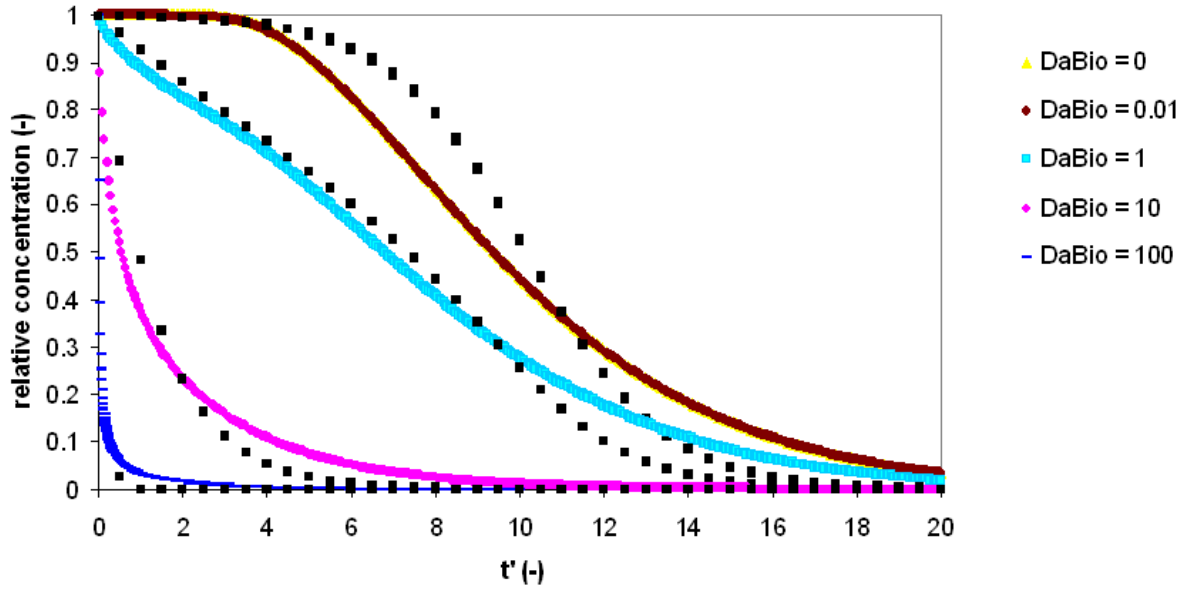

Fig. 4.12: Comparison of long term source strength functions of equation (4.1) (broken curves) with the SMART results (solid curves) for the case Da_{Des} = 1 with a retardation factor of R = 10.

The fitting of the source strength function after equation (4.1) to the SMART results is at least good in all cases and in some part very good. In view of the large range of parameter values considered and the uncertainity associated with the site-specific parameters, the source strength function after equation (4.1) can be considered as a reliable prognosis tool for the quantification of source strength behaviour of organic pollutants when $Da_{Des} \geq 0.1$. It is to be noted that, the function adjustments for the entire parameter range could be made solely by one full set of the function's coefficients.

4.5.2 Source term function for the parameter interval $0.001 \leq Da_{Des} < 0.1$

In addition to section 4.5.1, the Damköhler numbers for desorption within the interval $0.001 \leq Da_{Des} < 0.1$ were considered. The Damköhler number for degradation was varied for the entire investigation range as shown in Table 4.3. Using the appropriate SMART results from Fig. 4.13, the following source strength function was determined for the corresponding intervals of the Damköhler numbers Da_{Des} and Da_{Bio}:

$$\frac{c}{c_0} = \frac{\exp\left(-0.74 \cdot Da_{Bio} \cdot t'/R\right)}{1 + 5.07 \cdot \max\left\{0, t'-1\right\}^{0.6} / \left(Da_{Des}^{0.55} \cdot R^{0.93}\right)} \qquad 4.2$$

Table 4.3: Scenario parameters for slow desorption leaching behaviour of Phenanthrene.

Parameters / Scenario	Retardation factor	Dades	Dabio
s1	10	0.01	0, 0.01,1,10 and 1000
s2	32	0.01	0, 0.01,1,10 and 1000
s3	105	0.01	0, 0.01,1,10 and 1000
s4	340	0.01	0, 0.01,1,10 and 1000

As already described for equation 4.1, equation 4.2 also shows the relative leaching concentration as function of the dimensionless pore volume time t'. As function

parameters the two Damköhler numbers of Da_{Des} and Da_{Bio} as well as the retardation factor R appear explicitly again. The constant values appearing as coefficients, powers and / or exponents were optimally determined by the adjustment of the source term function to the results of the SMART simulations by means of the method of the least squares (using Excel solver) up to two decimal places.

The following curves (Figures 4.13 – 4.16) resulted for the case of "slow" desorption (Da_{Des} = 0.01) when parameter values were adjusted for different values of the retardation factor R and the Damköhler number for degradation Da_{Bio} as shown in Table 4.3. The black curves represent the source strength function in accordance with equation (4.2), and the coloured solid curves show the SMART results.

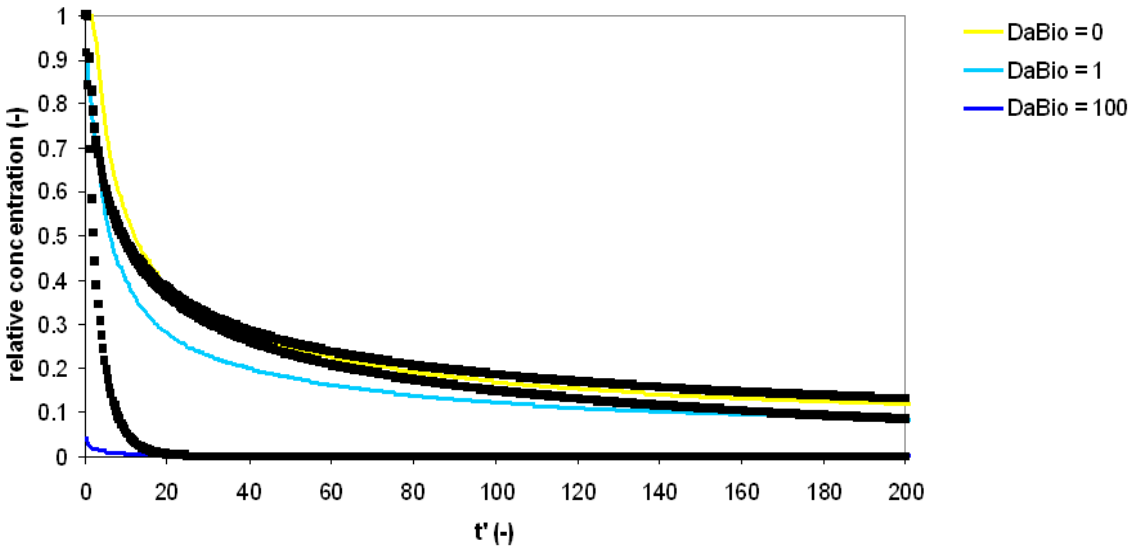

Fig. 4.13: Comparison of long term source strength functions of equation (4.2) (broken curves) with the SMART results (coloured solid curves) for the case Da_{Des} = 0.01 with a retardation factor of R = 340.

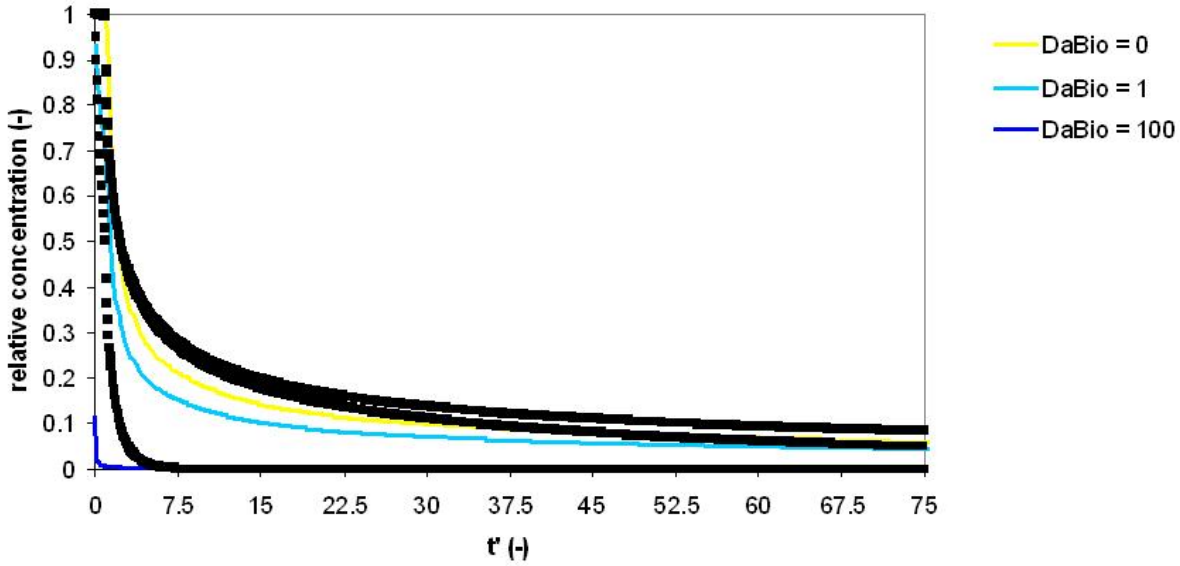

Fig. 4.14: Comparison of long term source strength functions of equation (4.2) (broken curves) with the SMART results (coloured solid curves) for the case Da_{Des} = 0.01 with a retardation factor of R = 150.

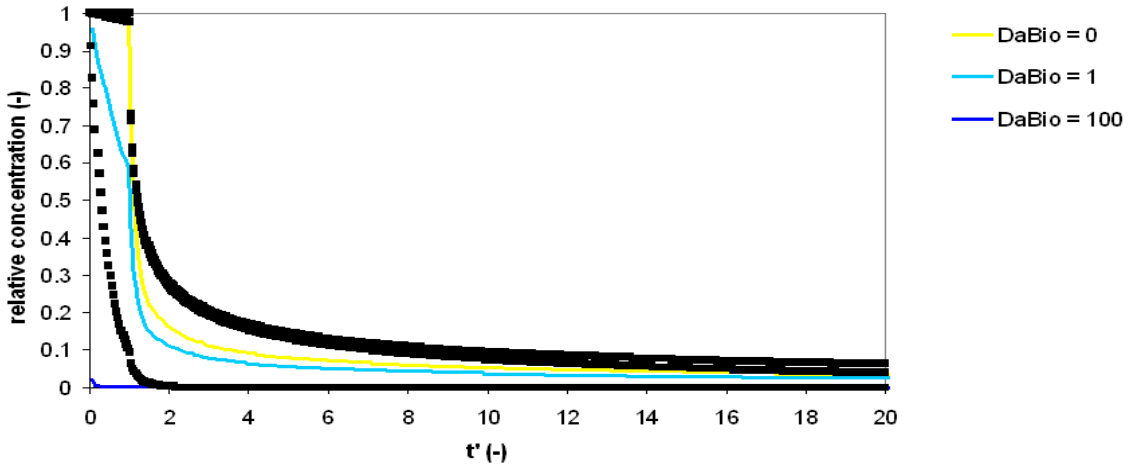

Fig. 4.15: Comparison of long term source strength functions of equation (4.2) (broken curves) with the SMART results (coloured solid curves) for the case Da_{Des} = 0.01 with a retardation factor of R = 32.

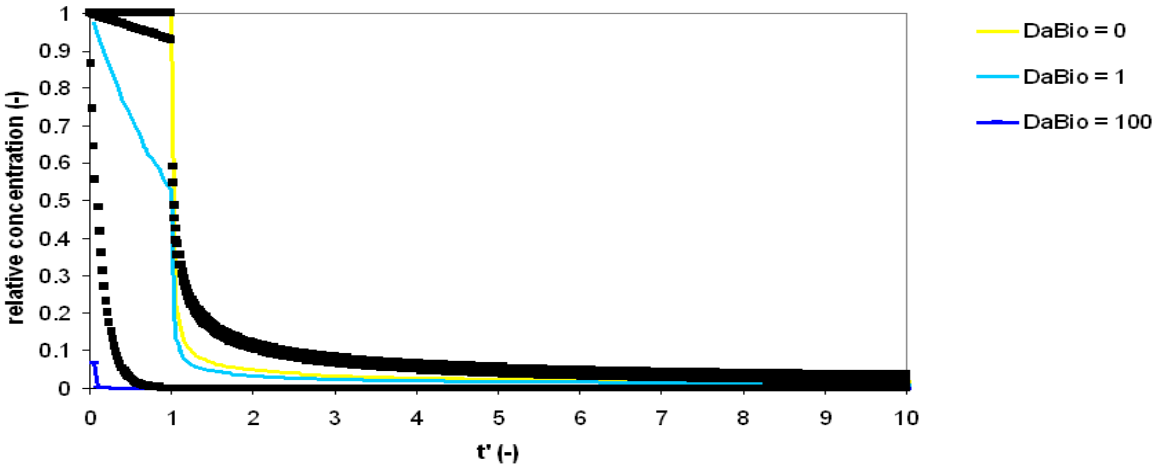

Fig. 4.16: Comparison of long term source strength functions of equation (4.2) (broken curves) with the SMART results (coloured solid curves) for the case Da_{Des} = 0.01 with a retardation factor of R = 10.

There is in general a good agreement between the source term function given by equation 4.2 and the SMART results as before. In view of the large range of parameter values considered plus parameter uncertainty, the source strength function after equation (4.2) can be considered as a reliable prognosis tool for the quantification of source strength behaviour of organic pollutants when Da_{Des} < 0.1. It is to be noted that the function adjustments for the entire parameter range could be made solely by one full set of the function's coefficients.

The relations for the relative discharge concentrations, indicated in equations 4.1 and 4.2 represent a practical aid to the quantification of the leachate behaviour of organic pollutants in the context of the seepage water prognosis. The derived equations 4.1 and 4.2 are therefore implemented in an Excel spreadsheet designed by Liedl (2006). A simple conversion is possible between the time t' and the water solid material relationship W/F standardized to the pore volume (see Appendix 2 for details of the Excel spreadsheet).

Chapter 5

5 TRANSPORT MODELLING AT THE LYSIMETER SCALE

5.1 Introduction

Quite an extensive amount of work was been undertaken within the BMBF research initiative ”Sickerwasserprognose” concerning the transport of contaminants from the unsaturated zone to the saturated zone. The main objective of this research activity was to propose a method that could reliably predict the concentration and mass of pollutants at the point of compliance, i.e. at the groundwater table, in accordance with the German Soil Protection Act (BBodSchV, 1998). One major item of “Sickerwasserprognose” was the model-based prediction of groundwater pollution. Corresponding tools were to account for all relevant processes, which are responsible for a decrease (sorption, biodegradation) or an increase of groundwater pollution risk (particle-facilitated transport, preferential flow). In this study lysimeter outlets were used as an index of the point of compliance. The modelling of the reactive material transfer on the lysimeter scale places an important link between the small-scale laboratory results (Rahman, 2000; Cata, 2003; Schmidt, 2003; Bold, 2004; Cai, 2004; Christ, 2004; Henzler, 2004; Madlener, 2004 and Susset, 2004) and the simulation of large scale or field scale scenarios (Boesten and van der Pas, 2000; Schierholz et al., 2000; Harris et al., 2000). Lysimeter data needed as model inputs information were made available from the research centre in Jülich and GSF, München-Neuherberg. In the following model results for both lysimeter locations with identical methodology are presented. Details of the modelling steps were described in each case by the example of the Jülich lysimeters.

5.2 Preparation and analysis of lysimeter data for transport modeling

5.2.1 Lysimeters from Jülich research centre.

Figure 5.1 shows a longitudinal cross section of the four identically constructed lysimeters, which are operated by the Jülich research centre at the Merzenhausen test site. Figure 5.1 also shows the source and transport zones, and the depths at which samples were taken for measurements. In three of the lysimeters, the source

zone layers were filled with the low contaminated BAM reference materials demolition waste (Bauschutt), contaminated soil (Altlastboden) and ashes of burned domestic waste (Hausmüllverbrennungsasche-HMVA). The fourth lysimeter was used as a reference lysimeter and the source zone was packed with gravel instead of polluted material. Apart from the lysimeter geometry, soil parameters relevant for the transport process were as shown in Tables 5.1 and 5.2 which were derived from an associated report prepared by Pütz et al. (2002) and Weihermüller (2005). The associated application report as well as data made available by the coordinating agency of the "Sickerwasserprognose" research initiative formed the bases of the definition of the other model parameters. The lysimeter flow was calculated using measured inflow and outflow data values. A temporally constant flow of $4.48*10^{-8}$ m³/s, corresponding to a specific flow rate of $2.24*10^{-8}$ m/s (lysimeter cross sectional area is 2 m^2) was obtained.

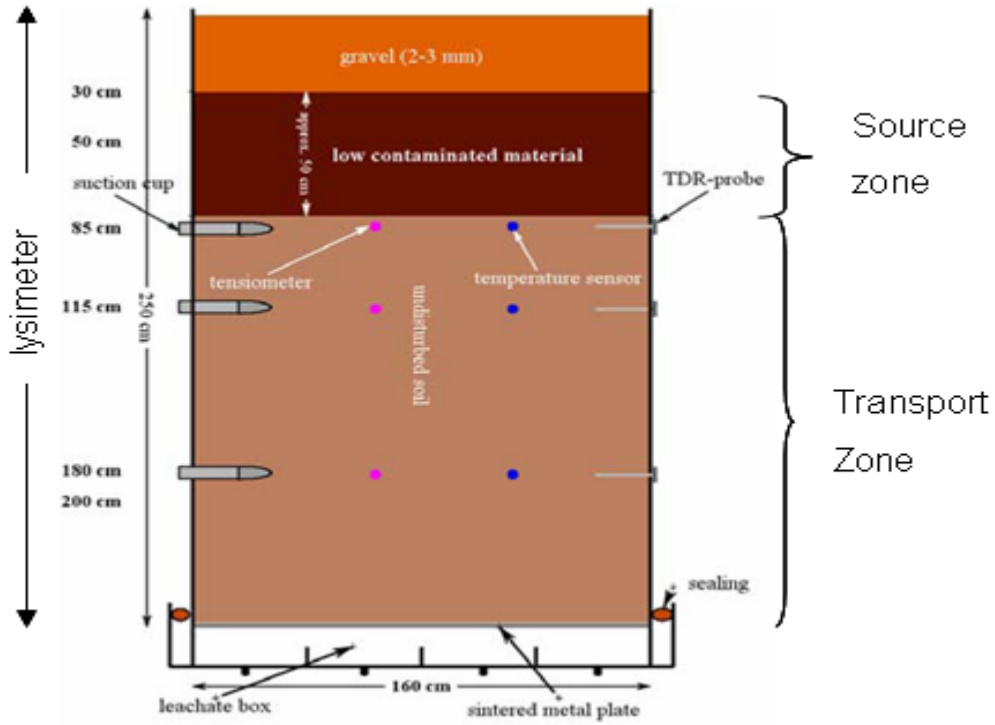

Fig. 5.1: Schematic longitudinal cross section of lysimeter (adopted and modified from Pütz et al., 2002).

Table 5.1: Physico-chemical soil parameters for the test site Merzenhausen. Soil types after AGBoden (1994). All units based on mass of dry matter except field capacity, (FC), based on saturated soil (adopted from Weihermüller, 2005)

Parameter	Horizon						
	Ap 0 -35 [cm]	Al 35 - 47 [cm]	Bt 47 -97 [cm]	Btv 97 -150 [cm]	Bv 150 - 210 [cm]	Bcv 210 - 225 [cm]	C 225 - 280 [cm]
clay (<2 m)[%]	13.4	18	22.7	18	16	12.7	13.1
silt (2 - 63 µm) [%]	81.9	78.9	74.9	79.4	81.1	82.8	81.9
sand (>63 µm) [%]	4.7	3.1	2.4	2.6	2.9	4.5	5
soil	Ut3	Ut4	Ut4	Ut4	Ut3	Ut3	Ut3
particle density [g cm−3]	1.48	1.53	1.54	1.56	1.52	1.45	1.59
particle density [g cm−3]	2.62	2.64	2.64	2.65	2.65	2.67	2.67
FC [%]	39.2	42.2	39.5	39.2	38	37.1	35
pH-value ($CaCl_2$)	7.1	7.1	7.1	7	6.8	7.6	7.6
humus [%]	1.8	0.6	0.4	0.2	0.1	0.2	0.3
CEC [meq 100 g−1]	10.5	10.5	11.9	16.3	12.5	10	15
S- value [meq 100 g−1]	13.56	11.58	14.29	14.41	11.6	14.1	17.39
carbonate [% $CaCO_3$]	0.5	0.4	0.4	0.3	0.4	11.9	15.6

Table 5.2: Soil parameters of the test site Merzenhausen: The saturated moisture content Θ_s as well as van Genuchten parameters *n* and *α* were fitted with the retention curve fit program RETC (van Genuchten et al., 1991). The saturated hydraulic conductivity *Ks* was taken from Pütz et al. (2002). The residual moisture content Θ_r was set to 0 for all fits.

Horizons	A_p	A_1	B_t	B_{tv}	B_v	B_{cv}	C
Depth	0-35	35-47	47-97	97-150	150-210	210-225	225-280
Θ_s [cm^3 cm^{-3}]	0.436	0.438	0.372	0.403	0.414	0.454	0.414
n [-]	1.353	1.215	1.234	1.259	1.338	1.490	1.411
α [cm^{-1}]	0.0064	0.0195	0.0048	0.0056	0.0053	0.056	0.0041
Ks [cm h^{-1}]	1.8629	0.1615	0.0595	0.05625	0.05625	0.05625	0.05625

The moisture content for a single horizon corresponding to the van Genuchten parameters α and n in Table 5.2 is given by

$$\theta = \theta_s\left(1+\left(\alpha\psi\right)^n\right)^{1/n-1} \qquad 5.1$$

The average moisture content corresponding to the van Genuchten parameters α and *n* in Table 5.2 was derived by using the relation:

$$\theta_{ave} = \frac{\Sigma \theta_s \left(1+\left(\alpha\psi\right)^n\right)_i^{1/n-1} * h_i}{\Sigma h_i} \qquad 5.2$$

where h_i [-] is the thickness of soil horizons, θ_s [-] the saturated moisture content, i is the index of soil horizon and ψ [L] the soil water pressure is head. The relation between the unsaturated hydraulic conductivity and soil water pressure is expressed according to the formula given by Mualem (1976)

$$K = K_s \frac{\left\{1-\left(\alpha\psi\right)^{n-1}\left[1+\left(\alpha\psi\right)^n\right]^{1/n-1}\right\}^2}{\sqrt{\left[1+\left(\alpha\psi\right)^n\right]^{1-1/n}}} \qquad 5.3$$

in which the average permeability K [LT^{-1}] could be simply equated to the specific flow($2.24*10^{-8}$ m/s). That assumption was fulfilled under the prevailing conditions (time-independent flow, no accumulation at the lysimeter surface area).

A value of 0.34 was obtained for θ_{ave}. Averaging the total porosity at each horizon produced a representative total porosity, n_{tot} of 0.42. This led to an average saturation, $S = \theta_{ave}/n_{tot}$ of 0.81.

Average bulk density of 1.536 g/cm³ was derived for the transport material, Parabraunerde. This value was obtained by finding the arithmetic mean of the horizon densities reported by Pütz et al. (2002) for the A and B-horizons as shown by the Merzenhausen data set. A material density of 2.647 g/cm³ was therefore calculated from the particle density and the total porosity.

The average grain size of the material was determined by the mass proportions of clay, silt and sand present in the Parabraunerde. The percentage proportions of the material which filled the transport layer of the lysimeter were 22.01% clay, 74.47% silt and 2.52% sand and the average grain diameters were 0.0002 cm (clay), 0.00266 cm (silt) and 0.0830 cm (sand) respectively. An average representative grain radius of 0.0013 cm was therefore calculated. In order to cover the range of grain radii in the

model domain and present the sensitivity of material transfer due to grain sizes, simulations of reactive transport for a “large”, “medium” and “small” (0.0415 cm, 0.0013 cm and / or. 0.0001 cm) grain radius were performed as shown in section 5.4.2.

According to (Kuntze et al., 1994) the fraction of organic (f_{oc}) could be equated to half of the average humus content in the transport material (Pütz et al., 2002). Using this accession and the linear distribution model by Seth et al., 1999 (equation 3.29) linear distribution coefficients k_d for model simulations of the PAHs Phenanthrene and Anthracene were therefore calculated. Model simulations were performed for the lysimeters with contaminated demolition waste and contaminated soil material as their source zones. These form the bases of the model prognoses since measured concentration values of Phenanthrene and Anthracene were present for comparative studies. The input parameters for the model are given in Table 5.2 below.
It is to be noted that the input (inlet) concentrations (at the interface of the source and transport zones) used for the transport model were the maximum measured concentrations from the GSF source term lysimeters (Klotz, 2003).

Table 5.3: Model input parameters for the lysimeters operated at the Jülich research centre.

Source reference material	Contaminated soil, Contaminated demolition waste
Transport reference material	Parabraunerde (loess)
Model Transport distances [m]	0.35 and 1.7
Tracer	Bromide
Contaminant	Phenanthrene (Phe), Anthracene (Ant)
Solubility of contaminant [mgL^{-1}]	6.18 (Phe); 5.9 (Ant)
Inlet contaminant concentrations [ugl^{-1}]	Cont. soil as source: 0.0259 (Phe); 0.374 (Ant), demolition waste as source: 16.84 (Phe); 4.638 (Ant)
Lysimeter height [m]	2.4
Lysimeter surface area [m^2]	2

Radius of lysimeter [m]	0.798
Grain size of Parabraunerde (radius) [cm]	0.0415 (large), 0.0013 (average) 0.0001 (small)
Total porosity [-]	0.42
Average water content [-]	0.34
Intraparticle porosity [-]	0.001
Degree of saturation [-]	0.81
Material density [kgl^{-1}]	1.536
Particle density [Kgl^{-1}]	2.647
Fraction of organic carbon [-]	0.002255
Distribution coefficient (k_d), [Lkg^{-1}]	22.29 (Phe); 23.21 (Ant)
Aqueous diffusion coefficient [cm^2s^{-1}]	$7.684 \cdot 10^{-6}$ (Phe); $6.84 \cdot 10^{-6}$ (Ant)
Volumetric flow rate [m^3s^{-1}]	$4.48*10^{-8}$

5.2.2 Lysimeters from GSF München-Neuherberg

Similar lysimeter and soil input parameters required for the simulation of transport processes with SMART (Table 5.3) were evaluated and prepared based on the associated report (Klotz, 2003) of the Institut für Hydrologie at GSF, Neuherberg following the procedure as described in section 5.2.1. Here the effluent concentrations of the six PAHs Naphthalene, Phenanthrene, Anthracene, Fluoranthene, Anthraquinone (Anthrachinon) and Pyrene leaching from the source layer filled with contaminated soil (Altlastboden) reference material through the transport layer filled with Sandboden (soil sands) were simulated. The model input parameters are shown in Table 5.3 below:

Table 5.4: Model input parameters for the lysimeters operated at the GSF München-Neuherberg research centre.

Source reference material	Contaminated soil
Transport reference material	Soil sand
Transport distances [m]	1.25
Tracer	Bromide
Contaminant	Napthalene (Nap). Phenanthrene (Phe), Anthracene (Ant), Fluoranthene (Fth) Anthraquinone (Atn), Pyrene (Pyr)
Solubility of contaminant [mgL^{-1}]	112 (Nap); 6.18 (Phe); 5.9 (Ant): 1.68 (Fth); 1.35 (Atn); 0.904 (Pyr)
Inlet contaminant concentrations [ugl^{-1}]	0.0219 (Nap); 0.0259 (Phe); 0.374 (Ant) 0.0933 (Fth); 1.831 (Atn); 0.174 (Pyr)
Lysimeter height [m]	2.05
Lysimeter surface area [m^2]	1.00
Radius of lysimeter [m]	0.564153
Grain size of Sandboden (radius) [cm]	0.1 (large) 0.027 (average) 0.00315 (small)
Total porosity [-]	0.36
Average water content [-]	0.13
Intraparticle porosity [-]	0.001
Degree of saturation [-]	0.3611
Material density [kgl^{-1}]	1.54
Particle density [kgl^{-1}]	2.42
Fraction of organic carbon [-]	0.0021
Distribution coefficient (k_d), [Lkg^{-1}]	1.22 (Nap); 20.75 (Phe); 21.61 (Ant) 72.87 (Fth); 90.74 (Atn); 125.96 (Pyr)
Aqueous diffusion coefficient [cm^2s^{-1}]	$9.15 \cdot 10^{-6}$ (Nap); $7.68 \cdot 10^{-6}$ (Phe); $6.84 \cdot 10^{-6}$ (Ant) ; $6.58 \cdot 10^{-6}$ (Fth, Pyr); $7.08 \cdot 10^{-6}$ Atn)
Volumetric flow rate [m^3s^{-1}]	$2.371*10^{-8}$

5.3 Determination of the distribution of mean residence time of Bromide in the lysimeters.

5.3.1 Lysimeters from Jülich research centre

The simulation of the reactive solute transport with the model tool SMART (Streamtube Model for Advection and Reactive Transport) requires retention time distribution of a conservative tracer in the lysimeters of the locations Merzenhausen and / or Neuherberg as the case may be as essential inputs for Merzenhausen. The results of such a Bromide tracer test after Pütz et al. (2002) at a transport distance 35 cm were therefore used. Figure 5.2 below shows the plot of the measured breakthroughs as well as their average values for four large lysimeters.

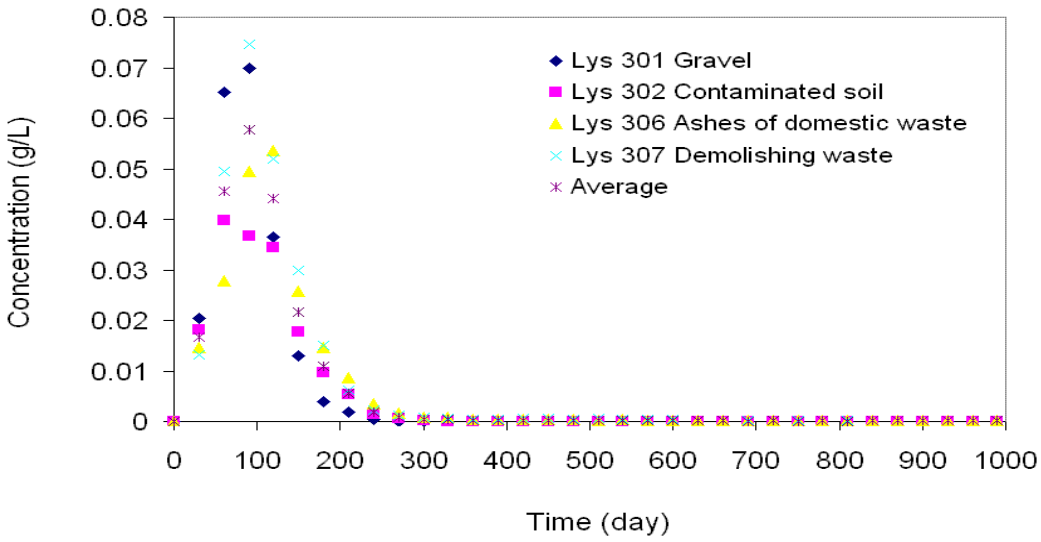

Fig. 5.2: Bromide breakthrough at a transport distance of 35 cm from the lysimeter station Merzenhausen (data from Pütz et al., 2002).

The measured data in Fig. 5.2 show deviations, which can be attributed to the effects of small-scale heterogeneities in the large lysimeter transport compartments.
These heterogeneities become irrelevant in the seepage water prognosis, which aims at the quantification of the long-term breakthrough behaviour of the pollutants in the groundwater. Therefore the seepage prognosis calculations can be accomplished in principle with an average retention time distribution. On the basis of these considerations two methods were used for the determination of this average retention time term:

(i) Method 1

As shown in Fig. 5.2, the measured concentrations were first arithmetically averaged. The retention time distribution was subsequently calculated by using the equation (3.6) (see details in section 3.4.2).

(ii) Method 2

The retention time distributions were first calculated separately for each of the lysimeters by using equation (3.6). The arithmetic mean of the individual retention time distributions was then subsequently computed.

Independent of the method chosen for the determination of the retention time distribution, the results are always calculated according to the general equation 3.6 (Bold, 2004). The concentration value C_l corresponding to a time, say t_l, would be the arithmetic mean of the associated four single concentrations at time t_l when method 1 is used. Figure 5.3 below depicts the comparison of both methods. It can be seen that the retention time distributions differ only insignificantly. This shows that the retention time distribution in question can be reliably be determined with both methods.

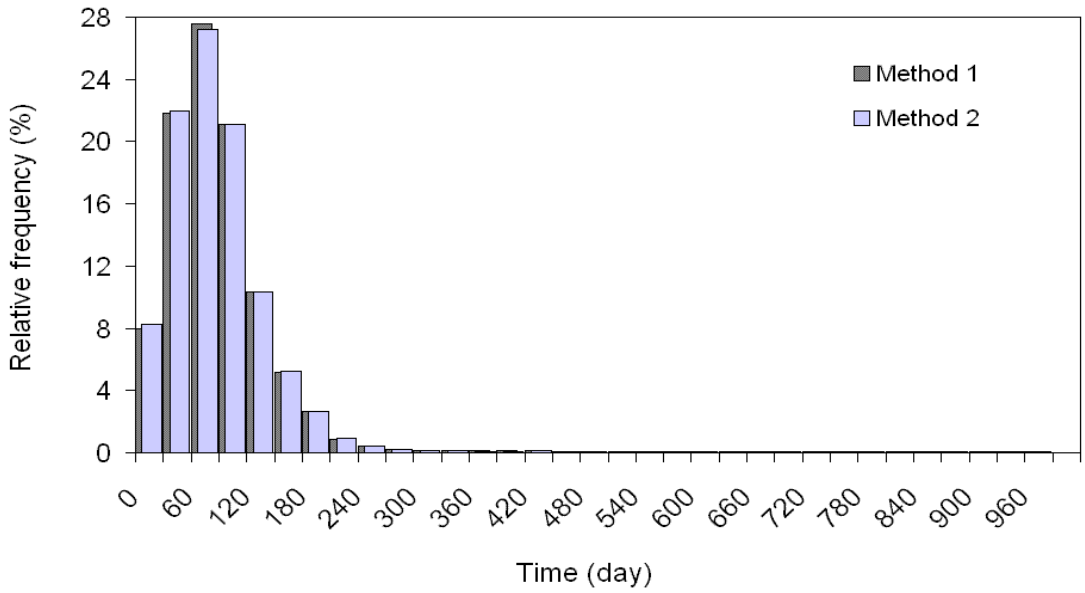

Fig. 5.3: Comparison of the retention time distribution at a transport distance of 35 cm.

Finally a plausibility check was accomplished to determine whether SMART could reproduce the measured bromide breakthrough of the calculated retention time

distribution. This procedure examined the correctness of the technical conversion of the concept, which is the basis for the model tool SMART (Finkel, 1999; Bold, 2004). The corresponding result for the retention time distribution was determined according to method 1 as shown in Figure 5.4 below. A very good match of the simulated results with the average values of the measured concentrations was determined. Almost identical results were obtained for the retention time distribution determined according to method 2 (not represented).

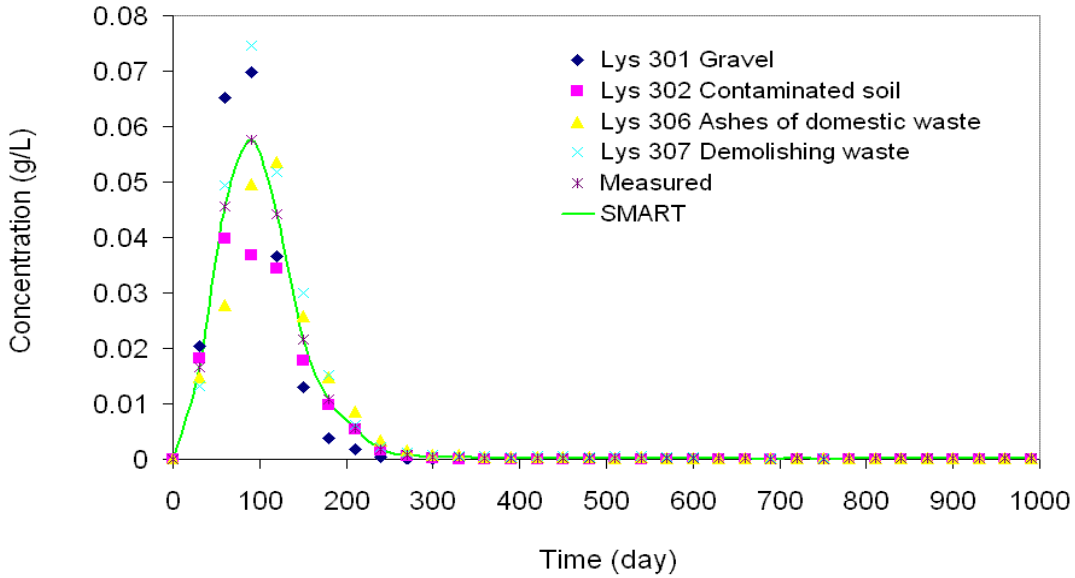

Fig. 5.4: Plausibility check of the SMART results for bromide transport at the plane of measurement of 35 cm.

The determination of the retention time distribution at the outlet of the Jülich lysimeters at a transport distance of 1.70 m, thus resulted in a frequency distribution, represented by Figure 5.5. A corresponding successful plausibility check of the model tool SMART is shown in Figure 5.6.

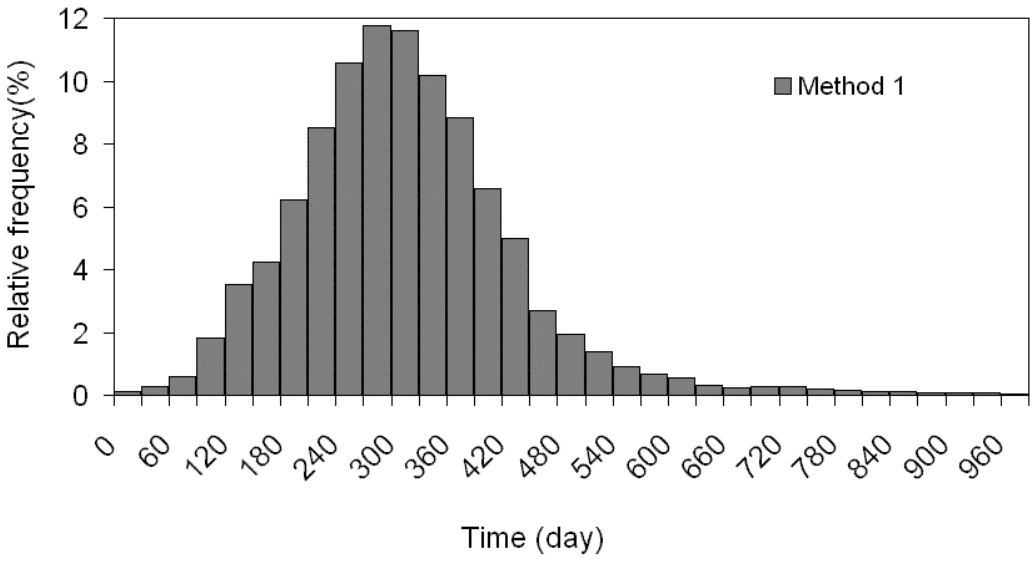

Fig. 5.5: Lysimeter at the research centre, Jülich: Retention time distribution evaluation by bromide transport at the discharge outlet.

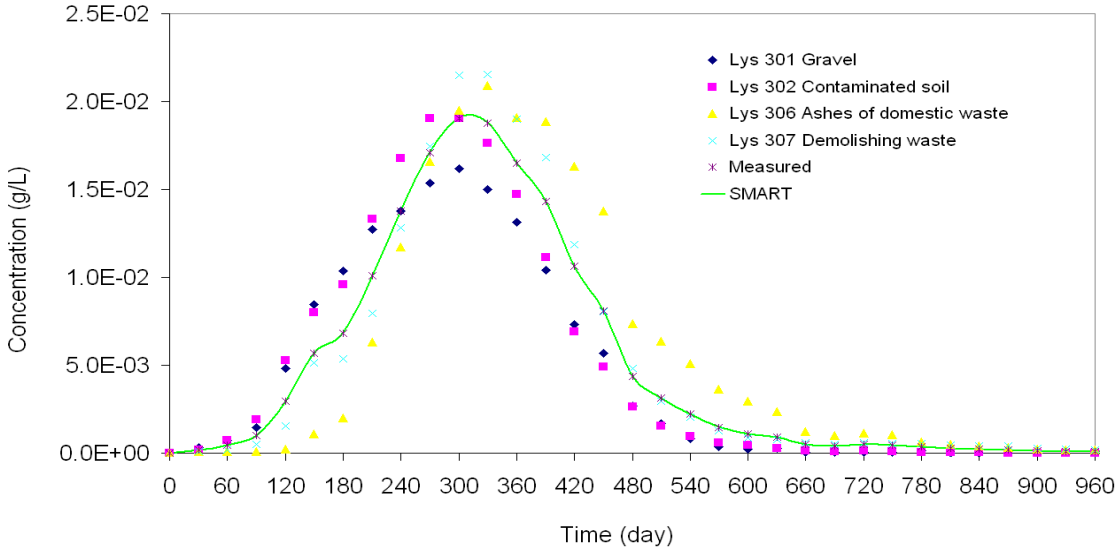

Fig. 5.6: Plausibility check of the SMART results for bromide transport at the Jülich lysimeter discharge outlet.

5.3.2 Lysimeters from GSF-München, Neuherberg

The mean retention time distribution at the discharge outlet of the lysimeters at the GSF München, Neuherberg (transportation distance 1.25 m) is shown in Figure 5.7 below. The different scale of the axes can be considered in comparison with the corresponding data of the Jülich lysimeters (Figure 5.5). The Jülich lysimeters

showed higher tailing in addition to higher peak values at the same time. Also the measuring interval at the München, Neuherberg site is shorter (7 days) in comparison with Jülich (30 days).

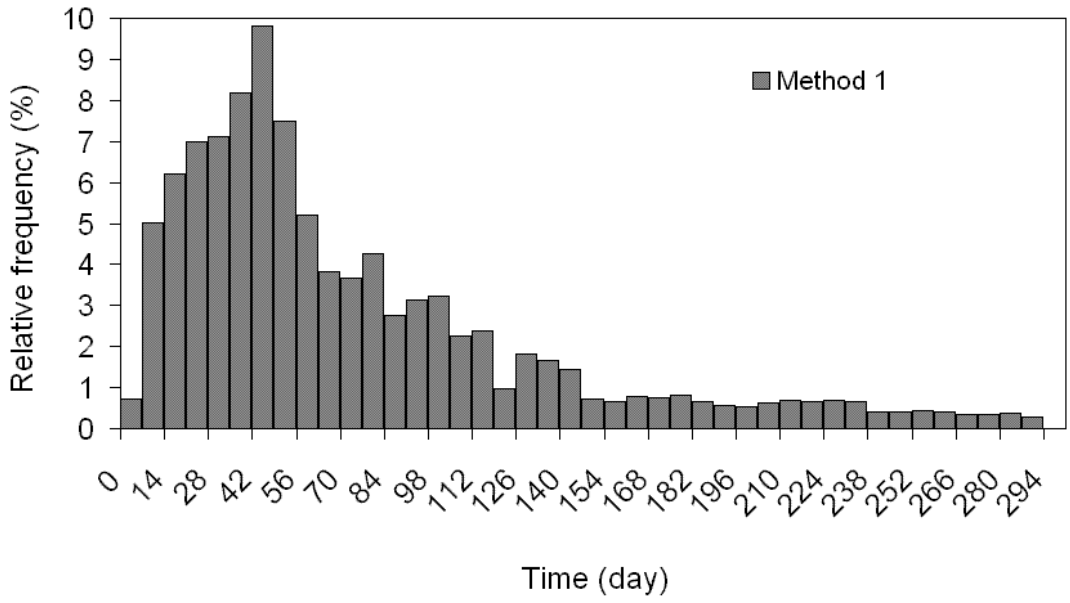

Fig. 5.7: Lysimeter from GSF-München Neuherberg: Retention time distribution evaluation of bromide transport at the discharge outlet.

For the sake of completeness, Figure 5.8 below shows the results of the plausibility check for the used software.

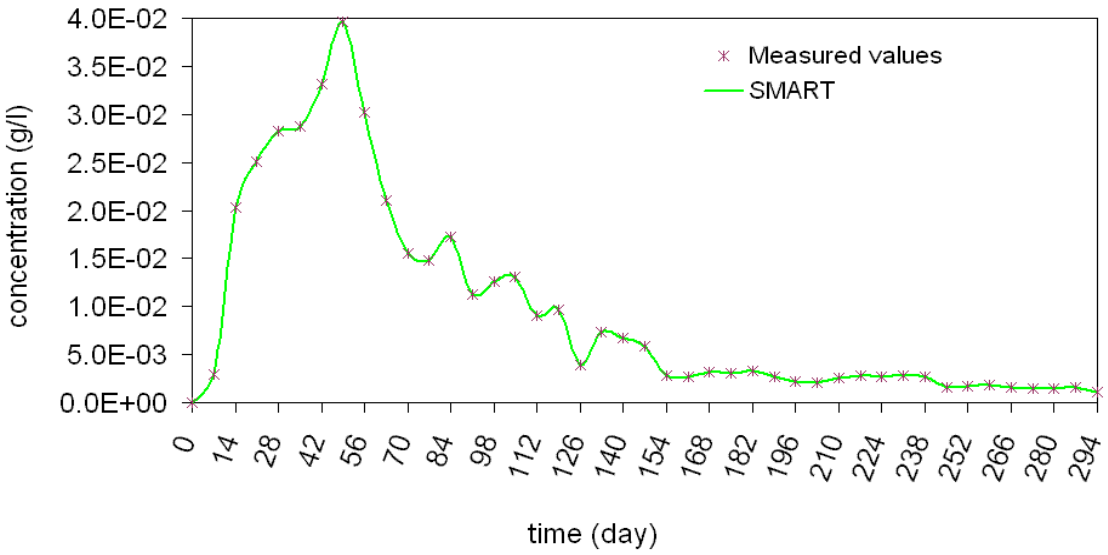

Fig. 5.8: Lysimeter from GSF-München Neuherberg: Plausibility check of the SMART results for bromide transport at the lysimeter discharge outlet.

5.4 Reactive contaminant transport

5.4.1 Lysimeters from Jülich research centre.

Reactive transport modelling was performed for the lysimeters located at the test site Merzenhausen (Jülich research centre) using the contaminants Phenanthrene and Anthracene as case studies (Table 5.3 and Appendix 3). The reference materials, demolition waste and contaminated soil were the source of pollutants occupying the source layer of the lysimeters. Since the choice of reference material as well as pollutants were purely based on the availability of lysimeter measured data, simulations were performed for both contaminants with each of the two named reference materials at a transport distance of 0.35 cm and 100 cm (only for demolition waste). Also the input concentrations used in the simulations were the maximum measured concentrations of the Phenanthrene and Anthracene data collected from GSF source term lysimeters. The simulations were carried out under the assumptions of physico-chemical equilibrium and non equilibrium conditions. In order to cover the possible range of grain size distributions the simulations were performed for three grain radii (0.0001 cm, 0.0013 cm und 0.0415 cm). Detailed copies of the simulation input files can be seen in Appendix 1. Figures 5.9 and 5.10 show the breakthroughs of Phenanthrene and Anthracene for the lysimeter with contaminated soil as source term material at a transport distance of 35 cm. As it is

well known the smaller the grains size the faster the pollutant uptake or absorption. As shown in the plots the curves for the grain radii 0.003 and 0.001 could hardly be differentiated from each other and slightly from the equilibrium breakthrough curve. The deviations of the modelled curves from the measured breakthrough were smallest for the simulations with largest grain radius in each case. While the forward model underestimates the Phenanthrene concentrations by approximately an order of magnitude, the Anthracene concentrations were well predicted.

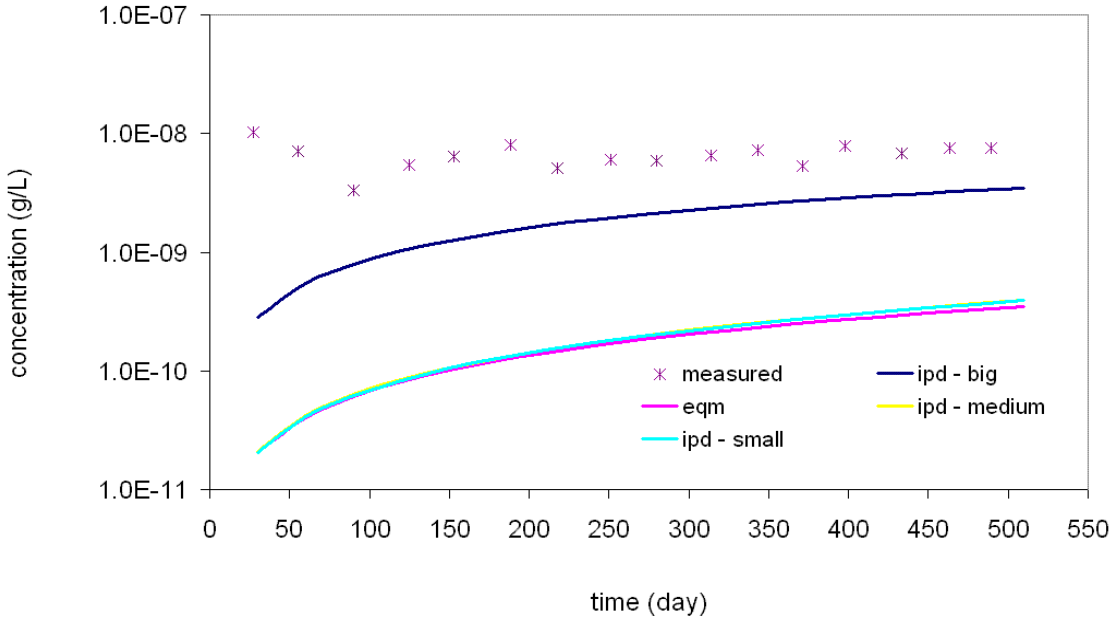

Fig. 5.9: Measured and simulated Phenanthrene breakthrough of the Jülich lysimeter with contaminated soil as source layer material at a transport distance of 35 cm under equilibrium (eqm) and non equilibrium conditions (ipd-small: grain radius 0.0001 cm; ipd-medium: grain radius 0.0013 cm; ipd-big: grain radius 0.0415 cm).

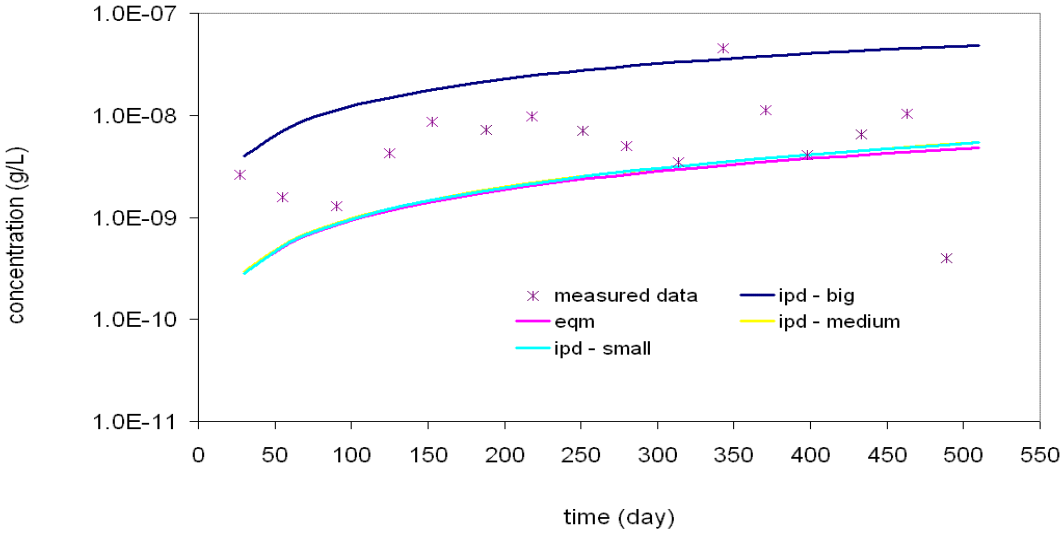

Fig. 5.10: Measured and simulated Anthracene breakthrough of the Jülich lysimeter with contaminated soil as source layer material at a transport distance of 35 cm under equilibrium (eqm) and non equilibrium conditions (ipd-small: grain radius 0.0001 cm; ipd-medium: grain radius 0.0013 cm; ipd-big: grain radius 0.0415 cm).

The long-term prediction of Phenanthrene and Anthracene breakthroughs for Jülich lysimeters with contaminated soil as source layer material is shown in Figure 5.11 below for a simulation period of over 800 years. The maximum concentrations were reached for both materials after approximately 70 years. Lower levels of breakthrough curves could be achieved if microbial degradation is considered as an additional process in the model. However no information about the presence and / or strength of the microbial processes were known in the lysimeters under consideration, hence the omission of degradation reactions in the transport simulations.

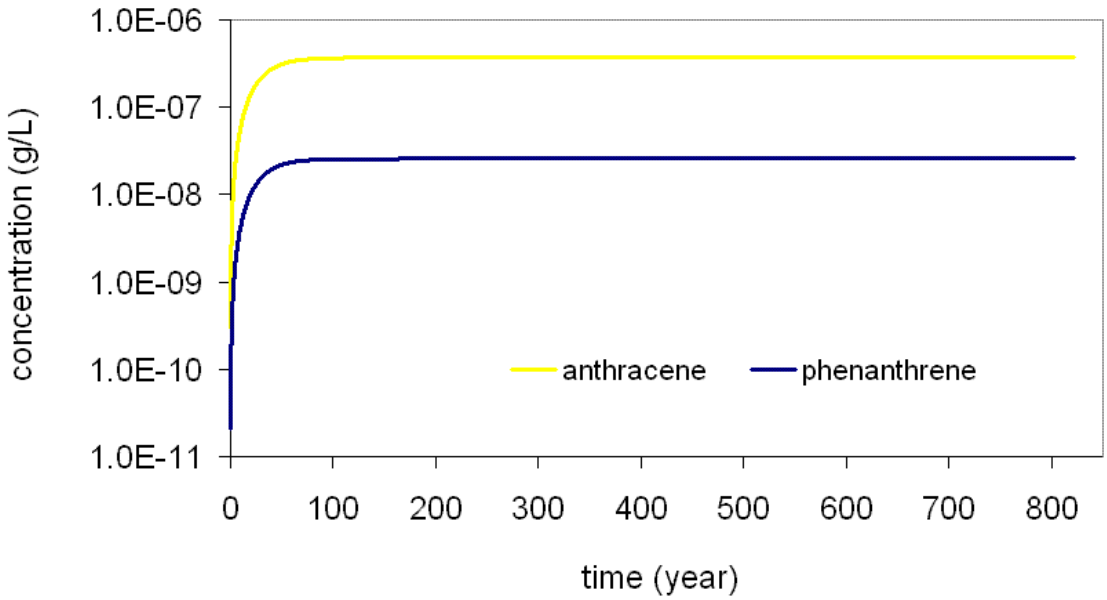

Fig. 5.11: Long term prediction of PAH breakthrough for Jülich lysimeter with contaminated soil as source layer material at a transport distance of 35 cm under non equilibrium conditions (grain radius 0.0013 cm).

Again a similar model study was accomplished for FZJ lysimeter but with demolition waste as source layer material (Figs. 5.12 – 5.14). In this case the Phenanthrene and Anthracene concentrations in the model prediction were over-estimated (Fig. 5.12 and 5.13). This may be due to the fact that the measured data are still in the range of background concentration values and with a total mass recovery less than one percent of the input concentrations in the model. Hence the modeled results are likely to improve over the longterm period. The long-term behaviour (Fig. 5.14) is basically equivalent to the breakthrough curves from Fig. 5.11, and the maximum concentrations were reached after almost 100 years.

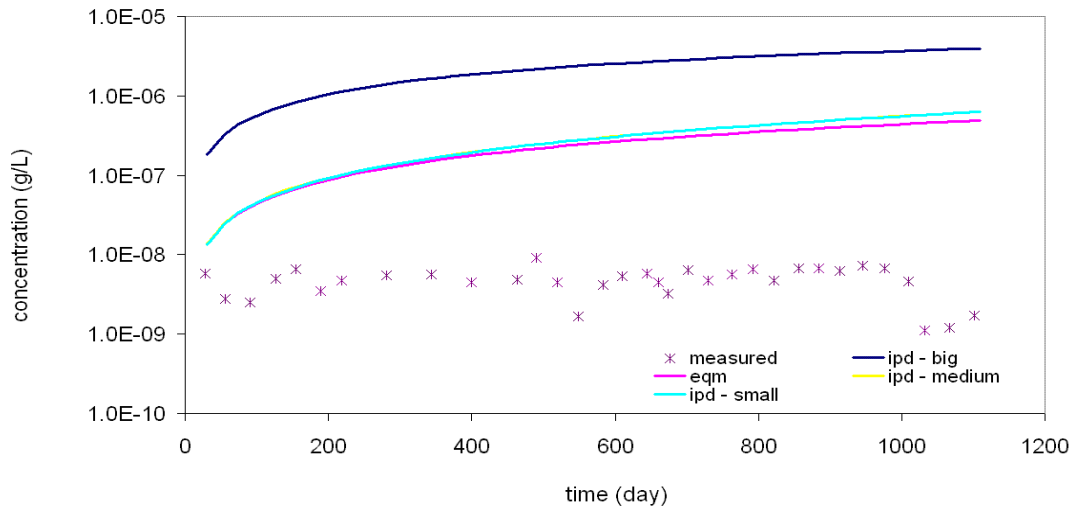

Fig. 5.12: Measured and simulated Phenanthrene breakthrough forJülich lysimeters with demolition waste as source layer material at a transport distance of 35 cm under equilibrium (eqm) and non equilibrium conditions (ipd-small: grain radius 0.0001 cm; ipd-medium: grain radius 0.0013 cm; ipd-big: grain radius 0.0415 cm).

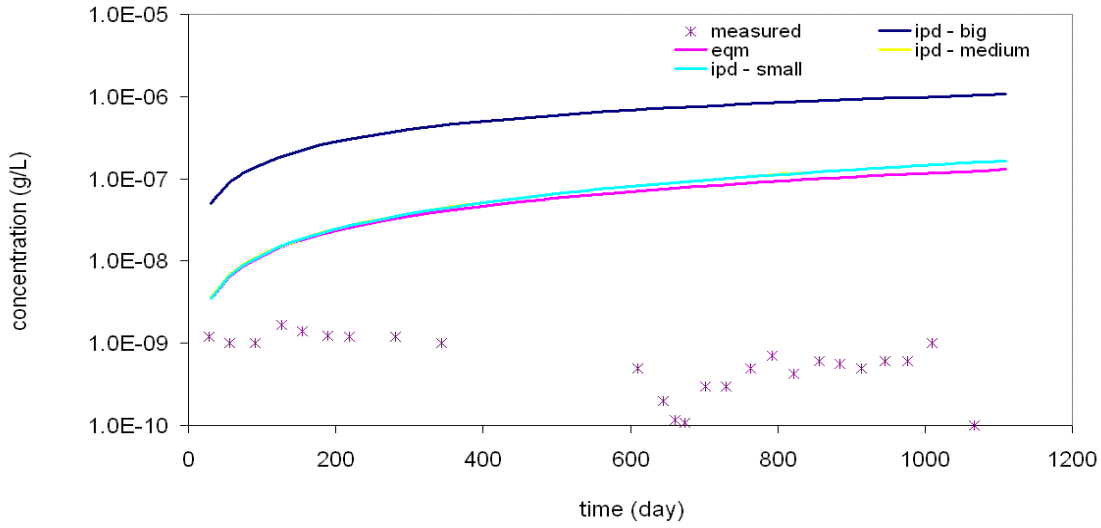

Fig. 5.13: Measured and simulated Anthracene breakthrough for Jülich lysimeter with demolition waste as source layer material at a transport distance of 35 cm under equilibrium (eqm) and non equilibrium conditions (ipd-small: grain radius 0.0001 cm; ipd-medium: grain radius 0.0013 cm; ipd-big: grain radius 0.0415 cm).

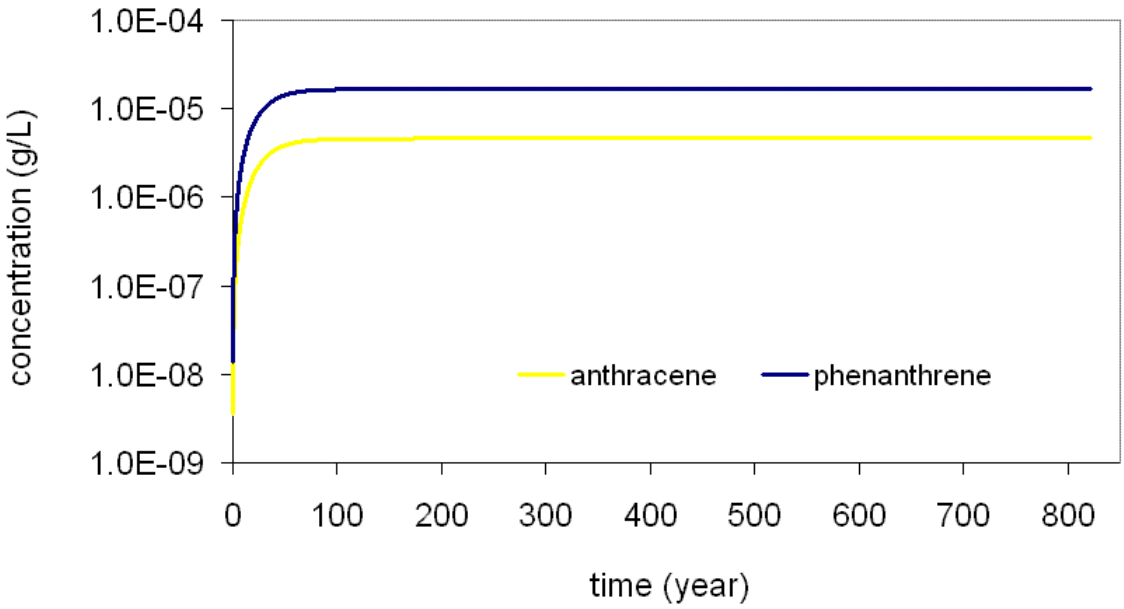

Fig. 5.14: Long term prediction of PAH breakthrough for Jülich lysimeter with demolition waste as source layer material at a transport distance of 35 cm under non equilibrium conditions (grain radius 0.0013 cm).

In addition to the above result for Jülich lysimeters with demolition waste as source layer material, model simulations were also run and compared with measured data collected from the lysimeter's discharge level 3, i.e. at a transport distance of 100 cm. The model results overestimate the experimental data for both Phenanthrene (Fig. 5.15) and Anthracene (Fig. 5.16) but within one order of magnitude as compared to Figs. 5.12 – 5.13. The sudden break in the measured data may be due to measurements below detection limits or instrumental and measurement errors.

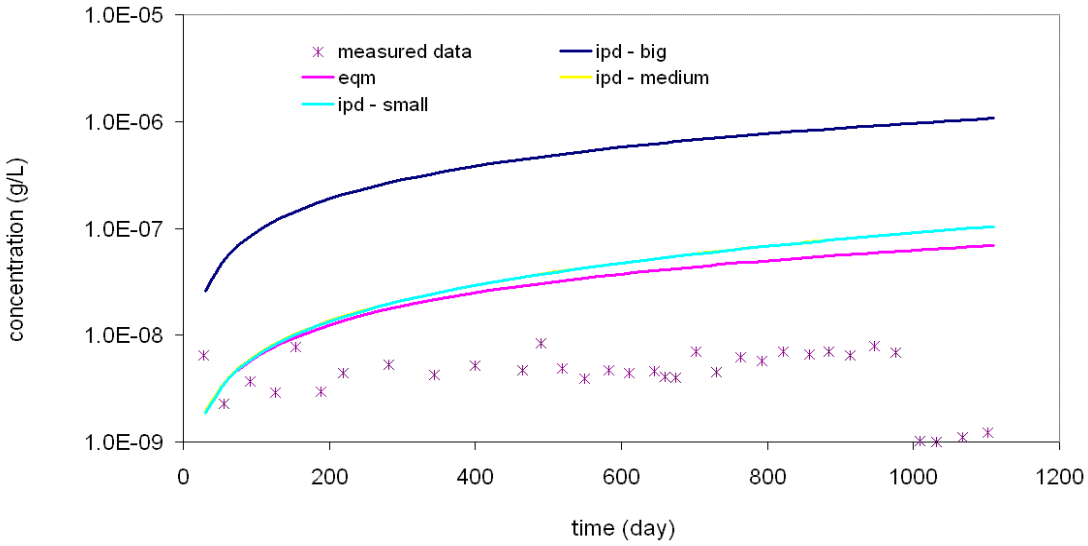

Fig. 5.15: Measured and simulated Phenanthrene breakthrough for Jülich lysimeters with demolition waste as source layer material at a transport distance of 100 cm under equilibrium (eqm) and non equilibrium conditions (ipd-small: grain radius 0.0001 cm; ipd-medium: grain radius 0.0013 cm; ipd-big: grain radius 0.0415 cm).

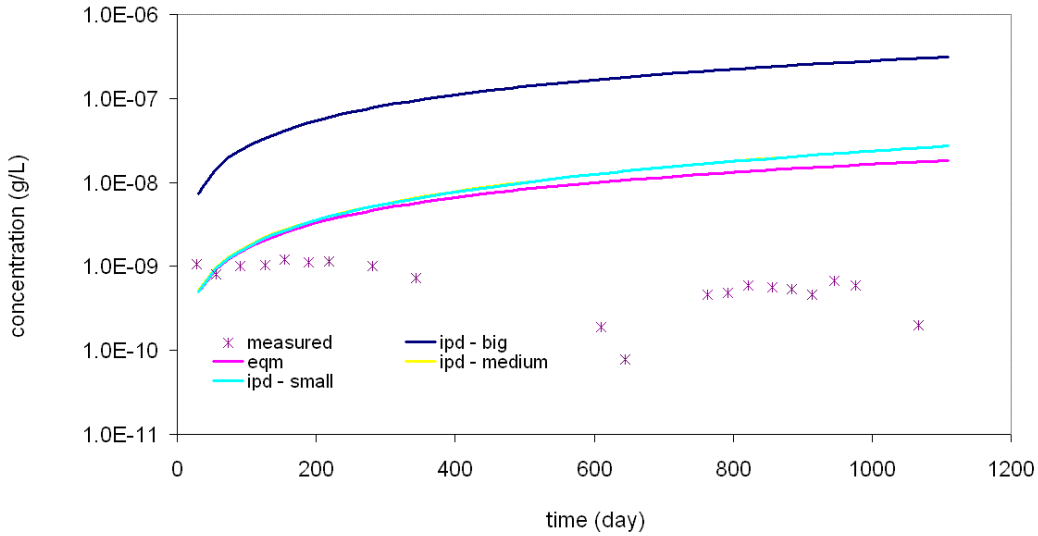

Fig. 5.16: Measured and simulated Anthracene breakthrough for Jülich lysimeters with demolition waste as source layer material at a transport distance of 100 cm under equilibrium (eqm) and non equilibrium conditions (ipd-small: grain radius 0.0001 cm; ipd-medium: grain radius 0.0013 cm; ipd-big: grain radius 0.0415 cm)

With reference to the long-term behaviour at the lysimeter discharge level 3 (Fig. 5.17) it was noted that the maximum concentrations of Phenanthrene and Anthracene respectively were reached after nearly 140 years as a result of the longer travel distance. According to the SMART model results, 50 % of the maximum concentrations were reached in each case after 51.37 years and 53.50 years (logarithmic scaling of the ordinate axis in Fig 5.17) for Phenanthrene and Anthracene respectively. If one calculates the breakthrough time by assuming a simplified approach in which physico-chemical equilibrium existed between the aqueous and the sorbed phases, a 50 % breakthrough time of 48.59 years and 50.96 years was obtained for Phenanthrene and Anthracene respectively. This means that the breakthrough times for the cases under consideration can be calculated by means of a back-of-the-envelope calculation with an error margin of less than 5 % (Table 5.5).

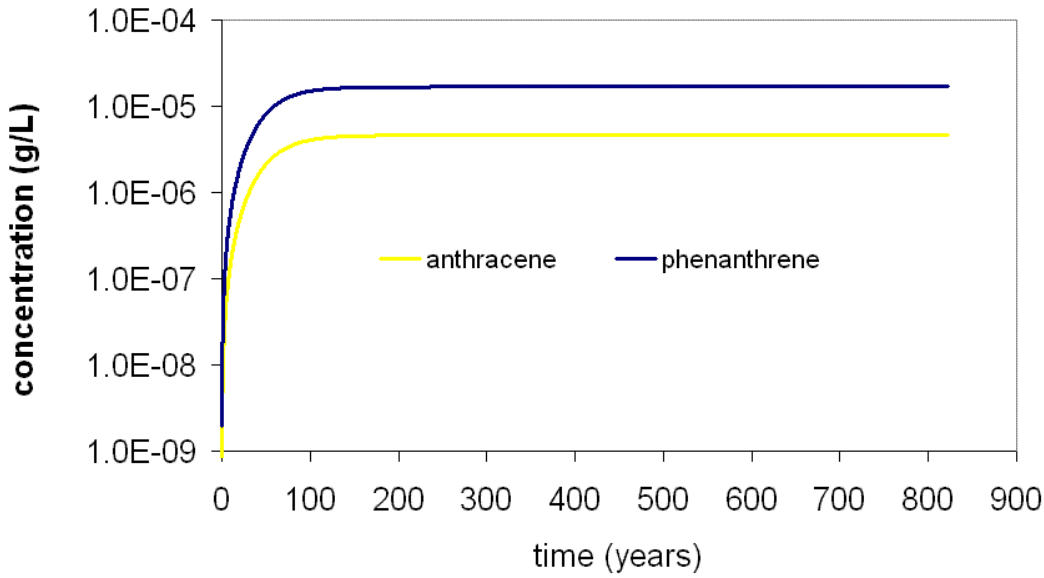

Fig. 5.17: Long term prediction of PAH-breakthrough for Jülich lysimeters with demolition waste as source layer material at a transport distance of 100 cm under non equilibrium conditions (grain radius 0.0013 cm).

The difference between the measured and modeled concentrations is about two and one orders of magnitude for Figures 5.12 -13 and Figures 5.15 – 16 respectively. This may be due to the fact that the measured data are still in the range of background concentration values. For the short-term simulations total mass recovery

is less than one percent of the input concentrations in the model. Hence the modeled results are likely to improve over the longterm period.

Table 5.5: Comparison of the 50 % breakthrough time for the GSF lysimeter with demolition waste as source layer material at a transport distance of 100 cm (grain radius 0.0013 cm)

Contaminant	50 % breakthrough time (years)	
	SMART	Equilibrium
Phenanthrene	51.37	48.95
Anthracene	53.50	50.96

5.4.2 Damköhler number for Jülich lysimeters

Also as shown in section 3.5.7, it is possible to express the degree of non-equilibrium by Damköhler numbers. With regards to sorption kinetics, these numbers are given in Tab. 5.6 for Jülich lysimeters.

Table 5.6: Sorption Damköhler numbers for FZJ lysimeters at a transport distance of 100 cm under non equilibrium conditions

Contaminant	Phenanthrene			Anthracene		
Grain radius (cm)	0.0001	0.0013	0.0415	0.0001	0.0013	0.0415
Damköhler number	197273.86	1167.79	1.64	168633.96	998.33	1.46

As shown in Table 5.5, the longterm breakthrough of both Phenanthrene and Anthracene is quite closed to the back-of-the-envelope calculation with an error margin of 5 %. This is clearly seen in Table 5.6 by the large Damköhler numbers for the modelled grain radius 0.0013 cm. Again the large Damköhler numbers for both Phenanthrene and Anthracene at grain radii 0.0001 cm and 0.0013 cm show that it

would be sufficient to model the contaminant matrix interaction with equilibrium sorption. However kinetic sorption is imperative for the larger grain sizes.

5.4.3 Lysimeters from GSF-München, Neuherberg

Similar simulations as in section 5.4.1 were accomplished for the lysimeters at GSF-München, Neuherberg. However, as compared to Jülich lysimeter the contaminants Naphthalene, Phenanthrene, Anthracene, Anthrachinon (Anthraquinone) Fluoranthene and Pyrene were considered (Tab. 5.3). Again the simulations were carried out under the assumption of physico-chemical equilibrium and non equilibrium conditions. Also the simulations were performed for three grain radii 0.00315 cm, 0.027 cm and 0.1 cm representing the possible range of grain sizes in the Sandboden. The results of the simulations in each case refer to the total transport distance of 1.25 m which allows a comparison with the measured outflow concentrations collected at the lysimeter discharge outlet.

With the exception of the big grains, all simulations tend to underestimate the measured concentrations at least for a certain time period. The modelled concentrations underestimate the measured concentrations for Naphthalene (Fig. 5.18), Phenanthrene (Fig. 5.19), Anthracene (Fig. 5.20), Anthraquinone (Fig. 5.21), Fluoranthene (Fig. 5.22) and Pyrene (Fig. 5.23) at early breakthrough. This may be due to background noise which is not accounted for in the model. Another source of error may be due to non stable conditions at the early stage of measurements within the lysimeters. At later times, the simulated breakthrough curves of the big grains lie over the measured results. With the exception of Naphthalene, a very good fit could be established for material grain sizes in between the big and the average grains. In contrast to this the modelled breakthrough curves of the small and medium simulations radii rise and barely approach the measured values and / or remain under it within the 1000 days of simulation. The unsual kink behaviour in the Napthalene equilibrium breakthrough occurred at the interface between the first and second time step in the PDF. The sharp constrast between the two time distributions coupled with the fast naphthalene release may have given rise to this stepwise breakthrough.

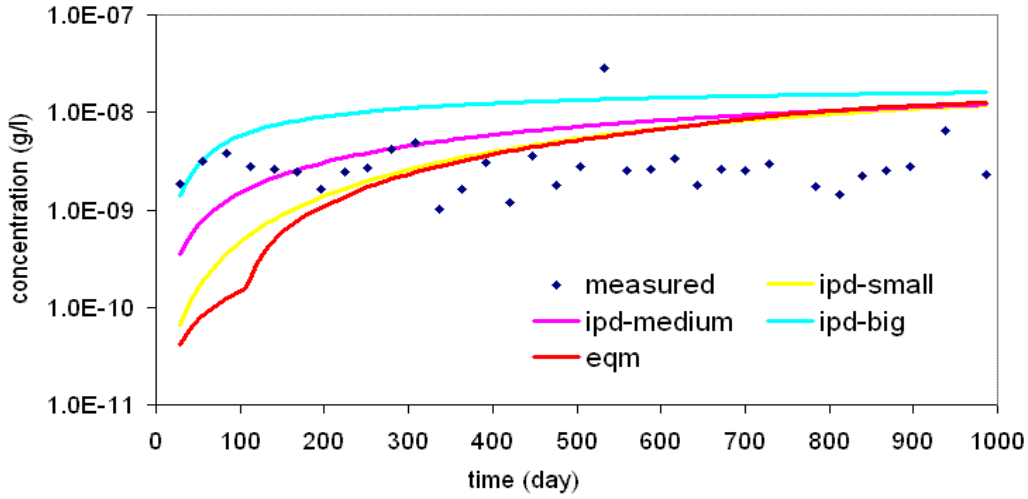

Fig. 5.18: Measured and simulated Naphthalene breakthrough of GSF lysimeters with contaminated soil as source layer material at a transport distance of 125 cm under equilibrium and non equilibrium conditions (ipd-small: grain radius 0.00315 cm; ipd-medium: grain radius 0.027 cm; ipd-big: grain radius 0.1 cm)

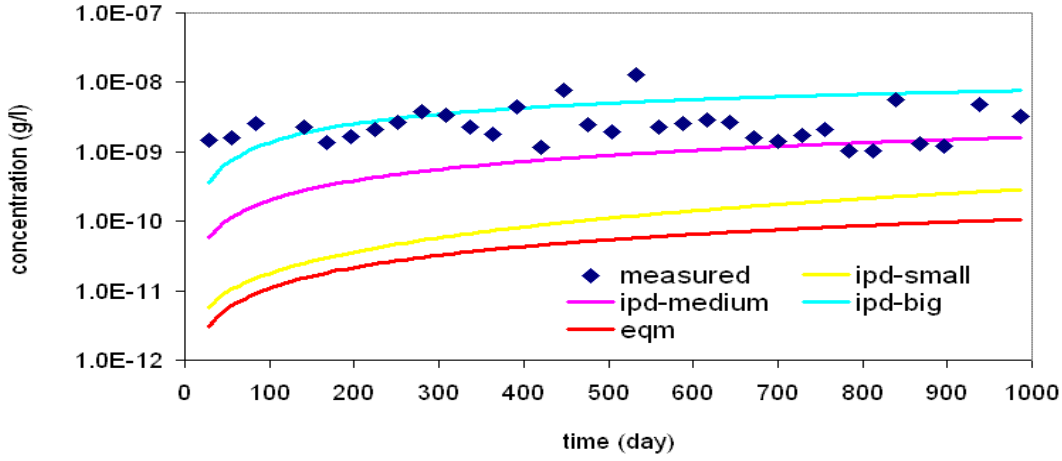

Fig. 5.19: Measured and simulated Phenanthene breakthrough of GSF lysimeters with contaminated soil as source layer material at a transport distance of 25 cm under equilibrium and non equilibrium conditions (ipd-small: grain radius 0.00315 cm; ipd-medium: grain radius 0.027 cm; ipd-big: grain radius 0.1 cm)

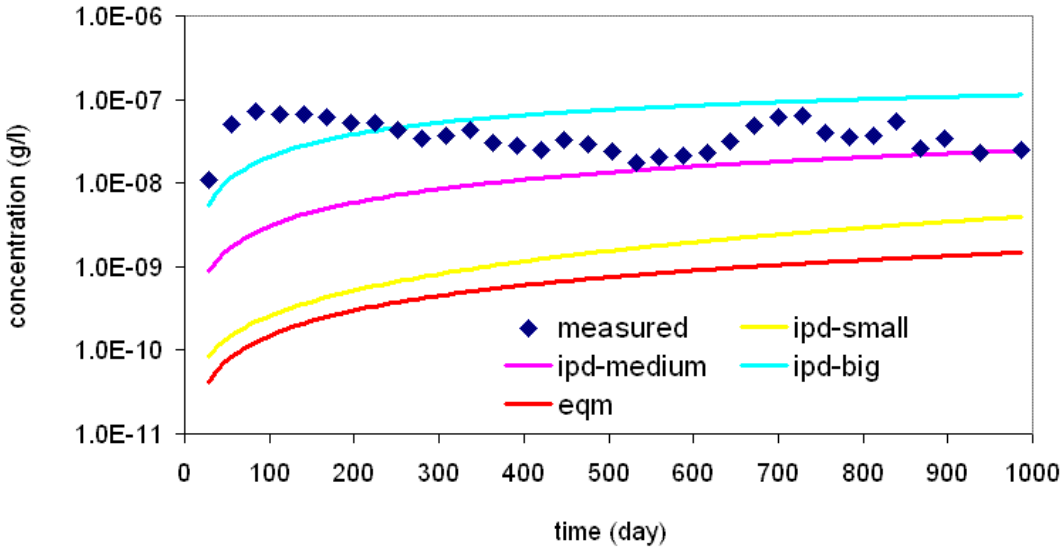

Fig. 5.20: Measured and simulated Anthracene breakthrough of GSF lysimeters with contaminated soil as source layer material at a transport distance of 125 cm under equilibrium and non equilibrium conditions (ipd-small: grain radius 0.00315 cm; ipd-medium: grain radius 0.027 cm; ipd-big: grain radius 0.1 cm)

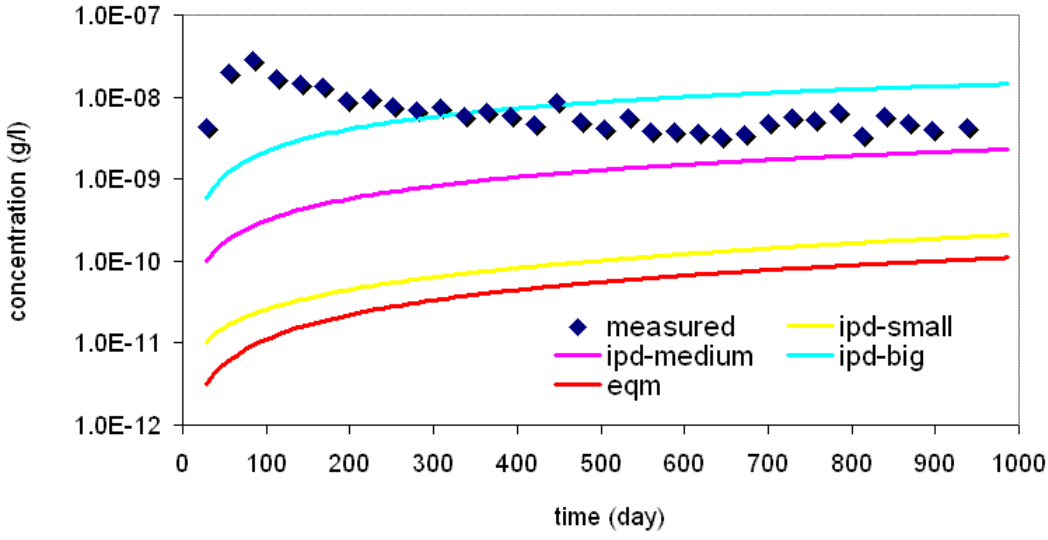

Fig. 5.21: Measured and simulated Fluoranthene breakthrough of GSF lysimeters with contaminated soil as source layer material at a transport distance of 25 cm under equilibrium and non equilibrium conditions (ipd-small: grain radius 0.00315 cm; ipd-medium: grain radius 0.027 cm; ipd-big: grain radius 0.1 cm)

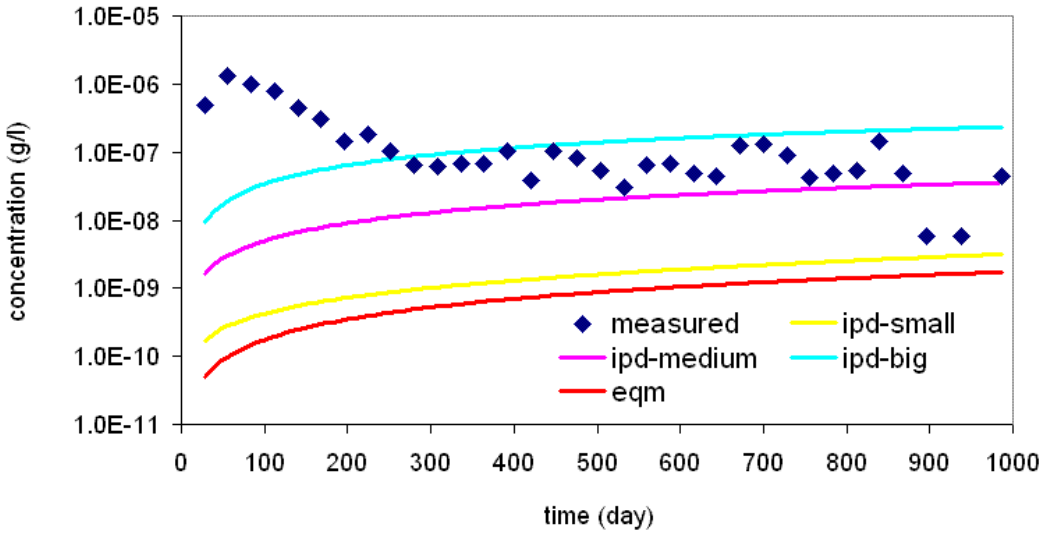

Fig. 5.22: Measured and simulated Anthraquinone breakthrough of GSF lysimeters with contaminated soil as source layer material at a transport distance of 25 cm under equilibrium and non equilibrium conditions (ipd-small: grain radius 0.00315 cm; ipd-medium: grain radius 0.027 cm; ipd-big: grain radius 0.1 cm)

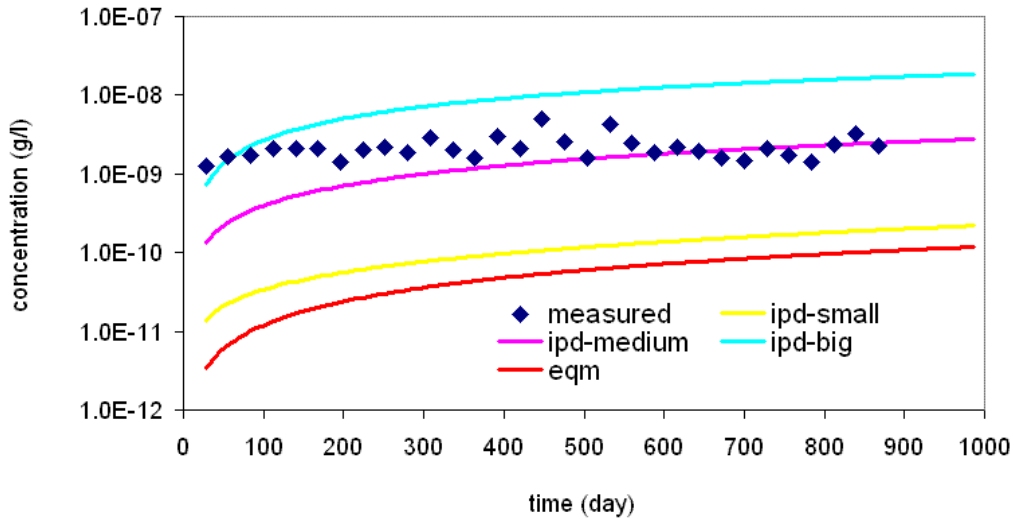

Fig. 5.23: Measured and simulated Pyrene breakthrough of GSF lysimeters with contaminated soil as source layer material at a transport distance of 125 cm under equilibrium and non equilibrium conditions (ipd-small: grain radius 0.00315 cm; ipd-medium: grain radius 0.027 cm; ipd-big: grain radius 0.1 cm)

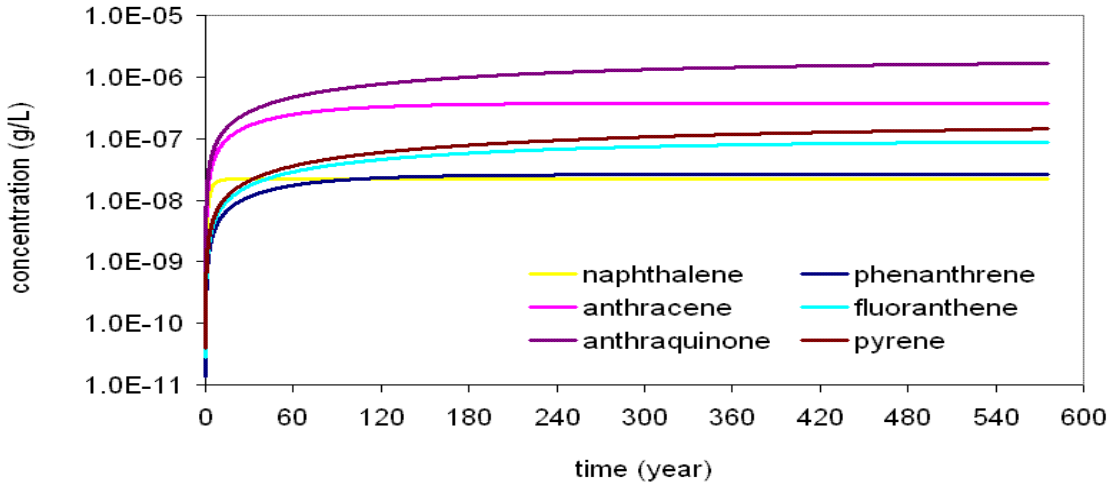

Fig. 5.24: Long term prediction of PAH breakthrough for GSF-lysimeters with contaminated soil as source layer material at a transport distance of 125 cm under non equilibrium conditions (grain radius 0.027 cm).

Figure 5.24 above shows the long-term predictions for the six PAHs, which were analysed at the GSF lysimeter filled with contaminated soil as the source layer material for the transport modelling. The time at which the maximum concentration is reached is strongly contaminant-dependent and increases with hydrophobicity.

Finally the 50 % breakthrough times which were determined based on SMART simulations for the pollutants Naphthalene, Phenanthrene, Anthracene, Fluoranthene Anthrachinon and Pyrene are given in Table 5.7 below. These values were compared to the results of the estimations of the back-of-the-envelope calculations, which were based on the assumption that physico-chemical (sorption) interactions proceeded under equilibrium conditions. The SMART results are overestimated by about 43 - 51 %.

In comparison with FZJ lysimeters, the reactive processes are less close to physicochemical equilibrium. The kinetic processes are therefore of more importance in the GSF lysimeters. In the long run, this is due to the larger grain sizes of the sandy materials in the GSF lysimeters. The associated longer diffusion length in the grains therefore represents a crucial factor of influence for sorption kinetics. Moreover the smaller Damköhler numbers (see Table 5.8 below) calculated for the GSF lysimeters further confirmed the importance of kinetic sorption.

Table 5.7: Comparison of the 50 % breakthrough time for the GSF lysimeter with contaminated soil as source layer material at a transport distance of 125 cm (outlet).

Contaminant	50 % breakthrough (years)	
	SMART	Equilibrium
Naphthalene	2.34	3.30
Phenanthrene	36.50	53.65
Anthracene	37.30	55.86
Fluoranthene	124.30	187.83
Anthraquinone	156.8	233.83
Pyrene	214.68	324.52

5.4.4 Damköhler numbers in GSF lysimeters

Damköhler numbers as mentioned earlier on have been used to characterise the relative importance of chemical processes as well as to ascertain how close a reaction may be to equilibrium. The results in Table 5.8 show that the contaminant-matrix interaction in GSF lysimeter is “most kinetic” for Pyrene while “least kinetic” for Naphthalene. Since all the values were well below 100, the contaminant–matrix interaction was highly influenced by kinetic sorption and diffusion limited under unsaturated conditions. This confirms the results by (Bold, 2004; Jennings and Kirkner, 1984) who reported that sorption kinetics control contaminant–matrix interactions with Damköhler numbers between 0.01 and 100.

Table 5.8: Sorption Damköhler numbers for GSF-lysimeters at a transport distance of 25 cm (outlet) under non equilibrium conditions (grain radius 0.027 cm)

Contaminant	Naphthalene	Phenanthrene	Anthracene	Fluoranthene	Anthraquinone	Pyrene
Da (sorption)	29.61	1.93	1.73	0.76	0.7	0.55

5.5 Discussion and Conclusion

The simulations of the reactive material transfer predict long residence times of the respective pollutants in the lysimeters for both sites. This could be attributed to the high sorption of the pollutants in the solid materials present in the transport layers. The small grain size in particular and its associated short diffusion length in the solid particles are regarded responsible for the fast contaminant sorption. It was also a fact that the equilibrium model in all Jülich cases predicted the 50 % breakthrough at the same time as the kinetic model. From the data in Tables 5.3 and 5.4 the respective retardation factors can be easily calculated. The retardation factors are between 101 - 107 and 15 - 1493 for Jülich and München respectively, indicating that sorption capacity is high. The overall results could be improved if background concentration and biodegradation data are included. In summary the applicability of the model tool SMART for the reactive material transfer at the lysimeter scale could be shown. This encompasses the consideration of different solid materials and pollutant characteristics.

Chapter 6

6 THE KWABENYA (GHANA) LANDFILL CASE STUDY: AN EXAMPLE OF FIELD SCALE MODELLING

6.1 Motivation

Environmental sanitation issues resulting from inadequate water supply, drainage, solid waste management as well as sanitation facilities have been a major bone of contention in Ghana for more than decades. The Ghana strategy for reducing poverty document for the years 2003 – 2005 emphasises the urgent need of environmental sanitation and capacity to deal with solid and liquid waste. The problems have adversely affected the urban poor. According to Mensah and Larbi (2005) the problem of solid waste disposal in Ghana is not only engineering but of multi-dimensional difficulties such as indiscriminate dumping of refuse, increasing difficulties of acquiring suitable disposal sites, lack of effective road network which aids in the conveyance of solid waste, rapid urbanization and poor financial and technical capacities of local authorities. The problems are further aggravated by effective planning and management lapses. Almost all landfills in Ghana are actually open dumps without leachate and gas collection facilities and hence operated not according to recommended standards and practices of sanitation. Recently the waste disposal situation was further worsened by creation and uncontrolled dumping of plastic bags. In 2002, the problem assumed a political dimension that led to the dismissal of the Accra City's mayor. A controlled dumping site which was in use at Oblogo, a site in the Accra metropolis, was usually compacted to ensure proper dumping. The dumping of waste at Oblogo began in January 2002. Since then Oblogo received an average daily waste load of about 1200 metric tons. The capacity of the facility was stressed up in July 2004. Other dumping sites were also available in or around the city but they were all temporary in nature. These sites were used or are being used partly because of limited capacity for collection of waste and partly because of the lack of suitable disposal sites. These temporary or ad hoc tips were unsightly and represent a risk to public health (Mensah and Larbi, 2005). Wastes deposited at these sites were picked over by scavengers and dispersed by animals.

In the absence of a new landfill site, solid wastes would be collected in similar uncontrolled dumps in numerous locations within the city. The number and size of such dumps would escalate. These waste dumps therefore obviously constitute a risk to public health and significantly cause environmental nuisance to the City.

There was therefore an urgent need for the development of a new site which could accept solid waste and retain the waste in such a manner as to protect public health and minimize damage to the environment. Foreign loads were therefore secured to help in tackle environmental sanitation especially engineered mediated landfills. One of the landfill that was sited in the Accra metropolis is the Kwabenya landfill. Environmental impact assessment (EIA) was conducted as a first phase of the overall landfill contraction. The modelling work done in the EIA report was exclusively for inorganic pollutants that may emanate from the landfill as a leachate. The objective of this chapter is therefore to model the spreading of organic contaminants, which is PAHs in this case. This is significant because the waste types are likely to change in the future as a result of industrialization and increased effluence (EIA report, 2000) towards organic contaminants.

6.2 The Kwabenya landfill

6.2.1 Description of the project area of interest

The growth of the cities of Accra and Tema has extended to neighbouring districts such as the district Ga in which the proposed landfill Kwabenya is located (Fig. 6.1). The principal objective of the landfill construction was to improve the surroundings, living conditions and quality of life of the entire citizenry of present and future generations. The Oblogo site is situated in the western part of Accra and was formerly a hard-rock quarry. The Accra Metropolitan Assembly (AMA) and other key stake holders in the region identified the urgent need for a landfill. Subsequently to site selection studies carried out by Accra Metropolitan Authority (AMA) and local consultants several years ago, the advisory committees of the AMA Waste Management Department advocated a site at Kwabenya for the proposed landfill after which the EIA had been conducted.

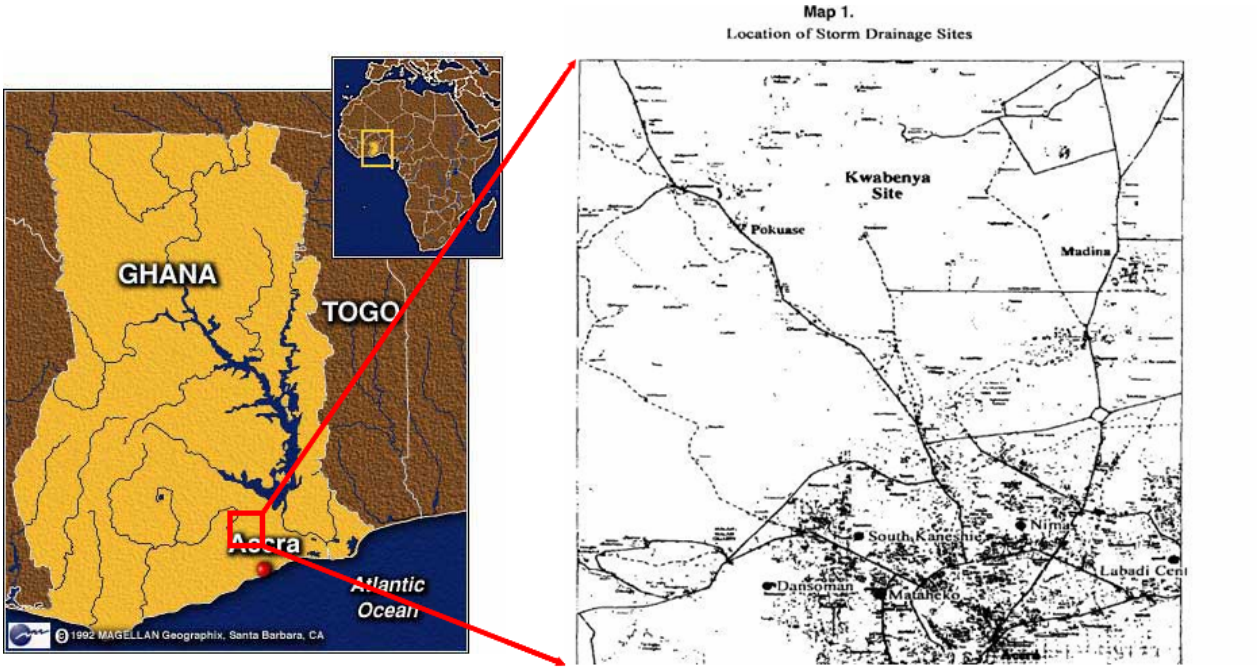

Fig. 6.1: The map of Ghana showing the landfill site at Kwabenya

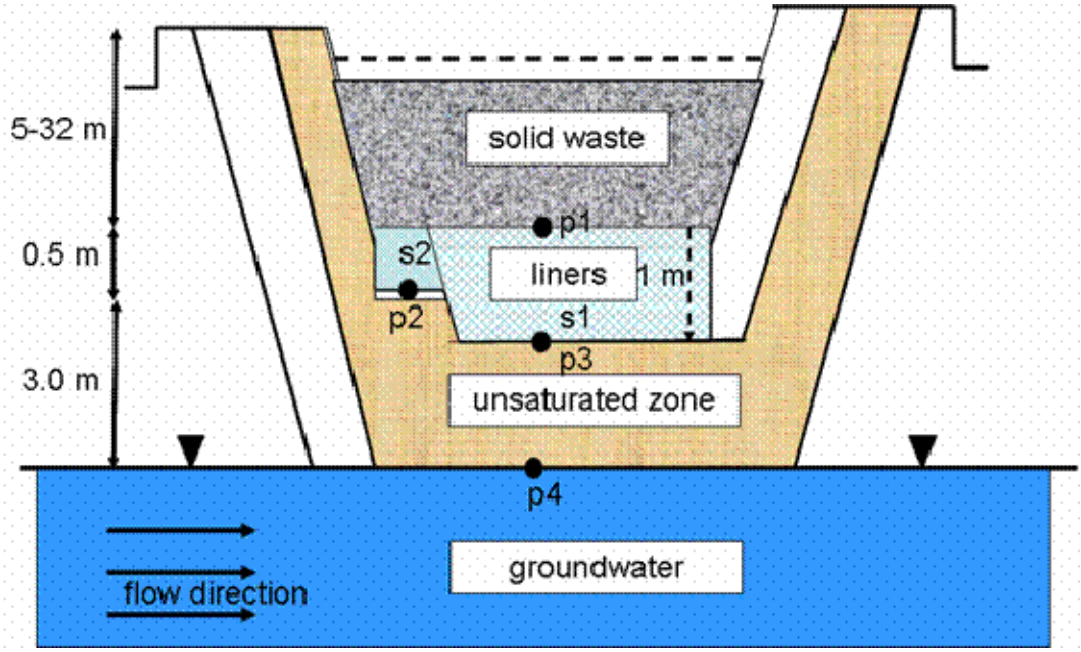

Fig. 6.2: Schematic diagram of the solid waste landfill scenario at Kwabenya

The EIA report proposed 3 design options one of which was approved. An initial development which comprised of a void space of 23 million m^3 for waste disposal for about 30 years was to be constructed. One of the major environmental impacts that

was identified and of concern to the study was groundwater. Its pollution would imply a far reaching local and national consequences. The chosen design scenario was to contain the leachate in the landfill site with an incorporated liner with permeability depending on the expected risk of leachate on different part of the landfill. The liner comprises of either geosynthetic clay or onsite soil mixed with bentonite. Three liners of different permeabilities were utilised: (i) at the bottom of the valley (right side of Figure 6.2). (ii) at the bottom of the valley (left side of Figure 6.2) where a sump was constructed to collect leachate for redistribution over the entire landfill and (iii) at the flanks of the valley where leachate was not likely to accumulate due to the steepness of the valley.

6.2.2 The geology of the site

The general geology of the area exhibits Quaternary to recent deposits. These consisted of unconsolidated sand, gravel and clay deposited by streams, of mine sand and gravel, forming beaches and spits, of materials deposited at times when sea level was higher or lower than at present, of sand blown inland by winds, and of sand and clay formed by the weathering of the underlying rocks. The thickness of these deposits was known to be somewhat greater than 25 metres. The site was underlain by overburden, which increases at the valley floor between 3 to 8 m and decreases at the sides down to less than 2 m, and eroded metamorphic bedrock. The overburden consisted of topsoils, colluvium / residential soil and some lateritic deposits. The topsoil consisted of loosely dark brown silty sands with interspersed coarser fractions. Along the valley bottom and the lower valley slopes was a distribution of the colluvium and residential soil. The residential soils were believed to be formed as a result of in situ weathering of the underlying bedrock. On the higher slopes of the valley the laterites seen as thin gravely layers overlying the bedrock were also found. The bedrock is mostly quartzite with occasionally interrupted maligned bands of phyllites formed as results of dynamic pressure variations in sediments. The outcrop is highly weathered at the surface with several sets of joints. The fresh, medium to fine grained, jointed quartzite is weathered to brown to reddish brown colour. Other geologic features such as joints, beddings and fractures were also present. Across the site is a fault believed to be beneath at an unknown depth (EIA report, 2000).

6.2.3 Hydrogeology of the site

The hydrogeology is influenced by the topology and geology of the site. Investigations conducted in situ on the silty sand soils showed a hydraulic conductivity varying from 10^{-7} m/s to 10^{-5} m/s. However laboratory tests with compacted samples recorded conductivity values of $1.4*10^{-8}$ m/s to $1.8*10^{-4}$ m/s. The conductivity results of the soils showed the existence of hydraulic continuity with the underlying bedrock. According to tests conducted in trial pits groundwater levels were shallow at the valley flanks due to the thin dry overburden present. This suggested a lateral flow towards the center of the valley or vertically to the underlying rocks which could occur at different seasons in different rates. The original (primary) porosity of the quartzite and phyllite was low due to their metamorphic origins. The presents of joints, beddings and fractures in the rocks resulted in secondary porosities and hence increased conductivities. Most of the in situ tests in these rocks showed a conductivity range of 10^{-6} m/s to 10^{-5} m/s which corresponded to moderate permeabilities normally encountered in fractured rocks. These values were further confirmed by borehole logs and drilling records. Effective porosities and storativities of the quartzites were assumed to be quite low since most of the water was believed to be stored in fissures. However storativity in the colluvium could be 10% or higher as compared to the 1 % that was guessed in the absence of pumping data. A groundwater level of 2 m was observed below the valley bottom which could rise to feed surface streams in time of rainfall event. The hydraulic gradients were 1/40 and 1/20 for the valley bottom and valley flanks respectively. Conceptually a nominal water flow through the active zone on the flanks of the valley and beneath the colluvium extended to a depth of 10 m. According to the EIA report a ground water flow of 0.75 L/sec and 0.19 L/sec was calculated for the rock and colluvium respectively by using the one dimensional Darcy method (EIA report, 2000).

6.3 The landfill leachate modelling

Emerging dilute and disperse leachate management was the main driving force of the landfill design. The target was to reduce and control ensuing leachate emerging from the landfill. As waste mass builds up at the landfill site, leachate would be generated. The input liquid component, changes in the soil moisture retentions and transmission characteristics of the waste as well as the infiltration through the successive layers

and ground surface would determine the volume of leachate generation. Potential leachate may migrate to contaminant surface water and ground water in and around the landfill hence the proposition of the lining system to minimise the risk. Drains are normally provided to take care of the leachates that are generated in the waste. However the lining may leak as the leachate heads build up in the landfill to contaminate the underlying groundwater (EIA report, 2000).

The conceptual model is described in terms of source (waste), pathway through the geosynthetic clay liner and receptor (the point of compliance between the unsaturated and saturated zone). The landfill is shown schematically in the Figure 6.2. In order to quantify the contaminant concentrations needed to assess the vulnerability of the underground water, breakthrough curves were calculated at the following levels of the landfill:

(i) p1, the level directly below the base of the waste
(ii) p2, the level directly below the liner at the left side of the landfill
(iii) p3, the level directly below the liner at the right side of the landfill
(iv) p4, the level of point of transition between the saturated and unsaturated zones.

Two pathway scenarios were considered in the model:

(1) s1: Leachate from the solid waste leaking through the liner (1 m thickness at the base of the valley) and through the unsaturated zone to the point of compliance, p4. The total vulnerability breakthrough is the time lag between p1, p3 and p4.

(2) s2: Leachate from the solid waste leaking through the liner (0.5 m thickness at the left side of the base of the valley) and through the unsaturated zone to the point of compliance, p4. The total vulnerability breakthrough is the time lag between p1, p2 and p4.

As a worst case scenario, the following assumptions were made similar to that of the inorganic contaminant model (EIA report, 2000):

(1) Groundwater and leachate migration are uniform through isotropic materials.
(2) There is no retardation or attenuation of the leachate in the lining system.

(3) The rate of infiltration is uniform throughout the whole year.
(4) The leachate concentration from the source (waste) is constant in time.
The leaching behaviour at the source (waste) was determined by using an Excel spreadsheet (Liedl, 2006) encoded with the source strength function derived in chapter 4 (section 4.5). The spread of the contaminant as well as the breakthrough concentration through the unsaturated zone was simulated with the aid of SMART.

6.3.1 Contaminant leaching through the source (waste)

The input parameters for the spreadsheet evaluation of PAH released in the waste is given below (Table 6.1). Measured parameters as well as literature values where not available were used for the landfill scenarios. According to Bold (2004) who reviewed the paper published by Gounaris et al. (1993), distribution coefficients as high as 15000 lkg^{-1} could be observed in batch experiments on the sorption behaviour of PAHs on micro particles. In this study a partition coefficient value of 10000 lkg^{-1} was used. A shift by 1 order of magnitude still has insignificant effect of the predicted concentration. Phenanthrene with a half-life of 500 days (Howard et al., 1991) was used as a representative for PAHs.

Table 6.1: Input parameter for the EXCEL spread sheet evaluation of the source concentration released at the Kwabenya landfill

scenario	Landfill waste
Source reference material	Municipal waste
Model source distances [m]	15
Contaminant	Phenanthrene
Solubility of contaminant [mgL^{-1}]	6.18
Flow (mm/a)	157
waste surface area [m^2]	725000
Radius (waste soil) [m]	0.0003
Total porosity [-]	0.3
Intraparticle porosity [-]	0.001

Degree of saturation [-]	0.67
Particle density [kgl^{-1}]	1.43
Material density [kgl^{-1}]	1
Distribution coefficient (k_d), [Lkg^{-1}]	10000
Aqueous diffusion coefficient [cm^2s^{-1}]	$7.68*10^{-6}$
Half life [s]	$4.32*10^7$

In Figure 6.3 below, contaminant breakthrough predicted directly beneath the landfill is shown at 15 m, a distance which represents the average thickness of the waste. A constant concentration was predicted over the simulation period of two pore volumes (equivalent to 38.4 years) by the source strength function. The release of PAHs from the solid waste would therefore not be diffusion limited within the waste over the life time of the landfill (30 to 40 years).

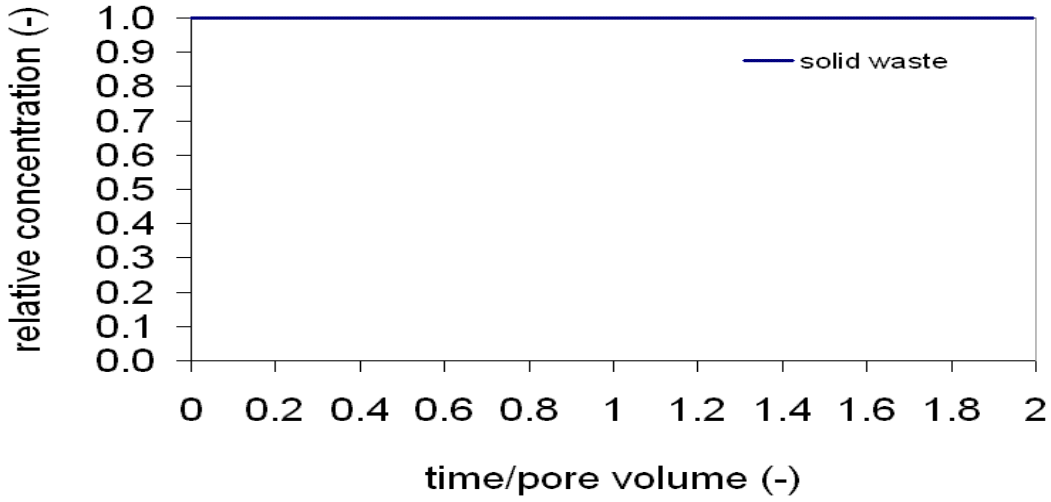

Fig. 6.3: Predicted contaminant concentrations at p1 for a waste layer of 15 m thickness.

6.3.2 Leachate transport through the liners.

The liners were made of geosynthetic clay consisting of clay and benthonite with different permeabilities.

Table 6.2: Input parameters of leachate leakage through the landfill liners

scenario	Base of valley (right side)	Base of valley (left side)
Thickness of liner [m]	1	0.5
Head gradient [-]	0.3	0.3
Conductivity of liner [ms^{-1}]	$1*10^{-9}$	$8*10^{-10}$
effective porosity [-]	0.1	0.1

Considering a worse case scenario, advective and diffusive time scales were computed and compared with the aid of the equations 3.12 – 3.15 (chapter 3). A time scale ratio of advection in relation to diffusion of 8:1 and 6.5:1 was obtained for the liners at the right side and left side of the base of the valley (waste) respectively. This means it would take a potential leachate at the bottom of the waste 3.3 years and 10.57 years to transverse through the left and right liners respectively, to the upper part of the unsaturated zone if diffusion is neglected. The overall leachate travel time would therefore be extended in favour of groundwater protection if retardation is considered in the liners.

6.3.3 Leachate transport in the unsaturated zone.

Considering a constant leaching concentration source (solid waste), contaminant breakthroughs at the point of compliance (p4) were simulated with SMART for two pathways, p3 – p4 (1 m) and p2 – p4 (3 m). The input parameters for the transport models are given in Table 6.3.

Table 6.3: Transport parameters for the Kwabenya landfill scenarios.

scenario	Unsaturated zone (s1 and s2)
Transport reference material	Colluvium (silty sand)
Model Transport distances [m]	1 (s1) and 3 (s2)
Inlet contaminant concentrations [mgl^{-1}]	10^{-3}
Grain size of colluvium [cm]	0.014
Total porosity [-]	0.35
Intraparticle porosity [-]	0.01
Degree of saturation [-]	50
Material density [kgl^{-1}]	1.58
Particle density [kgl^{-1}]	2.43
Distribution coefficient (k_d), [Lkg^{-1}]	10
Aqueous diffusion coefficient [cm^2s^{-1}]	$7.68*10^{-6}$
Volume flow rate [m^3s^{-1}]	$2.4*10^{-9}$ (s1); $2.0*10^{-9}$ (s2)

The flow rates in table Table 6.3 are vertical flow seeping from the base of the liners in the unsaturated zone.

In Figures 6.4 and 6.5 contaminant breakthroughs at 1 m and 3 m are shown for the pathways p3 - p4 and p2 - p4 respectively by taking into account sorption and biodegradation. The dotted line shows the drinking water standard of the World Health Organisation (WHO, 2003).

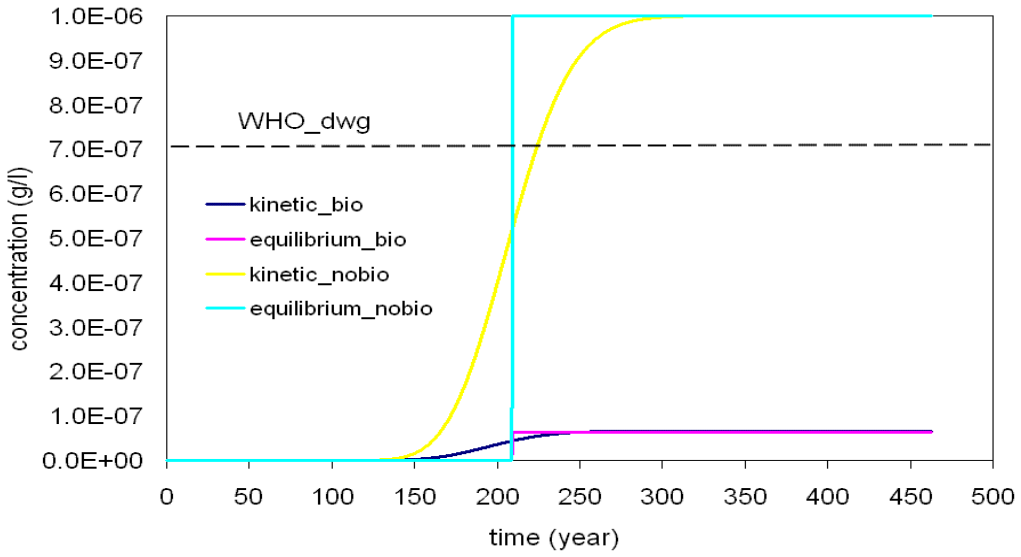

Fig. 6.4: Contaminant breakthroughs at the transport distance 1 m (p3 - p4) of the Kwabenya landfill scenario s1.

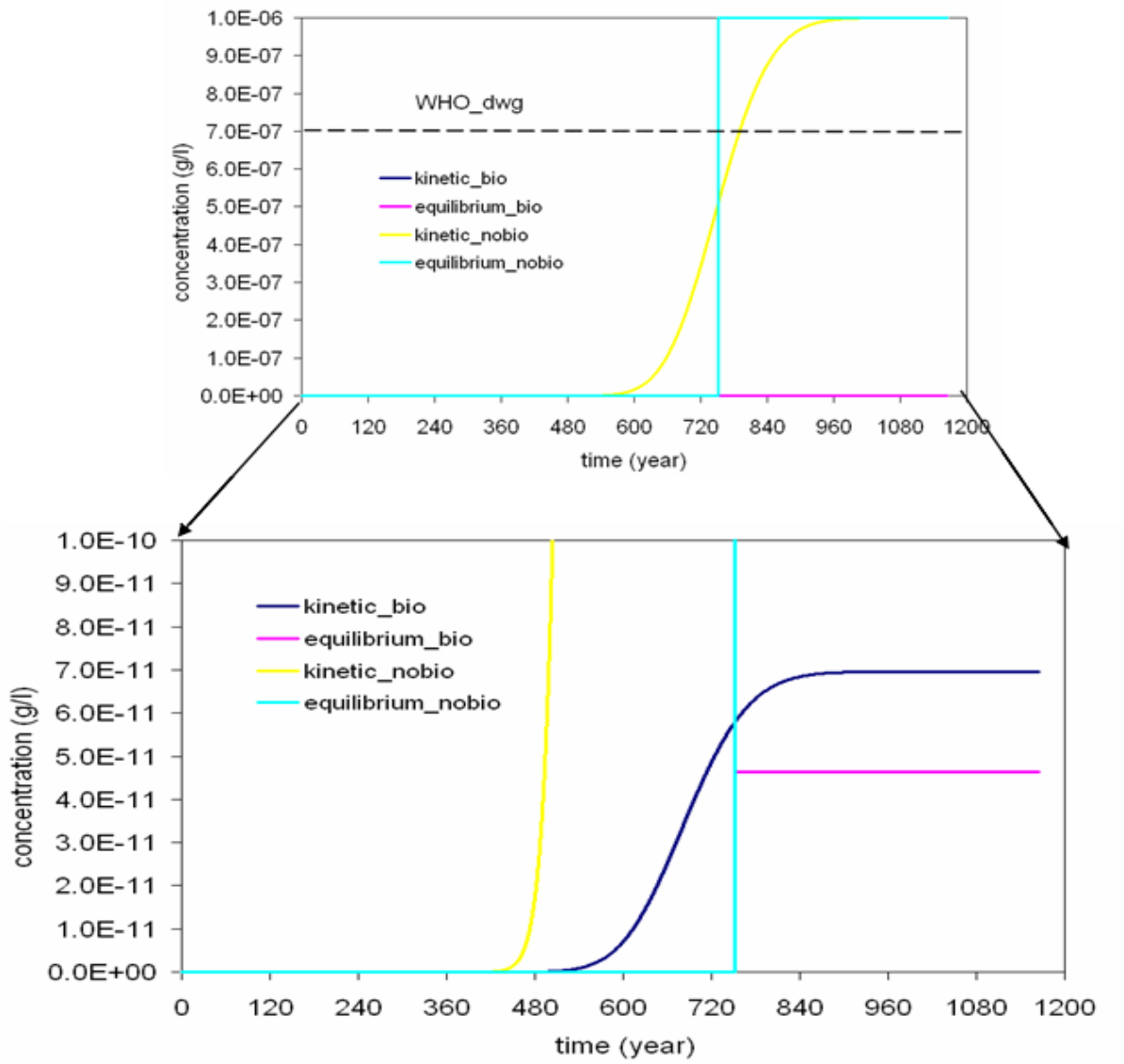

Fig. 6.5: Contaminant breakthroughs at the transport distance 3 m (p2 - p4) of the Kwabenya landfill scenario s2.

The 50 % breakthrough times at the point of compliance (p4) were 207.6 years and 754.14 years for the unsaturated zone of scenarios s1 and s2 respectively. Biodegradation reduced the contaminant levels by approximately 94 % (after 4 half lives) and 99.99 % (after 14.4 half lives) for scenario s1 and s2 respectively. Sorption Damköhler numbers computed for the scenarios s1 and s1 were 121.2 and 431.4 respectively. The higher sorption Damkohler numbers indicate that the kinetic sorption could be neglected, i.e. it would be sufficient to take into account only equilibrium sorption in the modelling process. Moreover first arrivals with insignificant concentrations of the pollutant occurred at time period of 2.4 years and 8.4 years for the scenarios s1 and s2 respectively.

6.4 Summary and conclusion

Two worse case scenarios (s1 and s2) were modelled for the Kwabenya, Ghana landfill. It was shown that the leachate concentration inside the source (waste) would stay constant during the 30 to 40 years life time of the landfill. However at any time the PAH leachates starts to leach through the liner and the unsaturated zone towards the receptor (groundwater table), the leachate would take 218.17 years and 434.70 years for the pathway scenarios s1 and s2 respectively. The World Health Organization (WHO) drinking water standards (dwg) of 0.7 ugl^{-1} (WHO, 2003) would therefore only be exceeded after a long period of 234.17 years and 973.4 years for scenarios S1 and S2 respectively. The large Damköhler numbers show that the kinetic behaviour of contaminant–matrix interaction could be neglected if the time evolution of the contaminant is to be monitored. The model shows that within the 30 year of landfill operation, the predicted concentrations would still be about 14 orders of magnitude lower than the WHO drinking standards. Biodegradation reduces the overall concentration levels thereby making the subsurface waters more secured. (Figures 6.4 and 6.5). The model therefore shows that the receptor, i.e. groundwater, is secured as far as leachate of the non volatile organic compounds such as PAHs through the geosynthetic liners and the underneath unsaturated zone of the landfill is concerned.

Chapter 7

7 SUMMARY AND CONCLUSION

Organic chemicals such as PAHs, though helpful domestically and industrially, can still be devastating and recalcitrant when entering the environmental media. Research in the behaviour, toxicity, carcinogenicity and modelling of PAH fate and transport is still ongoing. One of the objectives of this thesis was the development of a source strength function which could be used to predict the behaviour of organic leachate that could form the upper boundary condition for transport modelling. Also a process based prediction of long term PAH concentrations at the lysimeter outlets, an index of groundwater risk assessment, was conducted with the modelling tool SMART. In addition the application of SMART was to be extended to a field scale study of a landfill site in Ghana (Kwabenya). The major identifiable processes involved in groundwater risk assessment were reviewed. Sorption and biodegradation are known to cause a decrease of groundwater pollution risk while particle facilitated transport and preferential flow mostly increase groundwater pollution risk. Other tools such as GLEAMSS, PELMO, PRZM, VARLEACH, SIMULAT, MACRO, WAVE, LEACHP used in lysimeter studies were summarily described in terms of their flow and transport characteristics and equations.

Most of the aforementioned models solve the Richards equation for flow in the unsaturated zone and use the convection-dispersion equation to model solute transport. The SMART model is based on the Lagrangian streamtube approach which allows the separation of conservative transport and reactive processes under steady state flow conditions, thereby reducing numerical errors to the minimum. This software was validated successfully by authors Rahman (2002), Cata (2003), Schmidt (2003), Bold (2004), Cai (2004), Christ (2004), Henzler (2004), Madlener (2004), and Susset (2004) at the laboratory scale. The following conclusions are drawn for the source term, lysimeter and landfill modelling.

(1) Source term modeling

A source strength function was determined for the quantification of the possibly temporally variable discharge behaviour of organic pollutants from small-scale (point-like) sources of pollutant. With the aid of the source strength function, the temporal change of the pollutant concentration is determined in the seepage water at the transition from the pollutant source to the transport distance. In order to simulate transport and the reactive processes, the source strength function can be used as a time-dependent upper boundary condition for those pollutants migrating to the groundwater level (= point of compliance). In determining the source strength function, advection, desorption kinetics and microbial degradation were considered as relevant discharge processes. It was assumed that

- desorption kinetics can be simulated with an intraparticle diffusion model,
- seepage water flow is steady state,
- a concentration equilibrium exists between mobile and immobile phases at the beginning of the simulations,
- microbial degradation only occurs in the mobile phase.

In order to ensure the general applicability of the source strength function, dimensionless numbers and / or conditions were used throughout: The time t was standardized in terms of pore volumes, PV = n_eL/GWN (n_e = effective porosity, L = thickness of the source, GWN = seepage-water flow rate). The relative meaning of desorption in comparison to advection was expressed by means of the Damköhler number Da_{des}. The relative meaning of microbial degradation in comparison to the advection was expressed by means of the Damköhler number Da_{bio}. The pollutant source concentration C at the outlet of the source was normalised with the initial concentration C_o in the mobile phase. This value corresponds to the concentration under equilibrium conditions. In the seepage water prognosis, a conversion between the dimensionless time and water-solid mass ratio W/F is given by the relations:

$$t' = \frac{M/A}{n_e \cdot L} \cdot W/F \quad \text{and} \quad W/F = \frac{n_e \cdot L}{M/A} \cdot t'$$

where t’ = normalised pore volume time (t ' = t/PV), M/A = solid mass per unit cross sectional area. This conversion presupposes that flow can be accepted as steady

state (if necessary after suitable averaging). The use of the normalised pore volume time t' offers a crucial advantage in the context of setting of tasks, because the retention time of the pollutant in the mobile phase is thereby included. This enters directly in the determination of the Damköhler numbers Da_{des} and Da_{bio}, with which the relative contributions of desorption kinetics and the microbial degradation in the discharge behaviour are quantified.

(1) The Damköhler number Da_{des} is given by

$$Da_{des} = \begin{cases} -\ln\left(1 - 6\cdot\sqrt{\frac{D_{app}\cdot PV}{\pi\cdot a^2}} + 3\cdot\frac{D_{app}\cdot PV}{\pi\cdot a^2}\right) & \text{if} \quad \frac{D_{app}\cdot PV}{a^2} < 0.1 \\ \pi^2\cdot\frac{D_{app}\cdot PV}{a^2} - \ln\frac{6}{\pi^2} & \text{if} \quad \frac{D_{app}\cdot PV}{a^2} \geq 0.1 \end{cases}$$

with apparent diffusion coefficient: $D_{app} = \frac{D_{aq}\cdot n_{ip}^2}{n_{ip} + (1-n_{ip})\cdot\rho\cdot K_d}$

where a is grain radius, n_{ip} = intraparticle porosity, ρ is solid density und K_d is distribution coefficient.

(2) The Damköhler number Da_{bio} is given as $Da_{bio} = \lambda\cdot PV = \ln 2\cdot\frac{PV}{T_{1/2}}$

where λ is biodegradation rate constant and $T_{1/2}$ = half life.

The source strength function was derived from the results of many simulation runs with the model tool SMART. Within the SMART simulations both Damköhler numbers were varied independently from each other in the interval from 0.001 to 1000, in order to cover as large a range of the discharge behaviour as possible. Large values of the Damköhler numbers mean very fast, small values correspond to very slow reactions, where pore volume specification forms the comparison yardstick of typical advection time scales. With the help of the simulation results two function types were identified, which could be distinguished for the cases $Da_{des} \geq 0.1$ and $Da_{des} \leq 0.1$. Function parameters were obtained for both types by an optimum adjustment to the results of the SMART simulations.

(i) For case 1 ($Da_{des} \geq 0.1$) the relative discharge concentration is in the form

$$\frac{c}{c_0} = \frac{\exp\left(-0.74 \cdot Da_{Bio} \cdot t'/R\right)}{1+\exp\left[3.45 \cdot \left(Da_{Des}\right)^{0.15} \cdot \left(t'-R\right)/R^{0.74}\right]}$$

with the retardation factor $R = 1 + \frac{1-n_e}{n_e} \cdot \rho \cdot K_d$.

During the SMART simulations the retardation factor was varied up to a value of 340.

(ii) In the case of $Da_{des} \leq$ 0.1 the relative discharge concentration is in the form

$$\frac{c}{c_0} = \frac{\exp\left(-0.74 \cdot Da_{Bio} \cdot t'/R\right)}{1+5.07 \cdot \max\left\{0, t'-1\right\}^{0.6} / \left(Da_{Des}^{0.55} \cdot R^{0.93}\right)}$$

The relations for the relative discharge concentrations, indicated in the two discharge formulations represent a practicable aid to the quantification of the discharge behaviour of organic pollutants in the context of the seeping water prognosis. The derived equations have been implemented into an Excel sheet. A sample input and output files of this Excel formulation can be seen in Appendix 2. A simple conversion is possible between the dimensionless time t' and the water-solid material relationship W/F normalised with the pore volume as mentioned earlier. The constants arising in the equations for the relative discharge concentration were determined by adjustment of the source term function to the results of the SMART simulations. With additional test runs the database for the function adjustment could be widened and consequently lead to changes of the indicated constant values.

(2) Transport zone modelling at the lysimeter scale.

Lysimeter data from the research centers Jülich and GSF-München, Neuherberg were used, in order to determine the retention time distribution of a conservative tracer (bromide) over a transport distance from 35 cm to 100 cm and 125 cm respectively. This distribution formed a substantial input for the modelling of PAH pollutant transport with SMART, which was accomplished during the study. The model tool SMART was used to simulate the spread of the contaminants in the lysimeters. The very good agreement of the conservative breakthrough with the

observed tracer data in the Jülich and München lysimeters were a good technical basis for the modelling of the reactive transport with sufficient accuracy. During the model simulations, the initial model input parameters were defined independently from the PAH concentrations, which were recorded along the transport distance and / or at the lysimeter discharge outlet. This proceeding corresponds to a pure forward modelling of the reactive material transfer, i.e. there was no model calibration with regards to reactive processes as is the case in many modelling projects, in order to be able to examine the predictive capability of the model tool SMART. The 50 % breakthrough of the source term concentrations at the lysimeter measuring points were predicted to occur at 52 years for Jülich and between 2 to 215 years for München lysimeters. Large breakthrough times are due to the high PAH sorption capacity and rapid solute uptake of the predominantly fine-grained material and the associated, pronounced pollutant retardation along the travel distance. This was consistent with the very low recovery rate and low concentrations (Klotz and Schramm, 2006) detected in the lysimeter research facilities for more than 2.5 years of monitoring. However the appropriate breakthrough times could also be determined for many of the studied settings with simple calculation based on the measured data on the assumption of equilibrium conditions. The consistent good agreement between the observed data and the model predictions shows the usefulness of the model tool SMART as a prognosis instrument for pollutant risk assessment. Other lysimeter specific modelling with SMART, not presented in this study showed much improved agreement between the observed and the model results within the limit of experimental errors but limited in application.

(3) Landfill modelling

In addition to the Environmental Impact Assessment and inorganic leachate modelling with the Landsim model tool (Environmental Agency / Golder Associate, 1996) performed by (Taywood Environmental Consultancy) (Environmental Impact Assessment report, 2000) the process based reactive transport model SMART has been used to predict organic (PAH) contamination at a landfill site in Ghana (Kwabenya), a country whose solid waste is increasingly becoming organic in nature due to industrialisation with low waste recycling and minimisation programs.

Leachate released from the source (waste) was modelled with the source term functions encoded in the Excel spreadsheet introduced in chapter 3. The source term modelling of the organic leachate from the waste predicted a straight line horizontal breakthrough. This shows that the release of the leachate will be time independent at least for the 30 - 40 year operational period of the landfill i.e. the organic leachates were not affected by age within this period. Advective and diffusive time lags of leachate leaking through two liners with different permeabilities emplaced at the base of the landfill directly in contact with the waste were also determined. With the activation of sorption (equilibrium and kinetics) and biodegradation processes, two pathway scenarios were modelled with SMART for the unsaturated zone. Due to the relative longer half-life of PAHs, the effect of biodegradation is estimated to be minimal during the landfill operational period. The prediction of longer breakthrough times implies that the receptor (groundwater) would not be impaired if leachate leakage starts at any time within the operational period of the landfill. Even though there was no observed data for validation of the model as is often the case in field scale studies, SMART was found to be useful to a reasonable level of accuracy. SMART can therefore be used to establish waste acceptance criteria for organic contaminants in the landfill at Kwabenya.

REFERENCES

Abdel-Salam., A. and Chrysikopoulos, C. V. (1995): Modeling of Colloid and Colloid-Facilitated Contaminant Transport in a Two-Dimensional Fracture with patially Variable Aperture. Kluwer Academic Publishers. 20, 197-221.

Abelin, H. (1986): Migration in a single fracture: An in situ experiment in a natural fracture, Ph.D. dissertation, Dep. of Chem. Eng., R. Inst. of Tech., Stockholm, 170 pp.

Abu-Sharar, T.M., F.T. (1987): Bingham and J.D. Rhoades, Stability of soil aggregates as affected by electrolyte concentration and composition. Soil Sci. Soc. Am. J., 51, 309.

Adamczyk, Z., T. Dabros, J. Czarnecki and T.G.M. van de Ven (1983): Physical Chemistry of Colloid and Interfaces: Biotechnologies and Drug Research Adv. Colloid Interface Sci., 19 183.

Aden, K., Diekkrueger, B (2000): Modeling pesticide dynamics of four different sites using the model system SIMULAT. Agric. Water Mgmt. 44, 337±355.

Adriaens, P. (2003): Applied Environmental Geoscience lecture notes: Microbiology II. Sec 5.2p. Eberhard-Karls-Universität Tuebingen.

AGBoden (1994): Bodenkundliche Kartieranleitung, 4. Auflage, E. Schweizbart'sche Verlagsbuchhandlung, Stuttgart,.

Aitken, C.M., Jones, D.M., and Larter, S.R. (2004): Anaerobic hydrocarbon biodegradation in deep subsurface oil reservoirs. Nature 431: 291-294.

Akthar, M.S., B.K.Richards, P.A.Medrano, M. deGroot, and T.S.Steenhuis. (2003): Dissolved Phosphorus Losses from Undisturbed Soil Cores: Related to Adsorption Strenth, Flow Rate, or Soil Structure? Soil Science of America Journal 67:458-470

Alexander, M., (1999): Biodegradation and Bioremediation, 2. ed., Academic Press, San Diego,. an unsaturated field soil. Water Resour. Res. 27:2533–2541.

Amankwah, E.(2003). Modeling of Sorption and Desorption Hysteresis phenomena. Master Thesis. Eberhard Karls Universität, Tuebingen.

Anderson, M.P. (1979): Using models to simulate the movement of contaminant through groundwater flow system. Crit. Rev. Environ. Controls 9(2), 97-156.

Anderson, M.P., (1984): Movement of Contaminants in Groundwater: Groundwater Transport-Advection and Dispersion: in Groundwater Contamination, Studies in Geophysics. National Academy Press, Washington D.C., pp. 429-437.

Avogadro, A. and G. de Marsily, (1984): The Role of Colloids in Nuclear Waste Disposal, Mat. Res. Symp. Proc.,26 495.

BAL/Bundesanstalt für alpenländische Landwirtschaft Gumpenstein (ed.), 1991, 1992, 1993, 1994, 1995, 1996, 1997, 1999, 2001, 2003: Berichte über die Lysimetertagungen. – BAL Gumpenstein/Bundesministerium für Land- und Forstwirtschaft bzw. Bundesministerium für Land- und Forstwirtschaft, Umwelt und Wasserwirtschaft, Irdning.

Batycky, R.P., Thiele, M. and M.J. Blunt, (1996): A streamline simulator to model field scale three-dimensional flow, Proceedings of the 5th European conference on the mathematics of oil recovery, Leoben, Austria,.

BBA, (1990): Lysimeter investigations for the displacement of pesticides into the subsoil. In: Guidelines for the testing of agricultural pesticides with registration procedure, Part IV 4-3, Braunschweig, Germany, Biological Bundesanstalt.

BBodSchG, (1998): Gesetz zum Schutz des Bodens vom 17. März 1998. - Bundesgesetzblatt, 16, 505-510,.

BBodSchV (1999): Bundes-Bodenschutz- und Altlastenverordnung vom 16. Juli 1999. Bundesgesetzblatt, 36, 1554-1682.

Bear, J., (2001): Modelling groundwater flow and contaminant transport, http://www.cmdlet.com/demo/mgfc-course/mgfcmod.html

Beltaos, S., T.J. Day (1978): A field study of longitudinal dispersion, Can, J.Civil Eng.5, 572-585.

Böhm, K. E. et al. (2002): Lysimeter – Anforderungen, Erfahrungen, technische Konzepte/ Lysimeter – Demands, Experiences, Technical Concepts. – Beiträge zur Hydrogeologie 53, Graz, pp 115-232

Bold, S. (2004): Process-based prediction of the long-term risk of groundwater pollution by organic non-volatile contaminants. Zentrum für Angwandte Geowissenschaften. Tuebingen, Eberhard Karls Universität,Tuebingen.

Boesten, J.J.T.I., van der Pas, L.J.T., (2000): Movement of water bromide ion and the pesticides ethoprophos and bentazone in a sandy soil.: description of the Vredepeel dataset. Agric. Water Manage. 44, 21-42.

Bourke, P. J. (1987): Channeling of flow through fractures in rock, Proceedings, GEOVAL87 Symposium, Swed. Nucl. Power Inst., Stockholm, pp. 167-177.

Bresler, E; Dagan, G. (1981): Convective and Pore Scale Dispersive Solute Transport in Unsaturated Heterogeneous Fields. WATER RESOURCES RES. Vol. 17, no. 6, pp. 1683 -1693.

Brunauer, S., Emmett P.H., Teller E. (1938): Adsorption of gases in multimolecular layers. - J. Amer. Chem. Soc. 60 (2): 309-319, Washington.

Buddemeier, R.W. and J.R. Hunt, (1988): Appl. Geochem., 3: 535. Bundesgesetzblatt, 36, 1554-1682, 1999.

Butters, G.L., W.A. Jury, and F.F. Ernst. (1989): Field scale transport of bromide in an unsaturated soil. 2. Dispersion modeling. Water Resour. Res. 25:1583–1589. by EU-Commission**:** 66.

Cai, W. (2004): Effects of enhanced solute spreading in the unsaturated zone on the bioavailability of contaminants. Zentrum für Angewandte Geowissenschaften. Tuebingen, Eberhard Karls Universität of Tuebingen.

Cata, C. (2003): Prediction of contaminant transport in unsaturated layered porous media. Zentrum für Angewandte Geowissenschaften. Tuebingen, Eberhard Karls Universität of Tuebingen.

Cerda, C.M. (1987): Mobilization of kaolinite fines in porous media. Colloids Surf. 27:219–241.

Cerniglia, C.E. (1984): Microbial metabolism of polycyclic aromatic hydrocarbons. Adv. Appl. Microbiol. 30: 31-71.

Cerniglia, C.E. (1992): Biodegradation of polycyclic aromatic hydrocarbons. Biodegradation 3: 351-368

Champ, D.R., Young, J.L., Robertson, D.E., and Abel, K.H. (1984): Chemical speciation of long-lived radionuclides in a shallow groundwater flow system. Water Poll. Res. J. Canada, 19, 35-54.

Chen, J., Henderson, G., Grimm, C.C., Lloyd, S.W., and Laine, R.A. (1998): Termites fumigate their nests with naphthalene. Nature 392: 558-559.

Christ, A. (2004): Zum Transport von partikelgebundenen Schadstoffen in der ungesättigten Zone. Inst. f. Geowiss. der Johannes-Gutenberg-Universität Mainz.

Chu, J., Y. Jin, M. Flury, and M.V. Yates. (2001): Mechanisms of virus removal during transport in unsaturated porous media. Water Resour. Res. 37:253–263.

Clement, T.P. (1998): RT3D - A Modular Computer Code for Simulating Reactive Multi-Species Transport in 3-Dimensional Groundwater Aquifers Version 1.0.

Comanys, R., Gaganis, P., Gorostiza, I., Höhener, P., Kjeldsen, P. and Van (1999): Compounds in a New Jersey Coastal Plain Aquifer System. Groundwater Contaminated Sites (GRACOS). Tübingen, GRACOSConsortium, funded .

Council directive 1999/31/EC of 26 April 1999 on the landfill of waste, (1999):.Official Journal of the European Communities, L 182, 1-19,

Crank, J., (1975):.Mathematics of diffusion, 2nd ed., Oxford University Press, London,

Crittenden, J.C., Hutzler, N.J., Geyer, D.G., Oravitz, J.L. and G. (1986): Friedman, Transport of organic compounds with saturated groundwater flow: Model development and parameter sensitivity, Water Resour. Res., 22(3), 271-284.

Dagan, G. and V. Cvetkovic, Reactive transport and immiscible flow in geological media, I. General theory. Proc. R. Soc. London, A, 452, 285-301, 1996.

Dagan., G (1982). Stochastic modelling of groundwater by unconditional and conditional probilities.2. The solute transport, Water Resour. Res. 18, 835-848.

de Jonge, L.-W., C. Kjaergaard, and P. Moldrup. (2004): Colloids and Colloid-Facilitated Transport of Contaminants in Soils: An Introduction. Vadose Zone Journal 3:321–325

De Rooij, G.H., (1995): A three-region analytical model of solute leaching in a soil with a water repellent top layer. der Sloot, H. (2003). Guideline for Groundwater Risk Assessment.

Diersch, H.-J.G., (2002): FEFLOW – Reference manual, WASY Ltd., Berlin.

Dohse, D.M. and L.W. Lion, (1994): Effect of microbial polymers on the sorption and transport of phenanthrene in a low-carbon sand, Environ. Sci. Technol., 28(4), 541-548,.

Dust, M., Baran, N., Errera, G., Hutson, J.L., Mouvet, C., Schaefer, H., Vereecken, H., Walker, A., (2000): Simulation of water and solute transport in ®eld soils with the LEACHP model. Agric. Water Manage., 44, 225-245

Egli T. (1995): The ecological and physiological significance of the growth of heterotrophic microorganisms with mixtures of substrates. In: Advances in Microbial Ecology, Vol 14 (Jones JG, ed). New York: Plenum Press, 305–386.

Environmental Agency / Golder Associate (1996). LandSim: Landfill Performance Simulation by Monte Carlo. Release 1.0.

Environmental Impact Assessment report (2000): Proposed landfill at Kwabenya – Environmental sanitation project. Taywood Environmental Consultancy, investigation and cleanup, fourth edition. EPA-542-B-05.

Estrella, M.R., Brusseau, M.L., Maier, R.S., Pepper, I.L., Wierenga, P.J. and R.M. Miller (1993): Biodegradation, sorption, and transport of 2,4-dichlorophenoxyacetic acid in saturated and unsaturated soils. Appl. Environ. Microbiol., 59(12), 4266-44273.

Evans, P.J., Mang, D.T. and Young, L.Y., (1991): Degradation of toluene and m-xylene and transformation of oxylene by denitrifying enrichment cultures. Applied and Environmental Microbiology, 57: 450-454.

Federal Ministry for Environment, Nature Conservation and Nuclear safety (BMU) (2006): Water Resource Management in Germany.

Fetter, C.W., (2004): Applied hydrogeology, fourth edition.

Finkel, M., Liedl, R. and G. Teutsch, (1998b): A modelling study on the efficiency of groundwater treatment walls in heterogeneous aquifers, In: Groundwater quality: Remediation and protection, IAHS Publ., 250.

Finkel, M., Liedl, R. and G. Teutsch, (1998a): Modelling Surfactant Influenced PAH Migration, Phys. Chem. Earth, 23(2), 245-250.

Finkel, M., Liedl, R. and G. Teutsch, (1999): Modelling surfactant-enhanced remediation of polycyclic aromatic hydrocarbons, Environmental Modelling & Software, 14, 203-211.

Fischer, H.B. (1973): Longitudinal dispersion and turbulent mixing in open channel flow. Ann. Rev. Fluid Mech.5,59-78.

Fischer-Romero, C., Tindall, B.J., and Jüttner, F. (1996): Tolumonas auensis gen. nov., sp. nov., a toluene-producing bacterium from anoxic sediments of a freshwater lake. Int. J. Sys. Biol. 46: 183-188.

Flipse, W. J., Jr., B. G. Katz, J. B. Linder, and R. Markel. (1984): Sources of Nitrate in Ground Water in a Sewered Housing Development, Central Long Island, New York. Ground Water. 32:418-426.

Flury, M. (1996): Experimental evidence of transport of pesticides through fields. A review. J. Environ. Qual. 25:35-45.

Flury, M., (1996): Experimental evidence of transport of pesticides through field soils. A review, J. Environ. Qual., 25(1), 25-45.

Food and Agriculture Organization of the United Nations, (1982): Lysimeters. FAO Irrigation and Drainage Paper, 39, 67 pp.

Francaviglia, R., Capri, E., (2000): Lysimeter experiments in Tor Mancina (Italy). Agric.Water Manage. 44, 63±74.

Francaviglia, R., Capri, E., Klein, M., Hosang, J., Aden, K., Trevisan, M., Errera, G., 2000. Comparing and evaluating pesticide leaching models: results for the Tor Mancina data set (Italy). Agric. Water Manage. 44, 135±151.

Franck, H.G. (1963): The challenge in coal tar chemicals. Ind. eng. chem. 55: 38 - 44.

Frenkel, H., J.O. Goertzen and J.D. Rhoades, Soil Sci. Soc. Am. J., 42 (1978) 32. 1233.

Freundlich, H. (1909): Kapillarchemie, Leipzig (Akademische Verlagsgesellschaft m.b.H), 51.

Fried, J.J. (1975): Groundwater Pollution, Elsevier, Amsterdam, 330 pp.

Fusillo, T.V., J.J. Hochreiter and D.G. Lord. (1985): Distribution of Volatile Organics.

Galushko, A., Minz, D., Schink, B., and Widdel, F. (1999): Anaerobic degradation of naphthalene by a pure culture of a novel type of marine sulphate-reducing bacterium Environ. Microbiol. 1: 415-420.

Gelhar, L.W., and C. Axness. (1983): Three Dimensional Stochastic Analysis of Macrodispersion in Aquifers. Water Resour. Res. 19:161–180.

Gelhar, L.W., and C.L. Axness (1981): Stochastic Analysis of Macro-Dispersion in Three Dimensionally Heterogeneous Aquifer, Geophysical Research Centre, Hydrology Research Program, Rep. No. H8, New Mexico Inst. of Mining and Technology, Socorro, New Mexico, 140 pp. Golden, Colorado, p. 202.

Gelhar, L.W., Welty, C. and Rehfeldt, K.R., (1992): A critical review of data on field scale dispersion in aquifers. Water Resour. Res., 28(7): 1955-1974.

Gibson D.T, Subramanian V. (1984):. Microbial degradation of aromatic hydrocarbons. In: Gibson DT, editor. Microbial degradation of organic compounds. New York: Marcel Dekker.pp 181-252.

Gonçalves, M. C., J. Šimůnek, T. B. Ramos, J. C. Martins, M. J. Neves, and F. P. Pires (2006): Multicomponent solute transport in soil lysimeters irrigated with waters of different quality, Water Resour. Res., 42, W08401, doi: 10.1029/2005WR004802.

Good Modeling Practices handbook,: STOWA/RIZA, (1999): Smooth modeling in water management. STOWA report 99-05, Dutch depts. Public works, institute for inland water management and waste water treatment report 99.036.

Gounaris, V., Anderson, P.R. and T.M. Holsen, (1993): Characteristics and environmental significance of colloids in landfill leachate, Environ. Sci. Technol., 27(7), 1381-1387.

Grathwohl, P. and B. Susset, (2001): Sickerwasserprognose für organische Schadstoffe: Grundlagen und Stand der Forschung, Altlastenspektrum, 6, 285-293.

Grathwohl, P., (1990): Influence of Organic Matter from Soils and Sediments from Various Origins on the Sorption of Some Chlorinated Aliphatic Hydrocarbons: Implications on Koc Correlations. Environmental Science and Technology, 24: 1687-1693.

Grathwohl, P., (1998): Diffusion in natural porous media, Kluwer Academic Publisher, Boston,.

Grathwohl., P. (1997): Diffusion in natural porous media – Contaminant transport, sorption/desorption and dissolution kinetics, Kluwer, Dordrecht.

Grathwohl., P., (1998): Diffusion in Natural Porous Media: Contaminant Transport, Boston, 224.

Grbic-Galic, D. and T.M. Vogel, (1987): Transformation of Toluene and Benzene by mixed methanogenic cultures, Appl. Environ. Microbiol., 53(2), 254-260.

Grolimund, D., Borkovec, M., Barmettler, K. and H. Sticher., (1996): Colloid-facilitated transport of strongly sorbing contaminants in natural porous media: A laboratory column study, Environ. Sci. Technol., 30(10), 3118-3123.

Gschwend, P,M. and M.D. Reynolds (1987): Monodisperse ferrous phosphate colloids in an anoxic groundwater plume J. Contam. Hydrol., 1, 309.

Gschwend, P.M. and J.N. Ryan., (1994): Effects of ionic strength and flow rate on colloid release: Relating kinetics to intersurface potential energy. J. Colloid Interface Sci. 164:21–34 J. Colloid Interface Sci., 164, 21.

Guha, S. and P.R. Jaffé., (1996a): Biodegradation kinetics of phenanthrene partitioned into the micellar phase of nonionic surfactants Environ, Sci. Technol., 30(2), 605-611,.

Guha, S., and P.R. Jaffé., (1996b): The Bioavailability of Hydrophobic Compounds Partitioned into the Micellar Phase of Nonionic Surfactants, Environmental Science and Technology, Vol. 30, No. 4,. 1382-1391.

Guha, S., Jaffé, P.R. and C.A. Peters., (1998):.Bioavailability of mixtures of PAHs partitioned into the micellar phase of a nonionic surfactant, Environ. Sci. Technol., 32(15), 2317-2324.

Guha, S., Peters C., Jaffé P., (1999): Multisubstrate biodegradation kinetics of naphthalene, phenanthrene, and pyrene mixtures. Biotechnol Bioeng 65:491–499.

Gupta, D. and M.H. Peters, J., (1985): Colloid Interface Sci., 104 375.

Haldeman, W. R., Chuang, Y., Rasmussen, T. C. and Evans, D. D, (1991): Laboratory analysis of fluid flow and solute transport through a fracture embedded in porous tuff, Water Resour. Res. 27(1), 53-65.

Hance, R.J. and Führ F., (1992): Methods to study fate and behaviour of pesticides in the soil. In: Lysimeter studies of the fate of pesticides in the soil (eds. Führ F. and Hance R.J.), British Crop Protection Council Monograph, 53: 9-21.

Harris, G.L., Catt, J.A., Bromilow, R.H., Armstrong, A.C., (2000): Evaluating pesticides leaching models: the Brimstone farm dataset. Agric. Water Manage. 44, 75-83.

Henzler, R., (2004): Quantifizierung und Modellierung der PAK-Elution aus verfestigten und unverfestigten Abfallmaterialien. Zentrum für Angewandte Geowissenschaften. Tuebingen, Eberhard Karls Universät Tuebingen.

Hirner, A. V., Rehage, H., Sulkowski, M., (2000): Polyzyklische aromatische Kohlenwasserstoffe. In Umweltgeochemie. Darmstadt: Steinkopf, pp 308-317.

Howard, P.H., Boethling, R.S., Jarvis, W.F., Meylan, W.M. and E.M. Michalenko., (1991) Handbook of environmental degradation rates, Lewis Publisher, Chelsea,.

Hutson, J.L. and R.J. Wagenet., (1995): A multiple-region model describing flow and solute transport in heterogeneous soils, Soil Sci. Soc. Am. J., 59, 743-751.

Hüttmann, A., (2001): Jump-displacement: Eine Methode zur Modellierung des Transports von Stoffen mit nichtlinearen Sorptionsisothermen, Diplomarbeit, University of Tübingen, Tübingen.

IRC (2000): International water and sanitation center, Netherlands.

Jacques, D., D. Kim, J. Diels, J. Vanderborght, H. Vereeken, and J. Feyen., (1998): Analysis of steady state chloride transport through two heterogeneous field soils. Water Resour. Res. 34:2539–2550.

Jaeger, R. and R. Liedl., (2000): Prognose der Sorptionskinetik organischer Schadstoffe in heterogenem Aquifermaterial, Grundwasser, 5(2), 57-66,.

Jarvis, N., Brown, C., Granitza, E., (2000). Sources of error in model predictions of pesticide leaching: a case study using the MACRO model. Agric. Water Manage. 44, 247±262.

Jia, X. and R.A. Williams., (1990): The effect of ionic migration and diffusion on the roughness development of growing electrodeposits. Chem. Eng. Commun., 91 127.

Jia, X.; Williams, R.A., (1990): Particle deposition at a charged solid-liquid interface Chemical Engineering Communications, 91, pp.127-198.

Jia, X.; Williams, R.A.; Green M., (1990): The feasibility of selective separation of colloidal particles at a solid-liquid interface Chemical Engineering Communications, 91, pp.199-223.

Jørgensen, P.R., and J. Frederecia., (1992): Migration of nutrients, pesticides and heavy metals in fractured clayey till.Geotechnique 42:67–77.

Jury, W.A., (1982): Simulation of solute transport using a transfer function model parameters. Water Resour. Res. 18:363 – 368.

Jury, W.A. and K. Roth., (1990): Transfer functions and solute movement through soils, Birkhäuser, Basel.

Jury, W.A., and D. Scotter., (1994): A unified approach to stochastic–convective transport problems. Soil Sci. Soc. Am. J. 58:1327–1336.

Jüttner, F., (1988): Benzene in the anoxic hypolimnion of a freshwater lake. Naturwissenschaften 75: 151-153.

Jüttner, F., and Henatsch, J.J., (1986): Anoxic hypolymnion is a significant source of biogenic toluene. Nature 323: 797-798.

Kallay, N., E. Barouch and E. Matijevid., (1987): Diffusional detachment of colloidal particles from solid/solution interfaces. Adv. Colloid Interface Sci., 27.

Karathanasis, A.D., (1999): Subsurface migration of copper and zinc mediated by soil colloids, Soil Sci. Soc. Am. J. 63, 830-838.

Karickhoff, S.W., D.S. and Scott, T.A., (1997): Sorption of hydrophobic pollutants on natural sediments. Water Research, 13(3):241-248.

Kemmesies, O., (1999): Darstellung des Sachstandes. Umsetzung im Programm SIWAPRO/HYDRUS. BWK-AG 6.2, Instrumente zur Sickerwasserprognose.

Kinniburgh, D.G., (1986): General purpose adsorption isotherms. Environ. Sci. Technol. 20, 895-904.

Kladivko, E. J., G.E van Scoyoc, E. J. Monke, K.M. Oates, and W.J. Pask., (1991): Pesticide and nutrient movement into subsurface tile drains on a silt loam in Indiana. J. Environ. Qual. 20:264-272.

Klein, M., Hosang, J., Schaefer, H., Erzgraeber, B., Resseler, H., (2000): Comparing and evaluating pesticide leaching models. Results of simulations with PELMO. Agric. Water Mgmt. 44, 263±281.

Kleineidam S., Rügner H., Grathwohl P., (1999): Impact of grain scale heterogeneity on slow sorption kinetics, Environ. Toxic. Chem. 18 (8), 1673-1678.

Kleineidam, S., Rügner, H. and P. Grathwohl., (1999): Impact of grain scale heterogeneity on slow sorption kinetics, Environ. Tox. Chem., 18(8), 1673-1678.

Kuhn, E.P., Colberg, P.J., Schnoor, J.L., Wanner, O., Zehnder, A.J.B., and Schwarzenbach, R.P., (1985): Microbial transformation of substituted benzenes during infiltration of river water to groundwater: laboratory column studies. Environ. Sci. Technol. 19: 961-968.

KUTÍLEK, M. and D. R. NIELSEN., (1994): Soil Hydrology. – GeoEcology textbook, Catena Verlag, Cremlingen-Destedt, 370 p.

Lanthaler, C., (2004): Lysimeter Stations and Soil Hydrology Measuring Sites in Europe. Purpose, Equipment, Research Results, Future Developments. Diploma Thesis, Karl-Franzens-University Graz.

Lawes, J.B. Gilbert, and R.Warington., (1882):. On the amount and composition of the rain and drainage water collected at Rothamstead. Williams Clowes and Sons, Ltd., London

Lee, D. R., J.A. Cherry, and J.F Pickens., (1980):. Groundwater transport of a salt tracer through a sandy lakebed, Limnol.Oceanogr. 25, 45-61.

Lenhart, J.J., and J.E. Saiers., (2002): Transport of silica colloids through unsaturated porous media: Experimental results and model comparisons. Environ. Sci. Technol. 36:769–777.

Leonard, R.A., Knisel, W.G., Still, D.A., (1987): GLEAMS: groundwater loading effects of agricultural management systems. Trans. Am. Soc. Agric. Eng. 30(5), 1403±1418.

Liedl, R. and T. Ptak., (2003): Modelling of diffusion-limited retardation of contaminants in hydraulically and lithologically non-uniform media, J. Contam. Hydrol., 66(3-4), 239-259,.

Lui, H.H. and J.H. Dane., (1996): An extended transfer function model of field-scales solute transport: Model development. Soil Science Society of America Journal [Soil Sci. Soc. AM. J.]. Vol. 60, no. 4, pp. 986-991.

Madlener, I., (2004): Quantifizierung und Modellierung der PAK- esorptionsverhaltens aus feinkörnigem Material mittels Säulenversuchen (DIN V 19736) und Hochdruck - Temperatur-Elution (ASE). Zentrum für Angewandte Geowissenschaften. Tuebingen, Eberhard Karls Universität Tuebingen.

Madlener, I., Henzler, R. and P. Grathwoh.l, (2003): Material investigations to determine the leaching behaviour of PAHs at elevated temperatures, In: D. Halm and P. Grathwohl (Eds.), Proceedings of the 2st international workshop on groundwater risk assessment at contaminated sites (GRACOS), TGA, C68, Tübingen.

Maidment D.R., (2003): GIS for water resources, ESRI Press, Redlands.

Matheron, C., and G. DeMarsily.,(1980): Is transport in porous media always diffusive? Water Resour. Res. 16, 901-917.

McCarthy, J.F. and B.D. Jimenez., (1985): Interactions between polycyclic aromatic hydrocarbons and dissolved humic material: Binding and dissociation, Environ. Sci. Technol., 19(11), 1072-1076,.

McCarthy, J.F., and L.D. McKay. (2004): Colloid transport in the subsurface: Past, present, and future challenges. Available at www.2004. – vadose zone journal.org. Vadose Zone J. 3:326–337 (this issue).

McCarthy., F.J and J.M. Zachara., (1989): Environ. Sci. Technol.,23, 496.

McCarthy., J.F., and J.M. Zachara., (1989): Subsurface transport of contaminants. Environ. Sci. Technol. 23:496–502.

McDowell-Boyer, L.M., Hunt, J.R. and N. Sitar., (1986): Particle transport through porous media, Water Resour. Res., 22(13), 1901-1921.

McDowell-Boyer, L.M., (1992): Chemical mobilization of micro-sized particles in saturated porous media under steady flow conditions. Environ, Sci. Technol., 26, 586.

Meckenstock, R.U., Annweiler, E., Michaelis, W., Richnow, H.H., and Schink, B., (2000): Anaerobic naphthalene degradation by a sulfate-reducing enrichment culture. Appl. Environ. Microbiol. 66: 2743-2747.

Meckenstock, R.U., (2002): Applied Environmental Geoscience lecture notes: Microbiology I. 78p. Eberhard Karls Universität Tuebingen.

Mensah, A., and E. Larbi., (2006): Fact sheet: Solid waste disposal in Ghana 1-6.

Meyer J.S, Marcus M.D, (1984): Bergman HL. Inhibitory interactions of aromatic organics during microbial degradation. Environ Toxicol Chem 3:583-587.

Molinari J.P., B.G. Plaudecerf, and M. Launay., (1977) : Essais conjoints en laboratoire et sur le terrain en vue d`une approche simplifie de la prevision des propogations des substances miscibles dans les aquiferes reels, in Prac. of the Symp. on Hydrodynamic Diffusion and Dispersion in Porous Media, Int. Assoc. for Hydraulic Research, Pavia, Italy, pp, 89-102.

Moulin,V and G. Ouzounian., (1992): Role of colloids and humic substances in the transport of radio-elements through the geosphere Appl. Geochem., Suppl. Issue No. 1 179.

Muller, J.-C. (ed.), 1996: Un point sur trente ans de lysimétrie en France. Une technique, un outil pour l'etude de l'evironnement. – INRA, editions, comifer, Paris, 390p.

Neretnieks, I., (2002): A stochastic multi-channel model for solute transport - analysis of tracer tests in fractured rock. J. Contaminant Hydrol., 55(3-4): 175-211.

Neuman, S.P., (1990): Universal scaling of hydraulic conductivities and dispersivities in geologic media. Water Resourc. Res. 26:1749–1758.

Nieber, J.L., (1996): Modeling finger development and persistence in initially dry porous media. Geoderma 70, 207-230.

Nielsen, P.H. and T.H. Christensen., (1994): Variability of biological degradation of aromatic hydrocarbons in an arobic aquifer determined by laboratory batch experiments. J. Contam. Hydrol., 15, 305-320.

Nießner, R., Zajic, A., Schäfer, O. and M. Kühnhardt, (1994): Einfluß der Wechselwirkung organischer Luftschadstoffe (PAH's, PCB's) in athmosphärischen Aerosol und Niederschlag auf die Qualität oberflächennaher Grundwässer, Abschlussbericht, Lehrstuhl für Hydrogeologie, Hydrogeochemie und Umweltanalytik, Technische Universität München, München,.

Noss, RR; Johnson, ET., (1984): The Fourth National Symposium and Exposition on Aquifer Restoration and Ground Water Monitoring May 23-25,. The Fawcett Center, Columbus, Ohio. p 356-362, 9 fig, 1 tab, 8 ref. Massachusetts Division of Water Pollution Control, Contract No. 80-32.

O`Loughlin, E.M., and Bowmer, K.H., (1975): Dilution and decay of aquatic herbicides in flowing channel. J. Hydrol., 26. 217-235

Ogata, A., (1964): Mathematics of dispersion with linear adsorption isotherm. U.S. Geol. Surv.Prof. Pap.No.411-H.

Ogata, A., and Banks, R.B (1961): Solution of the differential equation of longitudinal dispersion in porous media. US. Geol. Surv. Prof. Pap.No.411-A.

Parker, J.C. and van Genuchten, M.Th., (1984): Flux-averaged and volume-averaged concentrations in continuum approaches to solute transport. Water Resour. Res., 20: 866-872.

Parlange, J- Y., T.S. Steenhuis, R.J. Glass, T.L. Richard, N.B. Pickering, W.J Waltman, N.O. Bailey, M.S. Andreine, and J.A. Throop., (1988): The flow of pesticides through preferential paths in soils . N.Y. Food Life Sci. Quart. 8:20-23.

Penrose., W.R., W.L. Polzer, E.H. Essington, D.M. Nelson and K.A. Orlandini., (1990): Environ. Sci. Technol., 24 228.

Peter, A., (2002): Assessing natural attenuation at field scale by stochastic reactive transport modeling, Tübinger Geowissenschaftliche Arbeiten, C64, Tübingen.

Peter, A., Liedl, R., Ptak, T. and Teutsch, G., (2002): Comparing two approaches for modelling natural attenuation of organic compounds in heterogeneous porous media. In: H. Schulz and G. Teutsch (Editors), Geochemical Processes - Concepts for Modelling Reactive Transport in Soils and Groundwater. VCH Wiley.

Pickens, J.F., and G.E. Grisak., (1981b): Modeling of scale-dependent dispersion in hydrogeologic systems, Water Resour. Res. 17. 1701-1711.

Pivetz, B.E. and T.S. Steenhuis., (1995): Soil matrix and macropore biodegradation of 2,4-D, J. Environ. Qual., 24, 564-570,

Pivetz, B.E., Kelsey, J.W., Steenhuis, T.S. and M. Alexander., (1996): A procedure to calculate biodegradation during preferential flow through heterogeneous soil columns, Soil Sci. Soc. Am. J. 60, 381-388,.

Prommer, H., D.A Barry, W.H. Chiang and C. Zheng., (2003): PHT3D-A MODFLOW/MT3DS-based reactive multi-component transport model. Groundwater. 41(2).

Pütz T., Rützel H., Vereecken H., (2002): Erfassung von realitätsnahen Verlagerungsszenarien im Großlysimeterversuch und begleitende Simulationen Rahmen des BMBF-Projekts: Prognose des Stoffeintrages in das Grundwasser mit dem Sickerwasser (Sickerwasserprognose) – Applikationsbericht, Forschungszentrum Jülich GmbH, 25 S.

Pyrak, L. R., Myer, L. R. and Cook, N. G. W., (1985): Determination of fracture void geometry and contact area at different effective stress, Eos Trans. AGU Abstract, 66(46), 903.

Quirk, J.P., and R.K. Schofield. (1955): The effect of electrolyte concentration on soil permeability. J. Soil Sci. 6: 163–178.

Rahman, M.M., (2002): Sorption and transport behaviour of hydrophobic organic compounds in soils and sediments of Bangladesh and their impact on groundwater pollution - Laboratory investigations and model simulations. TGA, C63, Eberhard-Karls-Universität Tübingen.

Ramaro, B.V. and C. Tien, in R.P. Chabra and D. DeKey., (Eds.) (1991): Transport Processes in Bubbles, Drops and Particles, Hemisphere, New York, , p. 191.

Reardon, KF, D.C. Mosteller and J.D. Rogers., (2000): Biodegradation kinetics of benzene, toluene, and phenol as single and mixed substrates for Pseudomonas putida F1. Biotechnol Bioeng 69:385–400.

Rekolainen, S., Gouy, V., Francaviglia, R., Eklo, O.M., BaÈrlund, I., (2000): Simulation of soil water, bromide and pesticide behaviour in soil with the GLEAMS model. Agric. Water Mgmt. 44, 201±224.

Richards, L.A., (1931): Capillary conduction of liquids through porous mediums, Physics, 1, 318-333.

Ritsema, C.J., J.C. van Dam, J.L. Nieber, L.W. Dekker, K. Oostindie, and T. Steenhuis., (2001): Preferential Flow in Water Repellent Sandy Soils:

Principles and Modeling Approaches. In Proceeding of the 2nd ASAE International Symposium on Preferential Flow: Water movement and chemical transport in the environment. Honolulu, HI. January 3-5.

Ritsema, J.C., L.W.Dekker, J.L.Nieber, and T.S.Steenhuis., (1998): Modelling and field evidence of finger formation and finger recurrence in a water repellent sandy soil. Water Resources Research 34(4):555-567.

Road map to understanding innovative technology options for brownfields (2005).

Rose, D.A., (1977): Dilution and decay of aquatic herbicides in flowing channels. J. Hydro., 32, 399-400.

Rosen, J.B., (1954): General numerical solutions for solid diffusion in fixed beds, Ind. Eng. Chem., 46(8), 1590-1594.

Roth, K., W.A. Jury, H. Fluhler, and W. Attinger., (1991): Transport of chloride through an unsaturated fied soil Water Resour. Res. 27:2533–2541.

Rothschild, E.R. Manser, R.J. and M.P Anderson., (1982): Ground Water Vol. 20, No. 4, p 437-445, Fig, 1 Tab, 26 Ref

Rügner, H., Kleineidam, S. and P.Grathwohl., (1997): Sorptionsverhalten organisher Schadstoffe in heterogenem Aquifermaterial am Beispiel des Phenanthrens. Grundwasser, 3: 133-138.

Runkel., R.L., (1996): Solution of the Advective–Dispersion Equation: Continous Load of Finite Duration. U.S. Geol. Surv. Water Resource Division.

Russel., W.B., D.A. Saville and W.R. Schowalter., (1989): Colloidal Dispersions, Cambridge University Press, Cambridge,.

Ryan, J.N. and M. Elimelech., (1996): Colloid mobilization and transport in groundwater, Colloids and Surfaces A: Physiochem. and Eng. Aspects, 107, 1-56,.

Ryan, J. N. and M. Elimelech., (1995): Colloid mobilization and transport in groundwater .Colloids Surfaces A: Physicochem. Eng. Aspects 107.

Salanitro, J. P., Dorn, P. B., Huesemann, M. H., Moore, K. O., Rhodes, I. A., Jackson, L. M. R., Vipond, T. E., Western, M. M. and Wisniewski, H. L., (1997): Crude Oil Hydrocarbon Bioremediation and Soil Ecotoxicity Assessment. Environmental Sciences and Technology, 31(6): 1769-1776.

Sansoulet, J., (2007): Water flow and transport of potassium and nitrate ions in a variable charge soil under rainfall redistributed by crop. Experimental and modeling study in a banana plantation fertilized on an andosol, PhD thesis, Institut National Agronomique, Paris, Grignon, 136 pp.

Schäfer, A., P. Ustohal, H. Harms, F. Stauffer, T. Dracos, and A.J.B. Zehnder., (1998a): Transport of bacteria in unsaturated porous media.J. Contam. Hydrol. 33:149–169.

Schelde, K., P. Moldrup, O.H. Jacobsen, H. de Jonge, L.W. de Jonge, and T. Komatsu., (2002). Diffusion-limited mobilization and transport of natural colloids in macroporous soil.Available at www.vadosezonejournal.org. Vadose Zone J. 1:125–136.

Schierholz, I., Shäfer, H., Kolle, K., (2000). The Weiherbach dataset: an experimental data set for pesticide model testing on the field scale. Agric. Water Manage. 44, 43-61.

Schmidt, M., (2002): Validation of SMART for the transport of Phenanthrene through the unsaturated zone, Master thesis, University of Tübingen, Tübingen, Germany,

Schwartz, F. W. (1977): Macroscopic dispersion in porous media:The controlling factors, Water Resourc. Res. 13, 743-752.

Schwarzenbach R.P., Gschwend P.M., Imboden D.M., (1992): Environmental Organic Chemistry.255.

Seagren, E.A., B.E. Rittmann and Valocchi. A.J., (1993): Quantitative evaluation of flushing and biodegradation for enhancing in situ dissolution of non equeous-phase liquids. J. Contam. Hydrol., 12: 103-132.

Seiler, K.-P., (2000): Markierungen in der wasserungesättigten Zone, in Methoden der Sickerwassermodellierung – Theorie und Praxis, K.-P. Seiler and D. Klotz (Eds.), GSF-Bericht 18/00, 42-49.

Selker, J.S., T.S. Steenhuis, and J.-Y. Parlange., (1996): An Engineering Approach to Fingered Vadose Pollutant Transport. In: Fingered Flow in Unsaturated Soil: From Nature to Model, T.S. Steenhuis, C.J. Ritsema, and L.W. Dekker, Eds. Special Issue of Geoderma 70:197-206.

Seth R, Mackay D, Muncke J., (1999): Estimating the organic carbon partition coefficient and its variability for hydrophobic chemicals. Environ Sci Technol; 33:2390-4.

Simkins, S. and Alexander, M., (1984): Models for Mineralization Kinetics with the Variables of Substrate Concentration and Population Density. Applied and Environmental Microbiology, 47(6): 1299-1306.

Simkins, S and M., Alexander., (1984): Models for Mineralization Kinetics with the Variables of Substrate Concentration and Population Density.Applied Environmental Microbiology, p. 1299-1306.

Simůnek, J., M. Šejna and M, Th van Genuchten., (1998): The HYDRUS-1D software package for simulating the one-dimensional movement of water, heat, and multiple solutes in variably saturated media. Version 2.0, IGWMC-TPS-70, International Ground Water Modeling Center, Colorado School of Mines.

Simůnek, J., M, Th. van Genuchten, and M. Šejna., (2005): The HYDRUS-1D software. Version 3.0, HYDRUS.

Skibitzkie, H.E., and G.M. Robinson., (1963): Dispersion in groundwater flowing through heterogeneous materials. U.S. Geol. Survey.Prof. Pap.386-B, 5 pp.

Slater, J. H., (1979): Microbial population and community dynamics, p. 45-63. In J. M. Lynch and N. J. Poole (ed.), Microbial ecology: a conceptual approach. Blackwell Scientific Publications, Ltd., Oxford.

Slichter, C.S. (1905): Field measurement of the rate of underground water, U.S. Geol. Surv. Water supply Pap.140, pp. 9-85.

Smith, L., and F. W. Schwartz., (1980): Mass transport, 1, A stochastic analysis of macroscopic dispersion, Water Resour. Res. 16, 303-313.

Smith, L., and F. W. Schwartz., (1981a): Mass transport, 2 Analysis of uncertainty in prediction. Water Resour. Res. 17. 351-369.

Smith, L., and F. W. Schwartz (1981a): Mass transport, 3, Role of hydraulic conductivity data in prediction. Water Resour. Res. 17.,1463-1479. Software Series 1, Department of Environmental Sciences, University of California Riverside, Riverside, CA, 270pp., 2005.

Sposito, G., (1984): The Surface Chemistry of Soils, Oxford University Press, New York.

Sprague, L.A., Herman, J.S., Hornberger, G.M. and A.L. Mills, (2000): Atrazine adsorption and colloid-facilitated transport through the unsaturated zone, J. Environ. Qual., 29, 1632-1641,.

Steenhuis, T.S., J.-Y. Parlange, and M.S. Andreini., (1990): A Numerical Model for Preferential Solute Movement in Structured Soils. Geoderma 46:193-208.

Steenhuis, T.S., Y.-J. Kim, J.-Y. Parlange, M.S. Akhtar, B.K. Richards, K.-J.S. Kung, T.J. Gish, L.W. Dekker, C.J. Ritsema, and S.A.Abur- ime., (2001): An equation for describing solute transport in field soils with preferential flow paths. p. 137–140. In D.D. Bosch and K.W. King (ed.) Preferential flow, water movement and chemical transport in the environment. ASAE, St. Joseph, MI.

Steenhuis, T.S., J.-T. Christ, Y.,Zeve, J.-F. McCarthy,J.-A. Throop., (2005): Transport and Retention Mechanisms of Colliods in Partially Saturated Porous Media. Vadose Zone Journal 4:184-195.

Susset, B., T. Delschen, and Leuchs, W., (2004): Stoffaustrag aus mineralischen Abfällen: Untersuchung der zeitlichen Quellstärkeentwicklung in Großlysimetern des LUA NRW.- Beitrag in Tagungsband zur 37. Essener Tagung für wasser-und-Abfallwirtschaft vom 24.bis.26. März.

Susset, B., (2004): Materialuntersuchungen und Modellierungen zur Quantifizierung des Quellterms im Rahmen des „Sickerwasserprognoseverfahrens“, Ph.D. Thesis, TGA, C74, Eberhard-Karls-Universität Tübingen.

Taylor, G.I., (1921): Diffusion by continuous movements, Math.Soc.Ser.2.20, 196-212.

Taylor, G.I., (1953): The dispersion of matter in solvent flowing slowly through a tube, Prac. R. Soc. London. Ser. A 219, 189-203.

Thiele, M., Blunt, M.J: and F.M. Orr, Jr., (1995a): Modeling flow in heterogeneous media using streamtubes. 1. Misible and immisible displacements, IN SITU, 19(3), 299-339.

Thomann, R.V., and Mueller, J.A., (1987): Principles of Surface Water Quality Modeling and Control, Harper and Row, New York.

Tien, C., (1989): Granular Filtration of Aerosols and Hydrosols, Butterworth, Stoneham, MA.

Toran, L. and Palumbo, A. V. (1992): Colloid transport through fractured and unfractured laboratory sand columns, J. Contam. HydroL 9, 289-303.

Traub-Eberhard, U., K.-P. Henschel, W.Kördel and W. Klein. (1995): Influence of different field sites on pesticide movement into subsurface drains. Pestic. Sci. 43:121-129.

Trevisan, M., Errera, G., Goerlitz, G., Remy, B., Sweeney, P., (2000): PRZM-2 evaluation using Vredepeel dataset. Agric. Water Manage. 44, 317±335.

Trevisan, M., Errera, G., Vischetti, A., Walker, A., (2000): Varleach evaluation. Agric. Water Manage., this issue.

UBA (1998): IC-07 Leather Processing Industry. Assessment of the environmental release of chemicals from the leather processing industry. Draft. Umweltbundesamt, Berlin.

Utermann, J., Kladivko, E.J. and W.A. Jury, (1990): Evaluating pesticide migration in tile-drained soils with a transfer function model, J. Environ. Qual., 19, 707-714.

Van Dam, J.C., J. Huygen, J.G. Wesseling, R.A. Feddes, P. Kabat, P.E.V. van Walsum, P. Groenendijk, C.A. van Diepen., (1997): Theory of SWAP version 2.0. – Simulation of water flow, solute transport and plant growth in the Soil-Water-Atmosphere-Plant environment. Tech. Doc. 45, DLO Winand Staring Centre, Wageningen, Netherlands. pp. 167.

Van Dam, J.C., J.M.H. Hendrickx, H.C. van Ommen, M.H. Bannink, M.Th. van Genuchten, L.W. Dekker, 1990.

Van Genuchten, M.T., (1980): A closed-form equation for predicting the hydraulic conductivity of unsaturated soils, Soil Sci. Soc. Am. J., 44, 892 –898.

Van Genuchten, M.Th. and Wierenga, P.J., (1976): Mass transfer studies in sorbing porous media. I. Analytical solutions. Soil Sci. Soc. Am. J., 40: 473-481.

Vanclooster, M., Boesten, J.J.T.I., Trevisan, M., Brown, C., Capri, E., Eklo, O.M., GottesbuÈren, B., Gouy, V., Van der Linden, A.M.A., (2000): A European test of pesticide leaching models. Methodology and major recommendations. Agric. Water Mgmt. 44, 1±19.

Vinten, A.J.A., B. Yaron, and P.H. Nye., (1983): Vertical transport of pesticides into soil when adsorbed on suspended particles. J. Agric. Food Chem. 31:662–664.

Wackett, L.P., and Ellis, L .M., (1999): Predicting biodegradation. Environ. Microbiol. 1: 119-124.

Walter, M.T., J.-S. Kim, T.S. Steenhuis, J.-Y. Parlange, A.Heiilig, R.D. Braddock, J.S. Selker, and J.Boll., (2000): Funneled flow mechanisms in a sloping layered soil: Laboratory investigation, 2000. Wat. Resources Res. 36(4):841-849.

Wan, J., and T.K. Tokunaga., (1997): Film straining of colloids in unsaturated porous media: Conceptual model and experimental testing. Environ. Sci. Technol. 31:2413–2420.

Water and solute movement in a coarse-textured water-repellent field soil. J. Hydr. 120, 359-379. Water Resour. Res. 31, 2701-2707.

Weihermüller G. L., (2005): Comparison of different soil water extraction systems for the prognoses of solute transport at the field scale using numerical simulations, field and lysimeter experiments. Rheinischen Friedrich-Wilhelms-Universit¨at zu Bonn.

White, R.E., J.S. Dyson, R.A. Haigh, W.A. Jury, and G. Sposito., (1986): A transfer function model of solute transport through soil. - 2. Illustrative applications. Water Resour. Res. 22:248–254.

WHO, (2003): Polynuclear aromatic hydrocarbons in drinking water.Background document for preparation of WHO Guidelines for drinking-water quality. Geneva, World Health Organisation (WHO/SDE/WSH/03.04/59).

Wiedemeier, T.H., Rifai, H.S., Newell, C.J. and Wilson, J.T., (1999): Natural Attenuation of Fuels and Chlorinated Solvents in the Subsurface. John Wiley and Sons, New York, 617 pp.

Williams, C.F., M. Agassi, J. Letey, W.J. Farmer, S.D. Nelson, and M.Ben-Hur. (2000): Facilitated transport of napropamide by dissolved organic matter through soil columns. Soil Sci. Soc. Am. J. 64:. 590–594.

Wood, W.W. and G.G. Ehrlich. (1978): Use of baker's yeast to trace microbial movement in groundwater Ground Water. 16, 398.

Xia G, Ball W.P., (1999): Adsorption-partitioning uptake of nine low-polarity organic chemicals on a natural sorbent. Environ Sci and Technol, 33:262-9.

Yao, K.-M., M.T. Habibian, and C.R. O'Melia. (1971): Water and waste water filtration: Concepts and applications. Environ. Sci. Tech nol. 5:1105–1106.

Ying, R., Peters, M.H., (1991): Brownian dynamics simulation of rotational correlation functions for a three-body macromolecular model.The Journal of Chemical Physics . July 15, .Volume 95, Issue 2, pp. 1234-1241.

Zhang, R., (1995): Prediction of solute transport using a transfer function model and the convection–dispersion equation. Soil Sci. 160:18–27.

Zhang, R., A.J. Krzyszowska-Waitkus, G.F. Vance, and J. Qi. (2000): Pesticide transport in field soils. Adv. Environ. Res.

Zhang, X., and Young, L.Y.,(1997): Carboxylation as an initial reaction in the anaerobic metabolism of naphthalene and phenanthrene by sulfidogenic consortia. Appl. Environ. Microbiol. 63: 4759-4764.

Zheng, C., (1990): MT3D – A modular three-dimensional transport model for simulation of advection, dispersion and chemical reactions of contaminants in groundwater systems, S.S. Papadopoulos and associates, Inc.

Zheng, C., Wang, P.P., (1999): MT3DMS: A modular three-dimensional multispecies model for simulation of advection, dispersion and chemical reactions of contaminants in groundwater systems; Documentation and User's Guide, Contract Report SERDP-99-1, U.S. Army Engineer Research and Development Center, Vicksburg, MS.

APPENDIX

Appendix 1: Example of SMART input data set

The input data set for a simulation run with SMART essentially consists of one main input file as well as two catalog files with solid and / or pollutant characteristics. An example of a input data set, how it was used for the investigations of this subproject, is arranged in the following Tables A.1 - A.3.

Table A-1: Main input data set

```
__TITEL
        7             ! no. of titel lines,
SIWA-TASKFORCE-sourceterm-modelling
Desorption (IPD), only advection, saturated sat=100%
ne= 30%, GWR=300mm/a, saturated, l=1m, Kd= 55.4 L/kg
iitial conc: 10 mg/Kg (PAH(PHE))
1 Lithocomponent
1 grain size class (1 mm)
units: Meter, kg, seconds
-----------------------------------------------------------------------
__SIMULATION_MODE
        1     ! sim_mode: simulation mode
        1     ! sat_mode ! saturated

__DIMENSIONS
       250     ! # of cells (nix)
    125000     ! # of time steps (nit)
        1     ! # of lithocomponents (nj)
        1     ! # of grain size classes (nk)
        1     ! # of contaminants (ni)
        0     ! # of surfactants (nm)
  __FILE_DATA
   8
  12    source.out
  13    source.dat
```

```
  14    source.ba1
  15    source.ba2
  16    contam.clg
  17    soil.clg
  18    smart.dim
  19    source.btc
__OUTPUT_CONTROL
      31
   5    1
 1 0 0 0 0 0
 0 0 0

__
GEOMETRICAL_DATA
    1.0                    ! cross-sectional area
       0   0.004             ! delx: cell lengths

__BOUNDARY_CONDITIONS
       2   0.00000      1.0   9.51e-9   ! ibound,head1,head2, qq



__HYDRAULIC_DATA
       0   1.0e-05      ! Hydraulic conductivity
       0   3.0e-01      !interparticle porosity
       0   3.0e-01      !flow effective porosity

__SATURATION
0  1                 !saturation 100 %
__TIME_DATA
      1            ! time discretization mode
   126182.9  ! range of time step no. & length of time steps

__CALCULATION_DATA
       2     ! dmode: mode for evaluating Dapp
       2     ! dcal: ipd model mode (1: analytical, 2: numerical)
```

```
------------------------------------------------------------------------
__LITHOCOMPONENTS
  1   500        HMVA_BAM    !internal no., catalog no. & denotation

__GRAIN_SIZE_CLASSES
        5.465e-4               !1sr class: 1 cm loess
        0     1.0e0          ! fraction of first class:100%
        0     1.0e0          ! fraction of parabrown: 100%
__CONTAMINANTS
   1   6              PHE  ! internal no., catalog no. & denotation

__EQUILIBRIUM_FRACTIONS
        0   0.e-02           ! no equilibrium fraction
------------------------------------------------------------------------
__INITIAL_CONCENTRATIONS
__CONTAMINANTS
  __MASS_PER_MASS_SOIL
        0       8.0e-07           !  mg/kg Phe
------------------------------------------------------------------------
__INFLOW_CONCENTRATIONS

__CONTAMINANTS
         1         0    ! internal no. of contaminant & mode
        0.0
-----------------------------------------------------------------
__BIO_REDUCTION
0    1       31536000    1.0       0.0       !type,  bio_mode,  half_life,  second_parameter,
half_lif_conc
__ISOTHERM_DEFINITIONS
__SORPTION_ONTO_MINERALSURFACES
   1    1    1    ! internal no. of parabrown & contamin. & isoth. type
  5.54e-2         ! parameter: Henry isotherm Kd=54.4 l/kg
```

Table A-2: Material characteristics catalog

*** Specific properties of lithocomponents ***

No.	Stoff-Bezeichnung	m	foc	l_dens	nip	
units: kg, m						
__DATA						
1	limestone	2.5	0.001	2.00d+03	0.02	
2	clay-/Siltstone	2.5	0.005	2.50d+03	0.005	
3	sandstone	2.5	0.0005	2.50d+03	0.01	
4	clay/silt	2.0	0.005	3.00d+03	0.001	
10	Test-material	2.0	0.020	2.50d+03	0.130	
11	Neckarsand	2.0	0.020	2.73d+03	0.010	
12	Neckarsand2	2.0	0.020	2.73d+03	0.020	
13	Pseudo_Mat1	2.0	0.020	2.73d+03	0.020	
14	Pseudo_Mat2	2.0	0.020	2.73d+03	0.020	
15	Pseudo_Mat3	2.0	0.020	2.73d+03	0.020	
161	Quartz1	1.00	0.001	2.65d+03	0.0100	
241	Quartz2	1.00	0.001	2.65d+03	0.0050	
242	Keupersandstone1	2.10	0.00161	2.65d+03	0.0800	
243	limestone2	2.00	0.00244	2.73d+03	0.0057	
244	jurassic_limestone	2.10	0.00131	2.73d+03	0.0160	
251	Quartz3	1.00	0.001	2.65d+03	0.0100	
252	Keupersandstone2	2.00	0.005	2.69d+03	0.0880	
261	Quarz4	1.00	0.001	2.65d+03	0.0030	
262	Quarz5	1.20	0.001	2.65d+03	0.0050	
263	Quarz6	1.10	0.000033	2.65d+03	0.0020	
300	Quarz7	1.00	0.0001	1.00d+03	0.1000	
301	limestone2	2.0	0.00022	2.73d+03	0.012	!Data from Rügner and Kleineidam

302	limestone3	2.0	0.00034	2.73d+03	0.0071	!from Horkheim
303	sandstone2	2.6	0.00020	2.68d+03	0.08	! Stubensandstone from Horkheim
304	virtuell_limestone	2.0	0.00034	2.164502d+03	0.01	! EU landfill directive scenario
305	virtuell_jur_limestone	2.0	0.00022	2.164502d+03	0.02	! for EU landfill directive scenario
400	lignite_particle	2.0	9.9999	0.78d+03	0.01	
500	HMVA_BAM	2.0	0.5	2.65d+03	0.01	!Data from Rainer Henzler
501	Bauschutt BAM	2.0	0.6	2.57d+03	0.0347	!Data from Rainer Henzler
502	Boden(Atlas) BAM	2.0	0.3	2.66d+03	0.0122	!Data from Rainer Henzler
600	Parabrown	2.0	0.0056545	2.92d+03	0.002	!Data from Amankwah (MSc thesis), foc data from Jülich

Contaminant characteristics catalogue

No.	Contaminant	Daq	logKow	logKoc
_DATA				
1	benzene	1.02E-09	2.13	1.92
2	toluene	9.39E-10	2.69	2.48
3	trichloroethene	1.04E-09	2.42	2.21
4	naphthalene	9.1495E-10	3.36	3.06
5	fluorene	7.22E-10	4.18	3.87
6	phenantrene	7.684E-10	4.57	4.00
7	anthracene	6.84E-10	4.54	4.23
8	fluoranthrene	6.58E-10	5.22	4.91
9	pyrene	6.58E-10	5.13	4.82
10	benz(a)anthracene	5.97E-10	5.91	5.60
11	benzo(a)pyrene	5.79E-10	6.50	6.19
15	Anthrachinon	7.08E-10	3.51	4.64

Appendix 2: Excel spreadsheet for the evaluation of the source strength function

In the following an example of Excel spreadsheet is presented, which makes the evaluation for the source strength function possible for organic pollutants. Thus a simple and a practical tool is presented for the evaluation of the equations 4.1 and 4.2.

The computational part of the Excel sheet is divided into three ranges. Tab. A-4 shows the input area. The compulsory input fields are in green colour. For the intraparticle porosity (blue supported input field) in the column "default" a value (1 %) is suggested. This value is used in the computation steps only if no entry is made in the associated input field.

Tab. A-4: Eingabebereich des Excel-Arbeitsblatts

	EINGABE		**Voreinstellungen**
Mächtigkeit Quelle (m)	1,5		
Grundwasserneubildung (mm/a)	220		
Porosität (%)	28		
Sättigungsgrad (%)	82		
Korndurchmesser (m)	200		
Materialdichte (g/cm³)	2,73		
Intrapartikelporosität (%)			1
Verteilungskoeffizient (L/kg)	12,4		
aquat. Diffusionskoeff. (cm²/s)	7,68E-06		
Halbwertzeit (d)	180		

Tab. A-5 contains computed figures, which are derived from the input values. The appropriate calculation steps contain simple operations e.g. the conversion of units and serve as preparation for the actual evaluation of the source strength function. Changes to the input data are emphasized by bold print in each case.

Tab. A-5: Parameter values

Parameter:	
Mächtigkeit Quelle (m)	1,5
Grundwasserneubildung (m/s)	6,98E-09
Porosität (-)	0,28
mittlere Bodenfeuchte (-)	0,2296
Kornradius (m)	0,0001
Materialdichte (kg/dm³)	2,73
Intrapartikelporosität (-)	0,01
Verteilungskoeffizient (L/kg)	12,4
aquat. Diffusionskoeff. (m²/s)	7,68E-10
Halbwertzeit (s)	1,56E+07

Tab. A-6 shows numerical results of the sheet. These contain the function parameters of the equations (4.1) and (4.2) in the first block: the pore volumes test specification, the retardation factor R and the Damköhler numbers Da_{des} as well as Da_{bio} for desorption and microbial degradation. In the second block, which is only partly represented in Tab. A-6, the time t' and the relative discharge concentration c/c0 standardized to the pore volume are indicated. This connection is graphically shown in Fig. A-1 for a larger period.

Tab. A-6: Parameters with numerical results

	Results
Porenvolumen (s)	4,94E+07
Porenvolumen (d)	571,39
Retardationsfaktor (-)	107,16
scheinbarer Diffusionskoeff. (m²/s)	2,29E-15
Damköhler-Zahlfür Desorption (-)	112,18
Abbauratenkonstante (1/s)	4,46E-08
Abbauratenkonstante (1/d)	3,85E-03
Damköhler-Zahl für Abbau (-)	2,20

Zeit / Porenvolumen (-)	relative Konzentration (-)
0,00	1,000
0,66	0,990
1,32	0,980
1,98	0,970
2,64	0,961
3,30	0,951
3,96	0,942
4,62	0,932
5,28	0,923

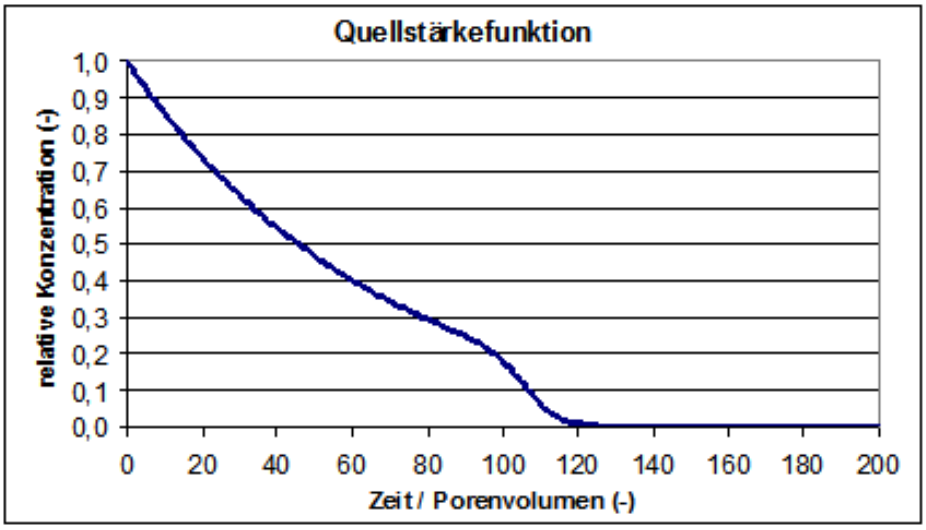

Fig. A-1: Plot of a source term function

Moreover the Excel sheet below contains information on the input data (Tab. A-7).

Tab. A-7: Information part of the Excel work sheet

Das Arbeitsblatt wertet eine Quellstärkefunktion für organische Schadstoffe aus. *Autor:* Rudolf Liedl

Es basiert auf den Ergebnissen des Teilprojekts TFQ-2 "Quellstärkefunktionen für organische Schadstoffe" *Datum: 26.10.2006*

der Task Force "Quellstärkefunktionen" im BMBF-Förderschwerpunkt "Sickerwasserprognose".

Die hier verwendete Quellstärkefunktion wurde durch Anpassung an Ergebnisse eines prozessbasierten Simulationsmodells ermittelt.

Als relevente Austragsprozesse wurden Advektion, kinetische Desorption und mikrobieller Abbau berücksichtigt.

Kinetische Desorption wurde im Prozessmodell mit einem Intrapartikeldiffusionsansatz nachgebildet.

Für den mikrobiellen Abbau wurde ein Ratengesetz erster Ordnung verwendet.

Die Felder für Eingabewerte sind grün bzw. blau gekennzeichnet.

Dabei wurde folgender Farbcode verwendet:

	Eingabefeld für Prozessparameter (Pflichteingabe, d. h. ohne Voreinstellung)
	Eingabefeld für Prozessparameter (vorhandene Voreinstellung kann abgeändert werden)

Eingabegröße:	*Einheit*	
Mächtigkeit Quelle	m	
Grundwasserneubildung	mm/a	
Porosität	%	
Sättigungsgrad	%	
Korndurchmesser	m	
Materialdichte	g/cm³	
Intrapartikelporosität	%	(Voreinstellung: 1 %)
Verteilungskoeffizient	L/kg	
aquatischer Diffusionskoeffizient	cm²/s	
Halbwertzeit	d	

Appendix 3: A sample lysimeter data set obtained from FZJ (Jülich)

QP	SiWa-Projekt Datenblatt org. Stoffe (PAK's)für eine Perkolationssäule Saugkerzenebene SKE-2					
A-1	AT1	AW1	AT2	AW2	AT3	AW3
A-2	Forsch.Einrich.t:	FZJ	Bearbeiter:	Pütz/Rützel	Bearb.-Datum	Febr.2004
A-3	Ausführ. Stelle	Institut Agrosphäre	Projekt-ID	218	Anmerkung:	
A-4	Unters.-Mat:	RM Boden	Herkunft:	BAM	Proben-ID:	
A-5	Versuchsanlage:	Großlysimeter	Lysim.-ID	302	Ort :	Jülich
Form-Version 14.2.04						

B	Hauptdaten der Versuchsanlage und Betrieb Saugkerzenebene SKE-2									
B-1	BT1	BT2	BW2	BT3	BW3	BT4	BW4	BT5	BW5
B-2	Vers.-Daten	Betr.-Beginn:	10.12.01	Ges.-Höhe [m]:	2.40	Fläche [m²]	2.0	Füllzustand:	ungesättigt
B-3	Zulauf	Zulaufrichtung:	oben	Zulauf-Ws:		Zusätze:	keine	TOC TraS-Mat. %	
B-4	Deckschicht	Material:	Quarzkies	Höhe [m]:	0.33	Masse [kg]:	943	KornGröße mm:	
B-5	Quellst.-Schicht	Material(OstS):	RM Boden	Höhe [m]	0.47	Masse [kg]:	1510	ρLager g/cm³:	
B-6	Transp.-Schicht	Material(TraS):	Parabraunerde	Höhe [m]:	1.60	Masse [kg]:		ρLager g/cm³:	
B-7	Filterschicht	Material:	Sintermetall	Höhe [m]:		Masse [kg]:		KorngGöße mm:	
B-8	Probenahme	Zeitschema:	monatlich	Entnahme-Art:	Sammel	Anz. SK-Ebenen:	3	Saugkerz.je Ebene	3
B-9	Analytik	Verfahren:		Vorfiltration:	1-2µm	Parallelproben:		Best.-Grenze	
B-10	Sonstiges	Beginn Ost-Bereg.	9.4.2002	W/F bez. auf		Feuchte OstS %		Feuchte TraS %	

C	AnalysenDaten des Quellstärkematerials (S4-Test)															
C-1	CS1	CS2	CS3	CS4	CS5	CS6	CS7	CS8	CG1	CG2	CG3	CG4	CG5	CG6	CG7	CG8
C-2	S4-2:1 Acena	S4-2:1 Anthra.	S4-2:1 Phenan.	S4-2:1 Pyren	S4-10:1 Acena.	S4-10:1 Anthra.	S4-10:1 Phenan	S4-10:1 Pyren	Phenol-Index	Acenaphthen	Anthracen	Fluoren	Naphthalin	Phenanthren	Pyren	Sum 16PAK
C-3	µg/L	µg/L	µg/L	µg/L	µg/L	µg/L	µg/L	µg/L	[mg/kg]	[mg/kg]	[mg/kg]	[mg/kg]	[mg/kg]	[mg/kg]	[mg/kg]	[mg/kg]
C-4																

D	Daten der Probenahme und der Parameterwerte Saugkerzenebene SKE-2															
D-1	DD1	DD2	DD3	DD4	DD5	DD6	DD7	DD8	DP1	DP2	DP3	DP4	DP5	DP6	DP7	P8
lfd. Nr	Datum	Samml Zeit	Betr.- Zeit kumul.	SZ-Zul kumul.	Ablauf SKE-2	Lysim. Ges.-Ablauf	W/F kumul.	W/F MiPkt	Phenol-Index	Acenaph-then	Anthracen	Fluoren	Naph-thalin	Phenant-hren	Pyren	Sum 15PAK
		[d]	[d]	[L]	[L]	[L]	[L/Kg]	[L/Kg]	[mg/L]	[µg/L]	[µg/L]	[µg/L]	[µg/L]	[µg/L]	[µg/L]	[µg/L]
1	9.4.02 12:00 AM	0.0	0.0		0.00	0.00										
2	6.5.02 12:00 AM	27.0	27.0	301.84	3.16	151.32	0.160	0.080		0.00	0.00	0.01		0.010		
3	3.6.02 12:00 AM	28.0	55.0	390.27	2.82	93.66	0.260	0.210		0.00	0.00	0.00		0.007		
4	8.7.02 12:00 AM	35.0	90.0	567.73	4.89	131.23	0.399	0.329		0.00	0.00	0.00		0.003		
5	12.8.02 12:00 AM	35.0	125.0	791.93	3.95	142.05	0.550	0.474		0.00	0.00	0.00		0.005		
6	9.9.02 12:00 AM	28.0	153.0	962.56	3.55	167.23	0.727	0.638		0.00	0.01	0.00		0.006		
7	14.10.02 12:00 AM	35.0	188.0	1032.96	2.93	56.07	0.786	0.757		0.00	0.01	0.00		0.008		
8	13.11.02 12:00 AM	30.0	218.0	1301.36	3.18	206.31	1.005	0.896		0.00	0.01	0.00		0.005		
9	16.12.02 12:00 AM	33.0	251.0	1385.96	2.81	90.44	1.101	1.053		0.00	0.01	0.00		0.006		
10	14.1.03 12:00 AM	29.0	280.0	1551.16	2.76	155.95	1.266	1.184		0.00	0.01	0.00		0.006		
11	17.2.03 12:00 AM	34.0	314.0	1636.36	2.78	85.24	1.357	1.312		0.00	0.00	0.00		0.007		
12	18.3.03 12:00 AM	29.0	343.0	1763.19	2.68	101.79	1.465	1.411		0.00	0.05	0.00		0.007		
13	15.4.03 12:00 AM	28.0	371.0	1870.65	2.45	74.82	1.54	1.50		0.00	0.01	0.00		0.005		
14	12.5.03 12:00 AM	27.0	398.0	1981.68	2.65	109.46	1.66	1.60		0.00	0.00	0.00		0.008		
15	16.6.03 12:00 AM	35.0	433.0	2237.88	5.26	168.03	1.84	1.75		0.00	0.01	0.00		0.007		
16	16.7.03 12:00 AM	30.0	463.0	2326.11	2.44	64.66	1.91	1.87		0.00	0.01	0.00		0.008		
17	11.8.03 12:00 AM	26.0	489.0	2496.00	2.79	120.16	2.03	1.97		0.00	0.00	0.00		0.008		
18																
19																
20																
21																
22																
24																
25																
26																
27																
28																
29																
30																
31																
32																
33																
34																
35																
36																
37																
38																
39																
40																
41																
42																
43																
44																
45																
46																
47																
48																
49																
50																
51																
52																
53																
54																
55																